UNIVERSITA' DEGLI STUDI DI PADOVA

Dipartimento di Anatomia e Fisiologia

SCUOLA DI DOTTORATO DI RICERCA IN
SCIENZE MEDICHE CLINICHE E SPERIMENTALI
INDIRIZZO
NEUROSCIENZE
CICLO XX

Calcium signals in myogenics cells and muscle fibers: an integrated study

Direttore della Scuola : Ch.mo Prof. Silvano Todesco
Supervisore : Ch.mo Prof. Carlo Reggiani

Dottorando : Marco Quarta

31 gennaio 2008

A mia moglie
To my wife

ABSTRACT
(english)

Calcium release during skeletal muscle excitation-contraction (EC) coupling occurs at the junctions between the sarcoplasmic reticulum (SR) and either the plasma membrane or T-Tubule. These Ca2+ release units are characterized by a specific molecular composition and their specific structural organization, both of which are important for the tissue-specific mode of skeletal muscle EC coupling. Though EC coupling has been known for over half a century, it is still an active area of biomedical research. The general scheme is that an action potential arrives to depolarise the cell membrane. By mechanisms specific to the muscle type, this depolarisation results in an increase in cytosolic calcium that is called calcium transient. This increase in calcium activates calcium-sensitive myofibrillar proteins that then trigger ATP hydrolysis by myosin causing cell shortening. However, the exact mechanism if EC coupling and the role of related Ca2+ singnaling in regulating intracellular skeletal muscle ptthways is far to be clear. To higlight some of these unclear and dark points, we realized two null-mice for SR proteins. The first lacks of a sarcoplasmic reticulum Ca2+-binding protein, termed Calsequestrin (Csq), which plays an important role in buffering $[Ca2+]_{SR}$ and modulating Ca2+ release and reuptake during EC coupling. Our findings reveal the essential role of Csq1 in reorganizing stores and an impaired calcium handling in mice lacking Csq1.

an essential role of Cs as presented in chapter 1. Our data suggest that Csq1 deficency may result in a myopathy similar to that caused by mutations of RyR1 in skeletal muscle, leading to *fulminant malignant hyperthermia (MH) episodes*, as presented in chapter 2.

To investigate the structural role of SR we realized a second model, Ank1.5-null mice. The highly regulated nature of the arrangement of the SR around myofibrils is such that specific domains of the SR involved in the mechanisms of Ca2+ release and uptake (i.e., terminal cisternae and longitudinal tubules, respectively) are positioned at regular intervals in

correspondence of specific regions of the sarcomere. However, the molecular mechanisms responsible of the interactions between these two cellular structures are not known. The small Ankirin 1.5 locates at SR level and participate in positioning SR and myofibrils. In chapter 3 we present evidence of contractile response impairment in skeletal muscles and altered animal performances of Ank1.5 deficient mices, without structural and ultrastructural morphological changes. The Ank1.5 could play a specific role not restricted to a correct positioning of the SR at specific sarcomere regions and its deficency may contribute to the generation of myopathies, and EC coupling dysfunctions.

To perform a deeper study of the development of the skeletal muscle cells, and in particular to better explore calcium signals in the context of EC coupling, we developed a muscle-cell / semiconductor chip device to induce EC coupling with non invasive long termed electric capacitive stimulation. We present in chapter 4 for the first time a new technique to study live EC coupling and Calcium signals in long term experiments and with high resolution, down to single cells, to induce muscle plasticity and synaptogenesis effects. The same approach is used for muscle fibers dissociated from mouse FDB muscle. To conclude, our hybrid device put an innovative base for new approaches aimed to better understand the muscle development and regeneration in normal and pathogenic conditions.

RIASSUNTO
(italiano)

Il rilascio di calcio durante i fenomeni di accoppiamento eccitazione-contrazione (EC) avviene al livello di giunzioni poste fra il reticolo sarcoplasmatico (SR) e elementi di membrane sarcoplasmatica ad essi associati, definiti tubuli T (TT). Quesit rilasci di unità di calcio sono caratterizzati da una precisa componente molecolare ad da una loro fine organizzazione strutturale, entrambi fondamentali per un corretto accoppiamento EC tessuto specifico del muscolo scheletrico. Nonostante il fenomeno dell'accoppiamento EC sia conosciuto da più di mezzo secolo, vi è tutt'ora una area di ricerca biomedica molto attiva per investigare sui meccanismi che regolano questo processo. Lo schema generale prevede che un potenziale di azione arriva e depolarizza il sarcolemma. Attraverso meccanismi specifici per tipo musclare, questa depolarizzazione è associata ad un incremento temporaneo di calcio citosolico, definito transiente di calcio. Questi transienti di calcio attivano proteine miofibrillari calcio-sensibili che attivano l'idrolisi dell'ATP da parte ella miosina causando un accorciamento delle miofibrille e con esse della celula musclare. Gli esatti meccanismi molecolari dell'accopiamento EC e il ruolo dei segnali di calcio ad essi associati nel regolare differenti vie di segnale cellulari sono però lontani dall'essere chiari e definiti.

Per chiarire alcuni di questi punti ancora oscuri, abbiamo realizzato due modelli di topi mancanti per proteine del SR. Nel primo modello murino, è stata tolta la proteina del SR legante il calcio, definita Calsequestrina del muscolo scheletrico (Csq1), che gioca un importante ruolo come sistema tampone del $[Ca2+]_{sr}$ e nel modulare il rilascio e il recupero di calcio dal reticolo durante i fenomeni di accoppiamento EC. I nostri risultati rivelano un ruolo fondamentale della Csq1 nella organizzazione di compartimenti per il calcio del SR, e la sua assenza o mutazione comporta variazioni strutturali del muscolo scheletrico e alterazioni funzionali nei segnali di calcio, come presentato nel capitolo 1. I nostri dati suggeriscono che alterazioni della Csq1 possa comportare miopatie simili a quelle causate dalla mutazione del recettore della rianodina scheletrico (RyR1), il canale del SR che rilascia calcio in seguito alla depolarizzazione del sarcolemma,

che portano a episodi fulminanti di ipertemia maligna, come presentato nel capitolo 2.

Per investigare il ruolo strutturale del SR abbiamo realizzato un secondo modello murino, mancante per la proteina del SR Ankirina 1.5. La natura altamente regolata nell'organizzazione del SR intorno alle miofibrille è così fine che specifici domini del SR coinvolti nei meccanismi di rilascio di Ca2+ e il suo recupero (le cisterna terminali e i tubuli longitudinali rispettivamente) sono posizionati a intervalli regolari in corrispondenza di specifiche regioni del sarcomero. I meccaniscmi molecolari responsabili delle interazioni fra queste due strutture sono però sconosciuti. La piccola isoforma di Ankirina 1.5 è posizionata in maniera specifica a livello di SR e partecipa nel posizionamento del SR sulle miofibrille. Nel capitolo 3 presentiamo l'evidenza di alterazioni funzionali nella risposta contrattile del muscolo scheletrico e di alterate performances nell'animale KO per la Ank1.5, senza però evidenze di variazini strutturali o ultrastrutturali. Questa proteina infatti potrebbe giocare un ruolo non limitato ad un corretto posizionamento del SR su specifiche rgioni del sarcomero e potrebbe contribuire nello sviluppo di miopatie e disfunzioni dell'accoppiamento EC.

Per sviluppare studi più approfonditi e precisi dello sviluppo del muscolo scheletrico e in particolare per meglio esplorare segnali di calcio nel contesto dell'accoppiamento EC a livello di singola cellula, abbiamo realizzato un dispositivo a microchip di silicio ibrido costituito da un semiconduttore accoppiato con cellule muscolari per indurre in vitro accoppiamenti EC non invasivi e protratti cronicamente nel tempo tramite stimolazioni elettriche di tipo capacitivo. Presentiamo nel capitolo 4 per la prima volta questa nuova tecnica che permette con un'altra risoluzione e nel tempo di indurre fenomeni di plasticita muscolare e sinaprogenesi in cellule muscolari e fibre singole dissociate dal muscolo FDB.

Per concludere, il nostro dispositivo ibrido getta le basi per nuovi approcci innovativi mirati ad un migliore comprensione dello sviluppo e della rigenerazione muscolare in condizioni normali o patogeniche.

INDEX:

Introduction:

1) Biology and physiology of EC coupling and calcium signals in skeletal muscle

2) Sarcoplasmic Reticulum: Functional and structural role of Calsequestrin

3) Ankyrins and organization of sarcoplasmic reticulum

4) A new approach with hybrid cell-semiconductor device for single cell investigtion of calcium signals in muscle plasticity at satellite cells, myotubes and single fiber level.

Cap1

Reorganized stores and impaired calcium handling in skeletal muscle of mice lacking calsequestrin-1.

Cap 2

Heat and anaesthesia cause a lethal crisis (malignan hyperthermia?) in CS1 null mice

Cap 3

Contractile response impairment in skeletal muscles of Ank1.5 deficient mices

Cap 4

A Novel Myo-Silicon Junction achieves single cell electric capacitive stimulation and modulates plasticity and differentiation of myogenic cells.

Conclusion

INTRODUCTION

1) Biology and physiology of EC coupling and calcium signals in skeletal muscle

Excitation-contraction (EC) coupling is a term coined in 1952 to describe the physiological process of converting an electrical stimulus to mechanical response (Sandow, 1952). This process is fundamental to muscle physiology, whereby the electrical stimulus is usually an action potential and the mechanical response is contraction. EC coupling can be dysregulated in many disease conditions.

Few years later, Huxley and Taylor, in 1958, managed to induce a local contraction by depolarizing limited region of a frog fiber's membrane near the I band, putting the base for the identification of the propagation system, later identified with the transverse tubular (TT) system already described by Veratti in 1902.

During the sixities, Ebashi and coworkers clarified the role of Ca2+ as key to the force generation reactions (review in 1968), while Weber and others established the function of the sarcoplasmic reticulum (SR) as intracellular Ca2+ storage and release organelle (Hasselbach, 1964). In the seventies a key discovery was the evidence of the voltage dependent charge movement of skeletal muscle (Scheider and Chandler, 1973), this was the first step toward the excitation-contraction coupling.

In the eighties the discovery process culminated with the identification of the main molecules involved in the EC coupling: the calcium-ryanodine receptor complex of skeletal and cardiac muscle (Pessah et al., 1985) first, immediately followed by the discovery of the calcium channel activity of the dihydropyridine-receptor (DHPR) of skeletal muscle (Smith et al., 1987). The final step that defined the moleculr terms in which the filed develops today was the confirmation in the ninetees of the DHPR in the process of EC coupling (Takeshima et al., 1995).

Though EC coupling has been known for over half a century, it is still an active area of biomedical research. The general scheme is that an action potential arrives to depolarise the cell membrane. By mechanisms specific to the muscle type, this depolarisation results in an increase in cytosolic calcium that is called a calcium transient. This increase in calcium

activates calcium-sensitive myofibrillar proteins that then trigger ATP hydrolysis by myosin causing cell shortening.

Calcium release during skeletal muscle excitation-contraction (EC) coupling occurs at the junctions between the sarcoplasmic reticulum (SR) and either the plasma membrane or TT. These Ca2+ release units are characterized by a specific molecular composition and their specific structural organization, both of which are important for the tissue-specific mode of skeletal muscle EC coupling. Upon depolarization Ca2+ is being released from the SR via the skeletal muscle ryanodine receptor (RyR1). The voltage sensor and trigger for this Ca2+ release process is the skeletal isoform of a L-type Ca2+ channel, the dihydropyridine receptor (DHPR), which activates the RyR1 faster and at lower voltages than its own conductance pore. It is assumed that this voltage-dependent activation of SR Ca2+ release occurs by (direct or indirect) physical interactions between the DHP-receptor and the RyR1. This physical interaction, in turn requires the close association of the two channels within the SR-T tubule or SR-plasma membrane junctions. Indeed, DHPRs in the junctional membranes are regularly arranged in groups of four, called the tetrads, which correspond in size and orientation exactly to the position of every other RyR in the opposing SR membrane. That this highly coordinated molecular arrangement of DHPR and RyR is important for the tissue specific mode of EC-coupling in skeletal muscle is further substantiated by the observation that in cardiac muscle, which requires the influx of trigger Ca2+ for the activation of EC coupling, the DHPRs do not form tetrads opposite the RyR arrays [Franzini-Armstrong et al., 1998].

The Chemical reactions underlyng the generation of force in muscle are blocked in the resting tissue, and only become possibile when free [Ca2+] in the aqueous medium bathing the contractile proteins rises from resting levels of about 100 nM to levels of 10-100 uM. This occurs physiologically after every action potential that propagates along the muscle cell membrane.

The early studies thus established that EC coupling requires low [Ca++]i at rest, then a rapid increase, and a return to resting levels in tens of milliseconds. Much effort was therefore devoted to measuring the

concentration of Ca++ in the myoplasm, and its changes upon action potential activation or voltage clamp depolarzation. Evaluated with optical techniques, considering the interfering effect of intracellular structures that bind the indicator dye, the values of resting [Ca2+]i range from 100 to 250 nM (Baylor and Hollingworth, 2000).

The important layers in myoplasmic and SR Ca2+ movements are illustrated schematically in fig1 of this introduction.

As introduced above, the voltage-sensitive Ca2+ channels of skeletal muscle are of L-type, implying that their resting Po will be extremely low. Voltage.insensitive “leak” Ca2+ channels have been described in cardiac and skeletal muscle (Rosenberg et al., 1988). They might be important in the regulation and adult fibres of mice with Duchenne muscular dystrophy, in which an increased proteolysis is a consequence of elevated [Ca2+]i [Alderton and Steinhardt, 2000]. Persistent elevation of [Ca2+]i triggers the opening of mitochondrial pores and releases cytochrome c, which activates the proteolytic caspases of apotosis. A second important group of voltage insensitive calcium channels are represented by the so-called store operated channels (SOC).

The active transport mechanism that mantains low the resting cytosolic [Ca2+]i include the (Ca2+ + Mg2+) – ATPase of the sarcoplasmic reticulum (SERCA), a similar protein in the plasma membrane (PMCA), the uniporter of the mitochondrial membrane and the Na+/Ca+ exchanger of the plasma membrane. SERCAs are crucial to the rapid restoration of low [Ca2+]i after a Ca2+ transient- Even though the flow of Ca2+ across the plasmalemma is too smal to be relevant to EC coupling in the short term, it is essential in Ca2+ homeostasis. Ultimately, the total calcium content of a cell can only be controlled by the flow trough its boundary, the plasmalemma.

At plasmalemma level is located another (Ca2+ + Mg2+) – ATPase (Schatzmann, 1989) in most cells. Four isoforms, termed PMCA 1 to 4, have been identified and are widely distributed. PMCA 1, 3 and 4 have been demonstrated in mammalian muscle (Penniston & Enyedi, 1998). The main functional difference with SERCAs is in their stochiometry (one Ca2+ transported per ATP hydrolyzed, while SERCA it is 2:1), and in the modulation of PCA activity by calmodulin. In the presence of

Ca2+:calmodulin, PMCA's myoplasmic Ca2+-binding KD is around 0.5 uM, while in its absence KD rises to > 1 uM. This implies that the pumps will have their activity reduced at resting [Ca2+]i therefore final bilance of fluxes at rest will depend to a greater degree on the other mechanism of active transport, Na+/Ca2+ exchange.

In most tissues the exchanger (of which there are isoforms NCX1, 2 and 3) operates at fixed stochiometry of 1 Ca2+ to 3 Na+. This exchamge is electrogenic rather than electroneutral, hence it is affected by membrane voltage. Near resting conditions it will extrude Ca2+ from the cell, but it becomes an influx pathway at positive voltages (reviewed by Gonzalez &Eduardo Rios, 2003) Because resting Vm (-90 mV) is more negative than ENa/Ca there will be a driving force to propel an outward current trough the exchanger. In other words, at resting membrane potential the exchanger will carry out active extrusion of Ca2+, sufficient to bilance some passive leak.

In addition to this role in setting resting [Ca2+], it may contribute significantly to Ca2+ removal after a transient in twitch muscle (Cifuentes et al., 1998). It appears, however, that the Na+/Ca2+ exchanger may play a greater role in contraction-related Ca2+ signaling in tonic muscle, as well as in slow-twitch fibers (reviewed by Blaustein and Lederer, 1999).

2) Sarcoplasmic Reticulum: Functional and structural role of Calsequestrin

The gradient of [Ca2+[between the lumen of the SR and the myoplasm is mantained by its Ca pumps. Isoforms SERCA1 (in its splice variant a) is the main contributor in adult fast twitch muscle fibres, while SERCA2a dominates in slow-twitch, cardiac and neonatal muscle (Brandl et al, 1987). A third isoform is also present in skeletal muscle. Inward Ca transport is matched 1:1 by H+ countertransport, and is hence electrogenic. Beacuse the SR membrane is leaky to many ions, this electric imbalance does not bilt up potential differences. It will alkalinize the SR lumen, however, which may play a role to balance the counterflow of protons associated with Ca2+ release (Kamp et al, 1998).

To evaluate the driving forces of Ca2+ release it is necessary to monitor [Ca2+] in the SR lumen. Detailed measurements were carried out by Chen

et al (1996) in heart using NMR and [Ca2+]SR was found near 1.5 mM, which is consistent with estimates of Inesi (1994) based on the sharp negative effects on ATP-ase rate upon increasing luminal [Ca2+] above 2 mM. The concentration gradient driving Ca2+ release is therefore of almost exactly four order of magnitudo, from 1.5 mM inside the SR to 150 nM in the myoplasm. In frog fast-twitch muscle, where stereologic (Mobley & Eisenberg, 1975) and functional measurements have been carried out in detail, the terminal cisternae (TC) of SR correspond to 4% of cell volume. The SR total calcium content, estimated at 2.5 mmoles/liter of fiber aqueous volume (Pape et al., 1995) is largely bound to buffers. The concentration of total Ca in the SR can be calculated as 2.5 mM x aqueous fiber volume (0.7 of total volume), or 43.75 mM. The buffer capacity is hence 43.75 mM or about 30. This buffer capacity is the role of calsequestrin (MacLennan and Wong, 1971) and others minor Ca2+ SR binding proteins. Calsequestrin (Csq) is located in the terminal cisternae of the SR (Meissner, 1975), where it forms multimeric chains visibile as electron-dense structures near the Ca2+ release channels, connected by thin “anchoring filaments” to the Ca2+ release channels. Triadin (Caswell et al, 1991) and junctin (Jone set al, 1995) are homologous proteins with a luminal C terminus. It appears that both proteins, separately or together, are part of the anchoring system, constituting both a link that position Csq and a conduit that directs flow of Ca2+ from buffer channels (Knudson et al, 193; Zhang et al, 1997).

Csq contains multiple low affinity binding sites fro Ca2+. Its stochiometry and affinity are somewhat ill-defined (KD is roughly in the mM range), as protein molecules tend to form multimers in Ca2+-dependent process that provides new binding sites of progressively lower affinity as [Ca2+] increases (Wang et al, 1998). In any case, Csq high capacity, low affinity, rapid equilibration rates, and strategic location, appear to be carefully designed to mantain [Ca2+]SR nearly clamped during release of a substantial portion of the SR Ca2+ content. There are indications that Csq may have dynamic interaction, including a change in its Ca2+ affinity upon RyR activation (Ikemoto et al, 1991) and reciprocal changes in channel activity might be induced by Csq (Szegedi et al, 1999).

Moreover, we have recently demonstrated (Paolini et al, 1997) an essential role of Csq in reorganizing stores and an impaired calcium handling in mice lacking Csq1, as presented in chapter 1.

Considering the role of Csq in potentially pathogenic conditions, where the protein carried out mutations or is totaly lacking, we described, in charter 2, that the mutation or the absence of this sarcoluminal calcium binding protein, together with heat and anaesthesia stress, cause a lethal crisis (malignan hyperthermia like phenotype) in Csq1 null mice. Our data suggest that Csq1 may result in a myopathy similar to that caused by mutations of RyR1 in skeletal muscle, leading to *fulminant malignant hyperthermia (MH) episodes.*

3. Ankyrins and organization of sarcoplasmic reticulum

How proteins are sorted into specialized domains of the sarcoplasmic reticulum, like the junctional region of the terminal cisternae or the longitudinal tubules, is not clear. A role for ankyrins in the localization of the proteins participating in the regulation of intracellular Ca2+ homeostasis in striated muscles was initially proposed by Tuvia et al. (1999). Ankyrins are a family of ubiquitously expressed proteins that participate in the organization of specific membrane domains by linking specific proteins on the plasma membrane with the sub plasma membrane cytoskeleton (Bennet et al., 2001). Vertebrate genome contains three ankyrin genes: Ank1 , Ank2 , and Ank3 , which encode proteins named originally Ankyrin-R, Ankyrin-B, and Ankyrin-G. Ankyrin gene products are often co-expressed within the same tissue and cells where they seem to have divergent and non-over- lapping functions. The primary structure of ankyrins can be divided in at least three common structural domains (membrane-binding domain, spectrin-binding domain, and death domain), where they share a high degree of sequence similarity. These proteins are, however, quite divergent in their C-terminal regulatory domains. Transcripts of all three ankyrin genes undergo a regulated splicing processing which results in the generation of several specific ankyrin isoforms from each gene.

In addition to their primary localization on the plasma membrane, specific ankyrin isoforms have been found to associate also with the membrane of intracellular organelles such as Golgi, lysosomes and the sarcoplasmic reticulum (Kordeli et al., 1999; gagelin et al., 2002). In striated muscles, ankyrins have been detected at specific sites, including costameres, the postsynaptic membrane and triads (Peters et al., 1995). More recent studies with ank2 deficient mice have better defined the role of this isoform in the localization of proteins involved in Ca2+ homeostasis, and especially of the InsP3 receptors at specific domains of the sarcoplasmic reticulum (Mohler et al., 2004b).

Cardiomyocytes derived from ankyrin-B+/- and ankyrin- B -/- mice display abnormal spontaneous contraction rates and abnormal Ca2+ dynamics

that may be caused by displacement of the ankyrin-B from the T-tubule/ sarcoplasmic reticulum sites. Indeed, cardiomyocytes from ankyrin-B+/- and ankyrin-B-/- mice present a reduction, in the T-tubule region, of proteins such as the Na/K ATPase, Na/Ca2+ exchanger, and inositol 1,4,5 trisphosphate (InsP 3) receptor (Mohler et al., 2004a)Since all of these proteins are known to bind ankyrin-B, it would appear that a role of ankyrin B is to favor the assembly of a complex of proteins responsible of Ca2+ homeostasis at the T-tubule region (Mohler et al., 2003). Accordingly, it has been postulated that reduction of the Na/K ATPase, by causing an increased intracellular Na content, would increase exchange of intracellular Na for extracellular Ca2+ by the Na/Ca2+ exchanger, thus resulting in the elevated Ca2+ transients observed in ankyrin B -/- cardiomyocytes. Interestingly, these studies in ankyrin-B -/- mice have provided a good experimental model to understand the molecular basis of an inherited cardiac arrhythmia (long QT syndrome type 4) reported in a family in which a mutation in the ANKB gene has been found (Mohler et al., 2003). Patients carrying ankyrin-B mutations display varying degrees of cardiac dysfunction including bradycardia, sinus arrhythmia, idiopathic ventricular fibrillation, catecholaminergic polymorphic ventricular tachycardia, and risk of sudden death. Similar symptoms can be observed in ankyrin-B +/- mice.

In striated muscles, a precise localizati of the sarcoplasmic reticulum relative to myofibrils is observed whereby the sarcoplasmic reticulum surrounds the myofibrillar apparatus forming a sleeve-like structure that favours a close apposition between the Ca2+ stores and the contractile apparatus (Franzini-Armstrong, 1994). The highly regulated nature of the arrangement of the sarcoplasmic reticulum around myofibrils is such that specific domains of the sarcoplasmic reticulum involved in the mechanisms of Ca2+ release and uptake (i.e., terminal cisternae and longitudinal tubules, respectively) are positioned at regular intervals in correspondence of specific regions of the sarcomere (Franzini-Armstrong, 1994)..

In this way, junctional complexes like diads and triads are positioned in correspondence of either the junction between the A-I bands or of the Z disk, as observed in skeletal and cardiac muscles of mammals,

respectively (Franzini-Armostrong, 1994; Veratti, 1902). However, although the precise localization of the sarcoplasmic reticulum with respect to myofibrils has been known since decades, the molecular mechanism(s) responsible of the interactions between these two cellular structures is not known (Meldolesi et al., 1998; Franzini-Armostrong, 1994; Veratti, 1902;). A set of muscle-specific transcripts of the ank1 gene has been identified in striated muscles (Birkenmeier et al., 1998). These transcripts encode characteristic muscle-specific ank1 isoforms that lack both membrane and spectrin binding sequences and retain only a short sequence from the COOH-terminus of the large ankyrin 1 (Gallagher et al., 1997). The NH2-terminal portion of these small muscle-specific Ank1 isoforms contains a transmembrane domain that anchors these proteins to the sarcoplasmic reticulum membrane, while the remaining amino acid sequence extends in the cytosol (Birkenmeier et al., 1998). Immunostaining of adult skeletal muscle has shown that small Ank1 isoforms are targeted to specific domains of the sarcoplasmic reticulum in correspondence of the Z-disks and M lines of the contractile apparatus (Zhou et al., 1997).

Studies aimed at identifying a possible cytosolic interacting protein for the small muscle-specific ankyrins have shown that one small muscle-specific ank1 isoform (ank1.5) is capable of interacting with the C-terminus of Obscurin (Bagnato et al., 2003). Obscurin is a recently identified muscle protein known to bind titin (Young et l., 2001). Obscurin is an extremely large protein characterized by a modular architecture that contains multiple immunoglobulin-like (Ig-like) domains, two fibronectin-like (FN3-like) domains, and a RhoGEF/PH domain. Additional transcripts of Obscurin have been detected that may also contain one or two serine-threonine kinase domains (Bang et al., 2001). The modular structure of Obscurin makes this protein a very good candidate for mediating multiple interactions both within the myofibrils and with other cellular structures (Sanger et al., 2002).

The interaction between ank1.5 and Obscurin is mediated by an amino acid sequence present in ank1.5, but not in other small ank1 proteins (e.g., ank1.6 and ank1. 7). On his own, ank1.5 recognizes a specific sequence present in the non modular region at the C- terminus of

Obscurin (Bagnato et al., 2003). Transfection of plasmids encoding ank1.5 and a fusion protein consisting of the C-terminus of Obscurin cloned in frame with the Green Fluorescent Protein resulted in the association of GFP- Obscurin with the endoplasmic reticulum. In cultured skeletal muscle cells ank1.5 was detected near or at the M line where it colocalizes with Obscurin. Localization of ank1.5 at the M line required the presence of an intact Obscurin-binding site since a mutation in this sequence prevented the localization of ank1.5 at the M line. These data are compatible with a model where these two proteins may contribute to holding a stable interaction between the sarcoplasmic reticulum and the myofibrils (Bagnato et al., 2003).

In conclusion, during the past few years, molecular techniques have helped to identify new genes encoding proteins that may participate in the formation of junctional complexes between the sarcoplasmic reticulum and the plasma membrane T-tubule system. In addition, there is initial evidence that cytoskeletal proteins may interact with proteins on the sarcoplasmic reticulum and help in assembling specific protein complexes required in the formation of stable interactions between the contractile apparatus and the sarcoplasmic reticulum. On this basis it can be expected that in the near future a more detailed understanding of the molecular mechanisms underlying the sub cellular organization of the sarcoplasmic reticulum shall be available (reviewed by Sorrentino, 2004). In our present work, in chapter 3 of this thesis, we present evidence of contractile response impairment in skeletal muscles of Ank1.5 deficient mices. Unexpectedly, Ank 1-5 null mices do not present any structural changes both at morphological and ultrastructural levels. On the other side, functional studies at whole animal and single muscle level clearly show differences in force and kinetics with a muscle specific distribution. Animals appear to be less coordinated and less resistant to exhaustion, while limb force is unaffected. According to our observation, Ank1.5 appears to play a functional role rather than structural, participating in the complex regulation of EC coupling patways.

4) **A new approach with hybrid cell-semiconductor device for single cell investigtion of calcium signals in a EC coupling dependent muscle plasticity: a satellite cells, myotubes and muscle fibers study.**

Neuro-electronics offers new avenues to biological investigation and application to excitable tissues, both in vitro and in vivo. In particular the studies, initiated at the beginnings of '90s (Fromherz at al., 1991) on interfacing neurons with semiconductors, have offered a new bio-electronics approach in terms of spatial resolution up to microscale and non-invasive two way interactions with cells.

Coupling without electrochemical process ion-conducing cells and electron-conducing semiconductor relies on a close contact between the cell membrane and the oxidised silicon with a high resistance of the junction and a high conductance of the attached membrane. Several studies in this direction have been progressed towards a neuron-semiconductor hybrid junction(Fromherz, 2006; Prasad et al., 2003; Micheal, 1999,) where neuronal excitation can be elicited and recorded from the chip by capacitive contacts and by field-effect transistors with an open gate (Fromherz, 2006).

In this model to obtain a perfect coupling between the two dielectrics, the lipid core of a cell membrane and the silicon dioxide should be fully attached (Fromherz, 2002). However in practical terms they are never in close contact, but a distance in between is created by dangling polymer molecules that protrude from the membrane (glycocalix) and that are deposited on the chip (Gleizner and Fromherz, 2006). They give rise to repulsive entropic forces that balance the attractive forces of cell adhesion between the integrins in the membrane and collagen, laminin and other molecules deposited on the silicon surface and a cleft is formed in the junction.

Such an approach was never applied to skeletal muscle cells, even if cardiac muscle cells were studied with non invasive recording and stimulation using microelectrodes arrays and field effect transitors arrays.

To perform a deeper study of the development of the skeletal muscle cells, and in particular to better explore calcium signals in the context of EC coupling, we developed a muscle-cell / semiconductor chip device to

induce EC coupling with non invasive long termed electric capacitive stimulation. We present here in chapter 4 of this thesis the model and in vitro results with single myotubes and muscle muscle fibers. Extracting satellite cells from hind limbs of wild type and knock out mices and plating/differentiating them on the chip, mature myotubes coupled with the semiconductor can be achieved. We present here for the first time a new technique to study live EC coupling and Calcium signals in long term and with high resolution, down to single cells, to induce muscle plasticity and synaptogenesis effects. The same approach is used for muscle fibers dissociated from mouse FDB muscle. To conclude, our hybrid device put an innovative base for new approach aimed to better understand the muscle development and regeneration in normal and pathogenic conditions.

REFERENCES

1. Aderto JM, Steihardt RA (2000) Calcium influx trough calcium leak channels is responsible for the elevated levels of calcium-dependent proteolysis in dystrophic myoubes. *J Biol Chem* 275:9452-60

2. P. Bagnato, V. Barone, E. Giacomello, D. Rossi, V. Sorrentino, Binding of an Ankyrin-1 isoform to the C-terminus of Obscurin identifies a molecular link between the sarcoplasmic reticulum and myofibrils in striated muscles, *J. Cell Biol*. 160 (2003) 245 – 253

3. Bang M.L., T. Centner, F. Fornoff, A.J. Geach, M. Gotthardt, M. McNabb, C.C. Witt, D. Labeit, C.C. Gregorio, H. Granzier, S. Labeit, The complete gene sequence of titin, expression of an unusual c700- kDa titin isoform, and its interaction with obscurin identify a novel Z- line to I-band linking system, Circ. Res. 89 (2001) 1065 – 1072.

4. Baylor SM and Hollingworth S (2000) Measurements and interpretationof cytoplasmic [Ca2+] signals from calcium-indicatoes dyes. *News Physiol. Sci*. 15:19-26.

5. Bennet V, Baines AJ (2001) Spectrin and ankyrin-based pathways: metozan invections for integratine cells tissues. *Physiol Rev* 81 1352-1292.

6. Blaustein and Lederer (1999) Sodium/Calcium Exchange: Its Physiological ImplicationsPhysiological Review 79 792

7. Birkenmeier C.S., J.J. Sharp, E.J. Gifford, S.A. Deveau, J.E. Barker (1998) An alternative first exon in the distal end of the erythroid ankyrin gene leads to production of a small isoform containing an NH2-terminal membrane anchor, Genomics 50 79 – 88.

8. Brandl CJ, deLeon S, Martin DR, MacLennan DH (1987) Adult forms of the Ca2+ ATPase os sarcoplasmic reticulum. Expression in developing skeletal muscle. *J Biol Chem* 262: 3768-74.

9. Chen W, Steenbergen C, Levy LA, Vance J, London RE, Murphy E. (1996) Measurements of free Ca2+ in sarcoplasmic reticulum in perused rabbit heartloaded with 1,2-bis(2-amino-5,6-difluorophenoxy)ethane-N,N,N',N'-tetraacetic acid by 19F NMR. *J Biol Chem* vol. 271 (13) pp7398-4

10. Du A., J.M. Sanger, K.K. Linask, J.W. Sanger, (2003) Myofibrillogenesis in the first cardiomyocytes formed from isolated quail precardiac mesoderm, Dev. Biol. 257 382 – 394.

11. Franzini-Armstrong, C., Protasi, F., and Ramesh, V. (1998*). Ann N Y Acad Sci*. 853:20-30.

12. Franzini-Armstrong C., The sarcoplasmic reticulum and the transverse tubules, in: A.E. Engel, C. Franzini-Armstrong (Eds.), Myology, vol. 1, McGraw-Hill, New York, USA, 1994, pp. 176 – 199.

13. Fromherz P (2006) Three levels of neuroelectronic interfacing: silicon chips with ion channels, nerve cells, and brain tissue. *Ann N Y Acad Sci* vol. 1093 pp 143-60.

14. Fromherz P, Offenhäusser A, Vetter T, Weis J. (1991) A neuron-silicon junction: a Retzius cell of the leech on an insulated-gate field-effect transistor, Science May 31;252(5010):1290-3

15. Gallagher P.G., B.G. Forget, (1998) An alternate promoter directs expression of a truncated, muscle-specific isoform of the human ankyrin 1 gene, *J. Biol. Chem.* 273 1339-1348.

16. Gallagher P.G., W.T. Tse, A.L. Scarpa, S.E. Lux, B.G. (1997) Forget, Structure and organization of the human ankyrin-1 gene, *J. Biol. Chem*. 272 19220 – 19228.

17.

18. Gagelin C., B. Constantin, C. Deprette, M.A. Ludosky, M. Recouv-reur, J. Cartaud, C. Cognard, G. Raymond, E. Kordeli (2002) Identification of AnkG107, a muscle-specific ankyrinG isoform, *J. Biol. Chem.* 277 12978 – 12987.

19. Gregorio C.C., H. Granzier, H. Sorimachi, S. (1999)Labeit, Muscle assembly: a titanic achievement? Curr. Opin. Cell Biol. 11 18 – 25.

20. Gonzalez A and Rios E (2003) Molecular Control Mechanism in Striated Muscle. Solaro and Moss ed.

21. Kamp F, Donoso P, Hidalgo C (1998) Changes in luminal pH caused by calcium release in sarcoplasmic reticulum vesicles *Biophys J* vol. 74 (1) pp.290-6

22. Kontrogianni-Konstantopoulos A., E.M. Jones, D.B. van Rossum, R.J. Bloch, Obscurin is a ligand for small ankyrin 1 in skeletal muscle, Mol. Biol. Cell 14 (2003) 1138 – 1148.

23. Kordeli E., M.A. Ludosky, C. Deprette, T. Frappier, J. Cartaud, (1998) AnkyrinG is associated with the postsynaptic membrane and the sarcoplasmatic reticulum in the skeletal muscle fiber, *J. Cell Sci.* 111 2197 – 2207.

24. Kordeli E, Ludosky MA, Deprette C, Frappier T, Cartaud (1993) Ankyring is associated with the postsynaptic membrane and the 3' ends are found among transcripts of the erythroid ankyrin gene. *J. Biol. Chem* 268 (1993) 9533-9540.

25. Inesi G (1994) Teaching active transport at the run of the twenty-first century: recent discoversies and conceptual changes. *Biophys J*. 66:554-60.

26. MacLennan D H, Wong P T (1971) Isolation of a calcium-sequestering protein from sarcoplasmic reticulum. Proc Natl Acad Sci USA. Vol. 68 (6) pp 1231-5.

27. Meldolesi J., T. Pozzan (1998), The heterogeneity of ER Ca2+ stores has a key role in nonmuscle cell signaling and function, *J. Cell Biol.* 142 1395 – 1398.

28. Meissner G., (1994). Ryanodine receptor/Ca++ release channels and their regulation by endogeneous effectors. *Annu Rev Physiol*. 56:485-508.

29. Meissner G (1975) Isolation and characterization of two types of sarcoplasmic reticulum vesicles. *Biochim Biophys Acta* vol 389 (1) pp 51-68.

30. MichaelP. Maher[a,] , Jerome Pine[b], John Wright[c] and Yu-Chong Tai[c] (1999) The neurochip: a new multielectrode device for stimulating and recording from cultured neurone, Journal of Neuroscience Methods V. 87 1 February 1999, P 45-56.

31. Mobley BA, Eisenberg BR (1975) Sizes of components in frog skeletal muscle measured by methods of stereology. *J Gen Physiol*, vol. 66(1) pp. 32-45.

32. Mohler P.J., J.Q. Davis, L.H. Davis, J.A. Hoffman, P. Michaely, V. Bennett, (2004a) Inositol 1,4,5-Trisphosphate receptor localization and stability in neonatal cardiomyocytes requires interaction with ankyrin- *B, J. Biol. Chem*. 279 12980 – 12987.

33. Mohler P.J., J.A. Hoffman, J.Q. Davis, K.M. Abdi, C.-R. Kim, S.K. Jones, L.H. Davis, K.F. Roberts, V. Bennett, (2004b) Isoform specificity among ankyrins, *J. Biol. Chem*. 279 25798 – 25804.

34. Mohler P.J., J.-J. Schott, A.O. Gramolini, K.W. Dilly, S. Guatimosim, W.H. duBell, L.-S. Song, K. Haurogne´ , F. Kyndt, M.E. Alı `, T.B. Rogers, W.J. Lederer, D. Escande, H. Le Marec, V. Bennett, (2003) Ankyrin- B mutation causes type 4 long-QT cardiac arrhythmia and sudden cardiac death, *Nature* 421 634 – 639.

35. Paolini C, Quarta M, Nori A, Boncompagni S, Canato M, Volpe P, Allen PD, Reggiani C, Protasi F (2007) Reorganized stores and impaired calcium handling in skeletal muscle of mice lacking calsequestrin-1 *J Physiol (Lond)* vol. 583 (pt2) 267-84.

36. Pape PC, Jong DS, Chandler WK (1995) Calcium release and its voltage dependance in frog cut muscle fibers equilibrated with 20 mM EGTAA, *J Gen Physiol*. 106:259-336.

37. Penniston J T, Enyedi A (1998) Modulation of the plasma membrane Ca2+ pump. *J Membr Biol.* Vol 165 (2) pp. 101– 9.

38. Pessah IN, Waterhouse AL, Casida JE. (1985) The calcium-ryanodine receptor complex of skeletal and cardiac muscle. *Biochem Biophys Res Commun*. Apr 16;128 (1)

39. Peters L.L., K.M. John, F.M. Lu, E.M. Eicher, A. Higgins, M. Yialamas, L.C. Turtzo, A.J. Otsuka, S.E. Lux, (1995) Ank3 (Epithelial Ankyrin), a widely distributed new member of the ankyrin gene family and the major ankyrin in kidney, is expressed in alternatively spliced forms, including forms that lack the repeat domain, *J. Cell Biol*. 130 313 – 330.

40. Prasad S, Yang M, Zhang X, Ozkan CS, Ozkan M (2003) Electricl Field assisted patterning of Neuronal Netorks for the Study of Brain Functions*. Biomedical Microdevices* 5:2, 125-137.

41. Rosenberg R L, P Hess, R W Tsien (1988) Cardiac calcium channels in planar lipid bilayers. L-type channels and calcium-permeable channels open at negative membrane potentials. *J. Gen. Physiol*. 1988 p2752

42. Russel M.W., M.O. Raeker, K.A. Korytkowski, K.J. Sonneman, (2002) Identification, tissue expression and chromosomal localization of human Obscurin-MLCK, a member of the titin and Ddl families of myosin light chain kinases, *Gene* 282 237 – 246.

43. Sandow A (1952). "Excitation-contraction coupling in muscular response.". *Yale J Biol Med* **25** (3)

44. J.W. Sanger, P. Chowrashi, N.C. Shaner, S. Spalthoff, J. Wang, N.L. Freeman, J.M. Sanger, (2002) Myofibrillogenesis in skeletal muscle cells*, Curr. Orthop. Relat. Res*. 403S S153 – S162.

45. Schatzmann H J (1989) Asymmetry of the magnesium sodium exchange across the human red cell membrane. *Biochim Biophys Acta*. 1993 p 2831.

46. Schneider MF, Chandler WK. (1973) Voltage dependent charge movement of skeletal muscle: a possible step in excitation-contraction coupling. *Nature*. Mar 23;242, 5395

47. Smith JS, McKenna EJ, Ma JJ, Vilven J, Vaghy PL, Schwartz A, Coronado R. (1987) Calcium channel activity in a purified dihydropyridine-receptor preparation of skeletal muscle Nov *Biochemistry*.3;26(22):7182-8.

48. Sorrentino V (2004) Molecular determinants of the structural and functional organization of the sacroplasmic reticulum. *Biochim Biophys Acta* vol. 1742 (1-3) pp-113-8 1585 – 1596.

49. Stromer M.H., (1998) The cytoskeleton in skeletal, cardiac and smooth muscle cells, *Histol. Histopathol*. 13 283 – 291.

50. Takeshima H, Yamazawa T, Ikemoto T, Takekura H, Nishi M, Noda T, Iino M. (1995) Ca(2+)-induced Ca2+ release in myocytes from dyspedic mice lacking the type-1 ryanodine receptor. *EMBO J*. Jul 3;14(13):2999-3006.

51. Trinick J., L. Tskhovrebova, (1999) Titin: a molecular control freak, *J. Cell Biol*. 9 377 – 380.

52. Tuvia S, Buhusi L, Davis M, Bennet V (1999) Ankyrin-B is reguired for intracellular sorting of structurally diverse Va2+ homeostasis proteins. *J Cell Biol* 147 995-1007.

53. Veratti E., Ricerche sulla fine struttura della fibra muscolare striata, Mem. Ist. Lomb. Cl. Di Sc. Matem. E Nat. 19 (1902) 87 – 133.

54. Young P., E. Ehler, M. Gautel, (2001) Obscurin, a giant sarcomeric Rho guanine nucleotide exchange factor protein involved in sarcomere assembly, J. Cell Biol. 154 123 – 136.

55. Zhou, C.S. Birkenmeier, M.W. Williams, J.J. Sharp, J.E. Barker, R.J. Bloch, (1997) Small, membrane-bound, alternatively spliced forms of ankyrin 1 associated with the sarcoplasmatic reticulum of mammalian skeletal muscle, *J. Cell Biol*. 136 621 – 631

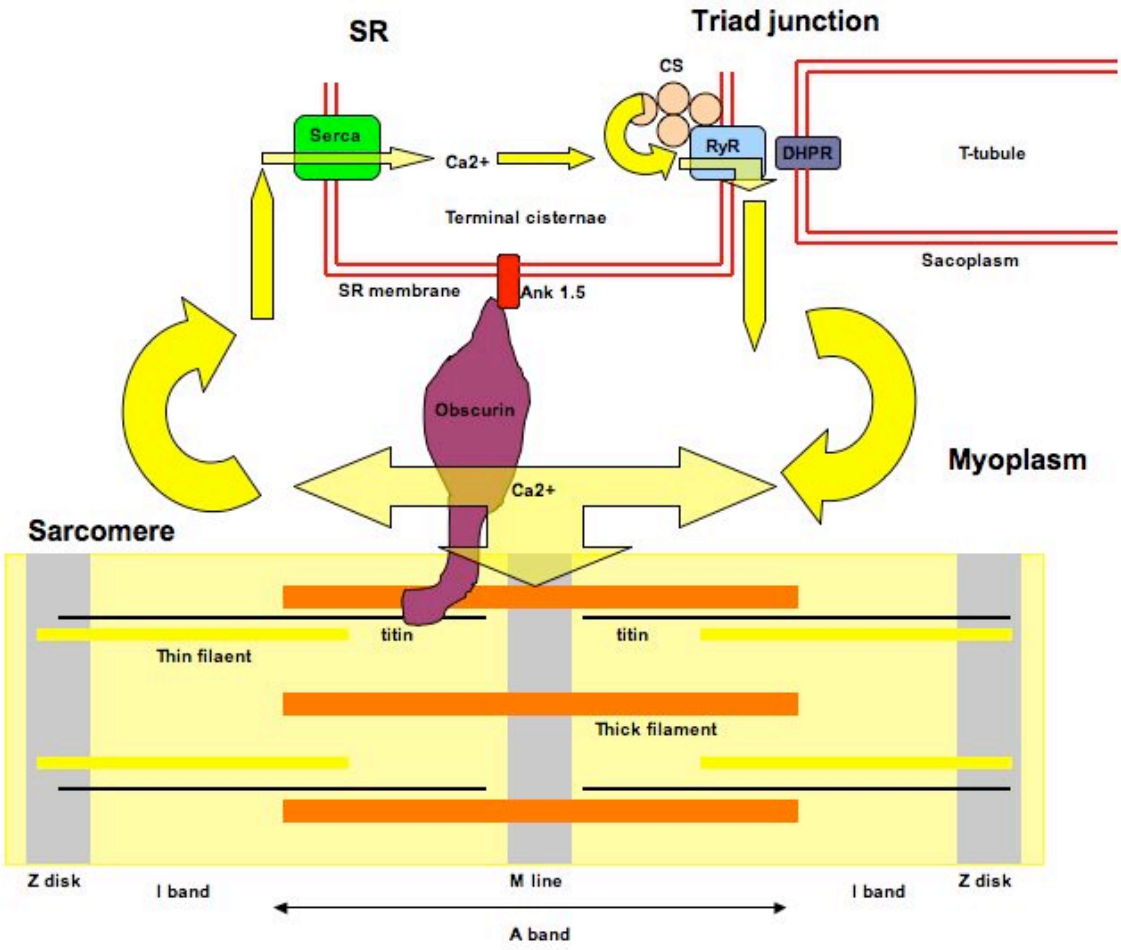

Fig 1 EC coupling multicomplex. Schematic rappresentation of calcium pathway in a EC coupling event within a triad. Terminal Cisternae is couppled to the sarcoplasm trough the RyR-DHPR interaction, and to the myofibril trough the Ank1.5-obscurin-titin binding which contributes in the correct positioning of the calcium releasing appartus on the sarcomere, at M line and Z disk regione. Calcium is released in the myoplasm by RyR after the DHPR signal trasduction, it induces contration on the myofibrils leading to twich events, and immediately reuptaked by SERCA within the SR where it buffered by CS.

CHAPTER 1

RE-ORGANIZED STORES AND IMPAIRED CALCIUM HANDLING IN SKELETAL MUSCLE OF MICE LACKING CALSEQUESTRIN-1.

Authors:

[1]Cecilia Paolini, [2]**Marco Quarta**, [3]Alessandra Nori, [1]Simona Boncompagni, [2]Marta Canato, [3]Pompeo Volpe, [4]Paul D. Allen, [2]Carlo Reggiani, and [1]Feliciano Protasi.

Affiliations:

[1,2,&3]IIM Interuniversity Institute of Myology; [1]Ce.S.I. Centro Scienze dell'Invecchiamento, University G. d'Annunzio, I-66013 Chieti Italy; [2&3]Dept. of Anatomy and Physiology and Dept. of Biomedical Sciences, University of Padova, I-35131 Padova Italy; [4]Dept. of Anaesthesia Research, Brigham and Women's Hospital, 02115 Boston MA.

Published in J Physiol (Lond) - 2007 vol. 583 (Pt 2) pp. 767-84

ABSTRACT

Calsequestrin (CS), the major Ca^{2+}-binding protein in the sarcoplasmic reticulum (SR), is thought to play a dual role in excitation-contraction coupling: buffering free Ca^{2+} increasing SR capacity, and modulating the activity of the Ca^{2+} release channels (RyR). In this study, we generated and characterized the first murine model lacking the skeletal CS isoform (CS1). CS1-*null* mice are viable and fertile even though skeletal muscles appear slightly atrophic compared to the control mice. No compensatory increase of the cardiac isoform CS2 is detectable in any type of skeletal muscle. CS1-*null* muscle fibers are characterized by structural and functional changes, which are much more evident in fast-twitch muscles (EDL) in which most fibers express only CS1, than in slow-twitch muscles (Soleus), where CS2 is expressed in about 50% of the fibers. In isolated EDL muscle, force development is preserved, but characterized by prolonged time-to-peak and half-relaxation time, likely related to impaired calcium release from and re-uptake by the SR. Ca^{2+} imaging studies show that the amount of Ca^{2+} released from the SR and the amplitude of the Ca^{2+} transient are significantly reduced. The lack of CS1 also causes significant ultrastructural changes, which include: a) striking proliferation of SR junctional domains; b) increased density of Ca^{2+}-release channels (confirmed also by ^{3}H-ryanodine binding); c) decreased SR terminal cisternae volume; d) higher density of mitochondria. Taken together these results demonstrate that CS1 is essential for the normal development of the SR and its calcium release units and for the storage and release of appropriate amounts of SR Ca^{2+}.

INTRODUCTION

Calcium ions (Ca^{2+}) are extremely versatile second messengers. Transient elevations of intracellular Ca^{2+} concentration ($[Ca^{2+}]_i$) play an important role in virtually all cell types and in many cellular functions: these processes include cell differentiation, gene transcription, generation of muscle force and metabolic regulation (Dolmetsch, 2003; Gerke *et al.*, 2005). In striated muscles, the changes in $[Ca^{2+}]_i$ that regulate myofibril function are caused by a large rapid Ca^{2+} release from internal stores, i.e., sarcoplasmic reticulum (SR), that follows depolarization of exterior membranes. The mechanism that links sarcolemmal depolarization to Ca^{2+} release is known as excitation-contraction (EC) coupling (Sandow, 1965; Schneider & Chandler, 1973; Rios *et al.*, 1991), and is governed by a coordinated interaction among several proteins localized in highly specialized intracellular junctions named Ca^{2+} release units (CRUs).

In skeletal muscles, CRU is a highly specialized system that finely controls the release and uptake of Ca^{2+} from the SR during muscle contraction and relaxation (Schneider, 1994; Protasi, 2002). In CRUs, two separate and well-organized membrane systems come in close contact with one another: the exterior membranes, i.e. sarcolemma and/or transverse-tubules (T-tubules), and the internal membranes, i.e. the SR. Several proteins are specifically localized in correspondence of these structures: the sarcolemmal slow voltage gated L-type Ca^{2+} channel (dihydropyridine receptor, DHPR), the SR Ca^{2+} release channel (ryanodine receptor, RyR1), and calsequestrin (CS) are three of the key elements in the EC coupling machinery (MacLennan & Wong, 1971; Lai *et al.*, 1988; Jorgensen *et al.*, 1989). DHPRs, organized in ordered arrays of tetrads in the T-tubule membrane, are thought to be physically coupled to RyR1, which is clustered in ordered arrays in correspondence of the SR terminal cisternae (Franzini-Armstrong, 1970; Saito *et al.*, 1984; Block *et al.*, 1988; Protasi *et al.*, 1997; Protasi *et al.*, 1998; Protasi *et al.*, 2000). Calsequestrin, located in the SR lumen in close proximity to the junctional SR domains containing RyRs, is an acidic protein that binds Ca^{2+} with a moderate affinity, but with high capacity, concentrating it near the sites of Ca^{2+} release (Jorgensen *et al.*, 1983; Franzini-Armstrong *et al.*, 1987). Two isoforms of mammalian CS (Campbell *et al.*, 1983; Damiani *et al.*,

1990), which are products of two different genes, have been identified and characterized: a skeletal muscle and a cardiac muscle isoform, abbreviated CS1 and CS2 respectively. CS2 is the only isoform expressed in the heart at all developmental stages, whereas both cardiac and skeletal CS genes are differentially expressed in various skeletal muscles (Fliegel *et al.*, 1987; Scott *et al.*, 1988). In slow-twitch fibers, CS2, is the most abundant isoform in fetal and neonatal muscles and is co-expressed with CS1 at a 1:3 ratio in the adult (Damiani *et al.*, 1990). In fast-twitch fibers, on the other hand, CS2 disappears completely after birth and CS1 remains the only isoform in the adult (Sacchetto *et al.*, 1993).

Active Ca^{2+} transport is limited by the intraluminal free Ca^{2+} concentration (Makinose & Hasselbach, 1965; Weber *et al.*, 1966; Weber, 1971; Inesi & de Meis, 1989). CS functions as a buffer of Ca^{2+} in the SR lumen keeping the free concentration relatively low and thus allowing more efficient inward transport by the SERCA pumps. This is particularly important in fast-twitch fibers where the amount of Ca^{2+} released and taken up is much greater than in slow fibers (Fryer & Stephenson, 1996). The higher concentration of CS in fast fibers (Leberer & Pette, 1986; Leberer *et al.*, 1988) reflects its important role. CS has also been implied in modulating the activity of the SR Ca^{2+} release channels (Ikemoto *et al.*, 1989; Gilchrist *et al.*, 1992; Beard *et al.*, 2005; Dulhunty *et al.*, 2006), but the details of this modulation and whether it is essential during EC coupling remain to be determined. Both the activation (Kawasaki & Kasai, 1994; Ohkura *et al.*, 1995; Szegedi *et al.*, 1999; Herzog *et al.*, 2000), and the inhibition (Beard *et al.*, 2002) of RyRs by CS have been reported. Given a possible dual role of CS as Ca^{2+} buffer and RyR modulator, it is not surprising that up or down regulation of CS expression levels in alterations in Ca^{2+} release, Ca^{2+} reuptake as well of store stability (Terentyev *et al.*, 2003; Wang *et al.*, 2006). Initial evidence from *null* CS mutations in C. Elegans (Cho *et al.*, 2000) and in cardiac muscle (Knollmann *et al.*, 2006) would suggest that CS is not absolutely essential for muscle function. These studies, however, involved muscles in which Ca^{2+} entry from the extracellular space during activation is substantial. This leaves open the question about the importance of CS in the activity of fast twitch skeletal muscle fibers that derive all the calcium needed for contraction from their

internal stores. Can mammalian skeletal muscle fibers function in absence of CS, as it occurs in C. Elegans (Cho *et al.*, 2000)? Will lack of CS affect fast and slow twitch fibers, which are known to handle different amounts of Ca^{2+} and at different rates during EC coupling, equally? How does the absence of CS1 change the structure and molecular composition of the CRU?

To address these specific questions and to elucidate the functional and structural roles of CS1 in skeletal muscle fibers, we developed a CS1 knockout model (CS1-*null* mouse). CS1-*null* mice are viable and fertile, and develop normally under standard housing conditions. Analysis of the skeletal muscles of CS1-*null* mice reveals structural alterations of the CRU and significant functional impairment in calcium handling, substantiating an important role of CS1 in calcium homeostasis and revealing an important, probably indirect, structural regulation of the membranes involved in calcium release.

Abbreviations used in the manuscript. Ca^{2+}, calcium ions; CBPs, Ca^{2+}-binding proteins; CRU, Ca^{2+} release unit; CS, calsequestrin; CS1, skeletal isoform of CS; CS2, cardiac isoform of CS; DHPR, dihydropyridine receptor; EC coupling, excitation-contraction coupling; EDL, extensor digitorum longus muscle; EM, electron microscopy; MHC, myosin heavy chains; RyR, ryanodine receptor; SERCA, sarco-endoplasmic reticulum calcium ATPase; SR, sarcoplasmic reticulum; T-tubule, transverse tubule; WT, wild type.

MATERIALS AND METHODS

- Creation of the CS1-null mouse. The SMCALSE1 gene trap allele (Fig. 1 A) was generated, using random insertional mutagenesis with retroviral vector VICTR24, as part of the OmniBank gene trap database (Zambrowicz *et al.*, 1998). This vector generates fusion proteins of neomycin with the 5' end of the gene and a fusion with BTK at the 3' end of the gene, introducing premature stop signals that prevent translation of the protein product. The OST82566 clone was identified as the one containing the mutated SMCALSE1 gene within the embryonic stem cell library of the 129/SvEvBrd mouse, in which the gene trap vector was randomly

introduced (OmniBank Library, Lexicon Genetics). Inverse genomic PCR (Silver & Keerikatte, 1989), was used to determine that the gene-trap vector had integrated in the intron between exons 3 and 4 (Fig. 1 A). Listed below is a portion of the mouse genomic sequence (50 nucleotides of sequence on either side) surrounding the gene-trap insertion site, which is denoted with an asterisk * (see Fig. 1 A). 5'…GATGGGGGAAGGGTAGTTAGCAACAAGTCATCTGGACAGCAATA GCAAAG*AGTCAGCCACTAGATACTTCAGAGTCTCTGGCAGGAATATT TGTCCCTGG… 3' The SMCALSE1 *null* line was generated by microinjection of the OmniBank ES cell clone represented by OST82566 into host blastocysts, using standard methods. Chimeric mice resulting from the ES cell injections were bred to C57BL/6J albino mice for germline transmission of the SMCALSE1 mutation. Multiplex Quantitative real-time PCR was used to genotype knockout mice (Charles River Laboratories, Boston MA).

- CS1-null Animals. All experiments involving animals were conducted according to the National Institutes of Health Guide for the Care and Use of Laboratory Animals and were approved by the animal welfare coordinator of our institution. C57BL/6J mice were obtained from the Charles River Laboratories Boston, MA. Mice were maintained in an accredited animal care facility and examined daily. Mice were first euthanized by an overdose of the anesthetic ethylic ether and their muscles were rapidly dissected.

- Preparation of homogenate total membranes, electrophoresis, western blot analysis, and ^{3}H-Ryanodine binding experiments. *1) Preparation of total homogenates from Soleus and EDL skeletal muscles.* EDL and Soleus muscles from control and CS1-*null* mice were homogenized in 3% SDS , 1mM EGTA, boiled for 5 min and centrifuged at 900g for 15 min. The protein concentration of the supernatants was quantified as described (Lowry *et al.*, 1951)*. 2) Western blot analysis.* For each sample, 20µg of total protein were loaded on a 8 or 10% SDS-polyacrylamide gel, electrophoresed and transferred to nitrocellulose. Immunostaining of blots was performed using the following primary antibodies: monoclonal antibody for SERCA1 (Affinity Bioreagents, USA), rabbit polyclonal antibody reactive with both isoforms of CS (Affinity

Bioreagents, USA); rabbit affinity-purified TRN6 antibody raised against residues 146-160 of mouse triadin (generous gift of L. A. Jones); secondary antibodies were anti-mouse or anti-rabbit AP-conjugated antibodies (SIGMA, Italia), respectively. Densitometric scans were analyzed with Scion Image Software to quantify protein band intensities. Normalization was performed with anti-GAPDH antibody (Abcam, UK) or total protein concentration for CS and SERCA1 with consistent results. Quantification of the signal for the 95kDa isoform of triadin and normalization to Ponceau Red staining was performed using QuantityOne Software from BioRad Laboratories (Hercules, CA). *3) Total membranes preparation*. Total membrane (TM) were prepared from a pool of ten-to-twelve EDL muscles from either WT or CS1-*null* animals, as described (Damiani *et al.*, 1991). *4) ^{3}H-ryanodine binding.* Bound ^{3}H-ryanodine was determined as described (Zorzato *et al.*, 1989).

- Cryostat sectioning and immunohistochemistry. EDL and Soleus muscles were dissected from both CS1-*null* and WT mice (4 to 9 months of age) and wrapped in a small piece of bovine liver. The samples were then frozen in liquid nitrogen and cryoprotected with Tissue-Tek II OCT compound (Miles Inc. USA). Transverse sections 10-12 μm thick were cut in a Leica cryostat (CM 1850, Leica Microsystem, Austria) and fixed with 0.8% para-formaldehyde. Sections were then blocked with 1% BSA and 10% goat serum in PBS to avoid non-specific detection and incubated with primary antibodies for 2h followed by secondary antibodies for 1h both at room temperature (CY3 conjugated goat anti-mouse and goat anti-rabbit, Jackson ImmunoResearch Laboratories, Lexington, KY). The specimens were viewed on a fluorescence microscope (Leica DMLB) or a confocal microscope (LS510 META or LSM 5 Pascal, Zeiss, Germany). The following primary antibodies were used: pAB, reactive with both CS1 and CS2, diluted at 1:800; 4B1, specific for CS1, 1:400 (Jones *et al.*, 1998); BA-F8 monoclonal antibody specific for myosin heavy chain (MHC) slow, supernatant diluted at 1:10; SC-71 monoclonal antibody, specific for myosin heavy chain IIA, supernatant diluted at 1:40 (Schiaffino *et al.*, 1989). pAB and 4B1 were a generous gift of L. A. Jones, BA-F8 and SC-71 were a generous gift of S. Schiaffino.

- Force and contraction kinetics of isolated intact Soleus and EDL. Soleus and EDL muscles were dissected from hind limb of WT and CS1-*null* mice in warm oxygenated Krebs solution and mounted between a force transducer (AME-801 SensorOne, Sausalito, California) and micro-manipulator controlled shaft in a small chamber where oxygenated Krebs solution was continuously circulated. Temperature was kept constant at 25°C. The stimulation conditions were optimized and muscle length was increased until force development during tetanus was maximal. The responses to a single stimulus (twitch) or to a series of stimuli at various rates producing unfused or fused tetani were recorded. Time to peak tension, time to half relaxation and peak tension were measured in single twitches. Tension was measured in completely fused maximal tetani and twitch/tetanus ratio was determined. The resistance to fatigue was tested by stimulating the muscles with a fatiguing protocol based on 0.5s fused tetani with 1:4 duty ratio (low frequency fatigue).

- Preparation of samples for Electron Microscopy (EM). EDL and Soleus muscles were carefully dissected from CS1-*null* and WT mice (4 to 9 months of age). Muscles were fixed at RT in 3.5% glutaraldehyde in 0.1 M Na cacodylate buffer, pH 7.2 for 2h. Small bundles of fixed fibers were then post-fixed in 2% OsO_4 in the same buffer for 2h and block-stained in aqueous saturated uranyl acetate. After dehydration, specimens were embedded in an epoxy resin (Epon 812). Ultra thin sections were cut in a Leica Ultracut R microtome (Leica Microsystem, Vienna, Austria) using a Diatome diamond knife (DiatomeLtd. CH-2501 Biel, Switzerland). Sections, after staining in 4% uranyl acetate and lead citrate, were examined with a Morgagni Series 268D electron microscope (FEI Company, Brno, Czech Republic), equipped with Megaview III digital camera.

- Quantitative analysis of electron-micrographs. Micrographs, all at the same magnification (14,000X for counting CRUs and mitochondria; 28,000X for RyRs frequency and SR terminal cisternae width) with no overlapping regions, were randomly collected from 5 to 10 different fibers for each analyzed specimen, excluding peripheral areas, nuclei and Golgi regions. In both CS1-*null* and WT mice, 3 different time points for EDL and Soleus muscles (n=3) were quantitatively studied (ages: for CS1-*null* 5,

6.2 and 8.3 month old mice; for WT 5, 6 and 9.8 month old mice). *1) Average size of SR terminal cisternae lumen.* Width of the external SR vesicles was calculated using the Analysis Soft Imaging System (Germany), measuring the distance between the SR membrane facing the T-tubule and the opposite membrane in junctional SR vesicles at the outer borders of each CRU, as shown in panels A-D of Table 3, in which the two membranes are marked with dashed lines. The terminal cisternae to be measured were carefully selected based on clarity and definition of their outlines (Table 3, column I). *2) Average number of RyRs in junctional arrays.* In a set of micrographs at a higher magnification (28,000X), RyRs in the junctional gap were marked and counted, and their average number per sectional area was calculated (Table 3, column II). *3) Evaluation of the relative SR volume*. Estimates of the ratio between total SR volume and fiber volume were obtained using the well-established stereology point counting techniques (Loud *et al.*, 1965; Mobley & Eisenberg, 1975). Data were obtained from the same micrographs used for the other quantitative analysis. The images were covered with an orthogonal array of dots at a spacing of 0.20 μm. The ratio of the numbers of dots falling within the SR profile to the total number of dots covering the image gave the ratio of the SR volume to the total volume. Data are presented in Table 3, column III as percentages of fiber volume occupied by the SR. *4) Density of mitochondria.* The density of mitochondria was determined by counting the number of their sectioned profiles in EM images (14,000X) and referring them to the sectioned area. The same micrographs were used to calculate the percentage of fibers containing multiple junctions.

- Intracellular Ca^{2+} measurements in single intact muscle fibers. Single FDB (Flexor digitorum brevis) fibers were isolated with a modified collagenase/protease method as described previously (Defranchi *et al.*, 2005) from CS1-*null* and WT mice. There was no difference in fiber yield between the 2 groups of mice. On the day of the experiment (generally 48 hours after dissociation) isolated fibers were loaded with 5μM fura-2 acetoxymethyl ester (Molecular Probes, Invitrogen) in incubation buffer (125mM NaCl, 5mM KCl, 1mM $MgSO_4$, 1mM KH_2PO_4, 5.5mM glucose, 1mM $CaCl_2$, 20mM Hepes and 1% bovine serum albumine, pH 7.4 with NaOH) for 30 min at 37°C. After loading with Fura-2, fibers were washed

twice for 10 minutes with incubation buffer without BSA at 37°C to retain the indicator in the cytosol. After a minimum of 30 minutes calcium signals were recorded using a dual-beam excitation fluorescence photometry setup (IonOptix Corp.) at the temperature of 25°C. After 5–10 minutes of steady-state pacing at 0,5 Hz, 10 transients were recorded from each fiber which was then removed with a micropipette and transferred to an Eppendorf test tube containing Laemmli solution for CS isoform identification. About five fibers were analyzed from each Petri dish. Ca^{2+} transients were analyzed using the IonWizard software designed by IonOptixCorp (Milton, MA). $[Ca^{2+}]_i$ measurements are expressed as fluorescence ratio (F ratio) of the emission at 480nM with reference to the excitation wavelengths of 360 and 380 nm respectively.

- Calcium release in single permeabilized muscle fibers*.* Single fibers were manually dissected free from the superficial layers of Tibialis anterior muscle of CS1-*null* and WT mice and segments of 1-1.5-mm length were mounted with small aluminum clips between a force transducer (AME-801 SensorOne, Sausalito, California) and an electro-magnetic puller to control fiber length. The force transducer and the electromagnetic puller were part of a set-up composed of an aluminum plate equipped with seven small pedestals where drops containing different solutions were accommodated. The aluminum plate was placed on the stage of an inverted microscope (Axiovert 10, Zeiss, Germany). The fiber segment could be quickly moved from one small pool to the other allowing a complete change of solution within 5s. Dissection was carried out in a high potassium solution containing EGTA and the fiber was mounted in the same solution (*drop n 1*) whereas the other six drops were respectively composed of skinning solution containing 5 mg/ml saponin(*n 2*), relaxing solution (*n 3*), loading solution (*n 4*), washing solution (*n 5*), releasing solution (*n 6*), and maximal Ca^{2+} concentration activating solution (*n 7*). The compositions of the solutions were identical to those described in a previous paper (Rossi *et al.*, 2001). The floors of the pedestals were transparent so that specimens could be viewed at 320x through the eyepieces of the microscope and a video camera connected to a computer. Signals from the force and displacement transducer were displayed and recorded after A/D

conversion (interface 1401 plus; CED) on a computer where the software Spike 2 (CED) was used for analysis.

For measuring Ca^{2+} release fibers were transferred from the first drop (high potassium solution) to the second drop to be permeabilized with saponin for 30 s. Fibers were then immersed in relaxing solution (*n 3*), and then SR was loaded by immersing the fibers in a solution (*n 4*) at pCa 6.45 in the presence of 5 mM ATP. After the fibers had been washed (*n 5*) to remove excess EGTA, Ca^{2+} release was induced by transferring the fiber to solution *n 6* with low EGTA content (0.1 mM) containing caffeine in one of X variable concentrations from 0.1 to 20 mM (pCa 8). The fiber was finally transferred to activating solution (*n 7*) to measure the ability to develop force during a maximal activation (pCa 4.7). The fiber was then brought back to relaxing solution (*n 3*) to start a new cycle of loading and release. The release of Ca^{2+} was inferred by the transient tension development and quantified by the tension-time area, according to a method, first developed by Endo (Endo & Iino, 1988) and widely used (Launikonis & Stephenson, 1997; Rossi *et al.*, 2001). As discussed in a previous study (Rossi *et al.*, 2001), experimental and model analyses point to the tension-time area as the best indicator of the amount of Ca^{2+} released from the SR and later removed by EGTA and diffusion. The tension-time area was normalized to the tension developed during maximal activation (pCa 4.7, *solution 7*) to account for the variability of the ability of the myofibrillar apparatus in each fiber to develop force. After normalization, the tension-time area was expressed in seconds. Dose-response curves were interpolated using the sigmoid curve Y=T/[1+10^(logEC50-X)] where Y is the normalized area, X the caffeine concentration, T the maximal response amplitude, EC50 the concentration at which half-maximal response is achieved.

– ***Statistical analysis.*** Data were expressed as mean ± standard deviation (SD), unless differently stated. Student's unpaired *t* test was used for comparisons between CS1-*null* and WT data and statistical significance was set at $p<0.05$. GraphPad Prism software (Site company and location) was used for curve fitting.

RESULTS

CS1-null mouse. The CS1-*null* mutation is not lethal, mice are viable and fertile, and appear to develop and breed normally (Fig. 1 B). Western blots of total homogenates prepared from limb muscles with an antibody reactive with both CS1 and CS2 show that in CS1-*null* tissue CS1 is missing confirming the success of the knockout, whereas CS2 is still present (Fig. 1 C, right lane). Although CS1-*null* mice do not show any significant behavioral alteration under standard housing conditions, they do display signs of muscle atrophy (Table 1). In fact, the average body weight of CS1-*null* mice is about 10% lower when compared to WT group (Table 1, column I): 27.3 vs. 30.1g (male animals, age 4-6 months, n, number of animals: CS1-*null*, n=211; WT, n=150; $p<0.0001$). The average weight and muscle/body weight ratios of a predominantly fast-twitch muscle (EDL) in CS1-*null* mice is significantly lower than in WT mice of same sex and age ($p<0.0001$) (Table 1, column II and III). On the other hand, the Soleus does not show difference in mass between CS1-*null* and WT mice (Table 1, columns IV and V).

Immunoblot and Immunohistochemistry. Muscle-specific Western blots confirm the lack of CS1 in both EDL and Soleus. As in *WT* muscle CS2 is expressed in both muscle types and the expression of CS2 is higher in Soleus than in EDL (Fig. 1 D). There was no detectable compensatory increase of CS2 in either of the two CS1-*null* muscles. Immunohistochemical staining of transverse cryosections with an antibody specific for CS1 confirms that CS1 expression is completely abolished in CS1-*null* mice (Fig. 2, B and E). WT and CS1-*null* muscles were frozen next to each other: lack of fluorescence in CS1-*null* muscles is clearly evident in panels C and F (Fig. 2), which show the contact point between the two muscles. The fluorescence detectable in the interstitial spaces of CS1-*null* muscles is non-specific and is caused by our using a secondary antibody against murine immunoglobulin on mouse muscle sections. Immunostaining of sections with an antibody that recognizes both CS1 and CS2, indicates that CS2 – the only isoform expressed - is not present in all fibers, but is confined to a subpopulation (Fig. 3, A and D) of fibers. Fibers expressing CS2 are rare in the EDL (5 to 20 % depending on the section, n = 5, Fig. 3 A), but are abundant in the Soleus (about 40-50 %, n = 4, Fig. 3 D). Thus, most muscle fibers in the EDL of CS1-*null* muscle

(80% or more) lack any CS, whereas in the Soleus only about 50% of fibers do not express any CS.

To determine which type of fibers express CS2, serial sections from both EDL and Soleus muscles were labeled with antibodies specific for CS2 and with antibodies specific for either slow (type I) or fast IIA (type IIA) myosin heavy chain (MHC). Corresponding fibers in the different sections are marked with the same numbers in paired panels (Fig. 3: B-C, EDL; E-F, Soleus). The results indicate that in Soleus CS2 is almost exclusively expressed in type I fibers, whereas in the EDL, CS2 is predominantly expressed in a subset of type IIA fibers, i.e. oxidative fast-twitch. Labeling with the two anti-MHC antibodies does not suggest that there is any detectable fiber type switch towards type I fibers in CS1-*null* muscles when compared to WT muscles. This has also been confirmed by MHC isoform separation with gel electrophoresis (not shown). Thus, taking into account the known fiber type composition of murine EDL and Soleus (Pellegrino *et al.*, 2003), fibers lacking both CS1 and CS2 are mainly type IIX and IIB in EDL, whereas they are mostly type IIA and a few IIX in Soleus.

Tension development and contraction kinetics of Soleus and EDL. Maximum isometric tension in fused tetani of EDL and Soleus muscles of CS1-*null* muscles is not reduced compared to WT (80 Hz in Soleus and 100-120 Hz in EDL, Table 2, column II). However, twitch tension shows a trend to higher values in CS1-*null* than in WT muscles (Table 2, column I), and the twitch/tetanus ratio is significantly higher in EDL muscles of CS1-*null* compared to WT (Table 2, column III). This increase in the twitch/tetanus ratio is likely related to the altered kinetics of the contractile cycle in CS1-*null* muscle. These changes include a significant prolongation of both time to peak tension and time to half relaxation in EDL (Fig. 4, A and B), but not in Soleus muscles (Fig. 4, D and E), suggesting a delayed Ca^{2+} release and delayed Ca^{2+} removal from the myofibrils. An interesting alteration of the contraction kinetics found in CS1-*null* EDL muscles is the highly significant increase in fatigue resistance (Fig. 4 C): residual developed tension after 120s of repetitive stimulation is 100% higher than in WT muscles. One possible explanation for this increased resistance to fatigue may be related to the increased

mitochondria content in EDL muscles described below (see also Table 3). This does not occur in CS1-*null* Soleus muscles and they show no difference in fatigue resistance compared to WT.

Ultrastructural features of the EC coupling apparatus. The overall architecture of the EC coupling apparatus in EDL and Soleus is quite similar (compare Figs. 5 and 6, panels A-B). In WT skeletal muscle, the mature T-tubule network has a general transverse orientation, and is located at the edges of the A band, forming two transverse networks for each sarcomere. CRUs in mature skeletal muscle are usually in the form of triads, composed of two SR vesicles closely apposed to a T-tubule (Figs. 5 B and 6 B). In these mature junctions, RyRs form two ordered rows along each side of the T-tubule (Fig. 5 B, small arrows). Some general quantitative differences between CRUs of fast and slow twitch fibers involve a higher frequency of junctional SR-T tubule apposition in the former, resulting in a higher overall density of ryanodine receptors (Appelt *et al.*, 1989; Franzini-Armstrong *et al.*, 1999).

In CS1-*null* EDL muscle the general shape of CRUs is strikingly altered. In CS1-*null* EDL the most noticeable difference is the presence of multiple stacks of alternating SR and T tubule profiles, that occupy the place where triads are usually found. Junctions that are formed by 5, 7 or even 9 elements (pentads, heptads and nonads, Fig. 5, C and D) are seen in 71% of EDL fibers CS1-*null* EDL mice. In contrast, CRUs in Soleus retain their usual triadic disposition and CRUs formed by more than three elements are quite rare. It must be noted that in order to deploy the stacked arrangement, the T tubule in EDL muscles must bend repeatedly.

A second alteration seen in CS1-*null* muscles is in the width of SR terminal cisternae, which tend to be considerably narrower than in normal triads (Table 3, column I). In EDL, where multi-layered junctions are frequent both the central elements of the stacks and those at the two borders are narrower than the junctional SR in wild type triads. In Soleus, the junctional SR cisternae are also narrower, although multiple stacks are not formed (Figs. 5 and 6). The average width of the junctional SR cisternae is 25.0 ± 4.5 nm (n, number of measurements; n=487) and 30.0 ± 5.9 nm (n=404), respectively in CS1-*null* EDL and Soleus muscle, both

of which are significantly lower than in their respective WT counterparts (EDL: 62.4 ± 10.5; Soleus: 62.5±11.7).

A third alteration, which is present only in CS1-*null* EDL is a change in the orientation of the main axis of the T tubule within CRUs and thus a change in the axis of the whole CRU. CRUs often show transverse, oblique, and even longitudinal orientations with respect to the main axis of myofibrils (Fig. 5 C), while still maintaining their usual position at the edges of the A band.

Due to the multiple stacking, many of the junctional SR cisternae in EDL are flanked by RyRs on two sides, both of which face T tubules. This, together with the fact that the junctions are formed by multiple layers, and that RyRs form multiple rows, implies that CRUs of CS1-*null* EDL fibers contain a larger number of RyRs than triads in WT fibers. The density of RyRs related to the area of thin section, obtained by counting "feet" directly in the images (see methods) is proportional to the density of RyRs per fiber volume. RyR density is approximately double in CS1-*null* EDL when compared to WT fibers: 71.8 RyRs/10μm^2 vs. 39.2 RyRs/10μm^2 (Table 3, column II - n, number of micrographs; 111 and 143 for CS1-*null* and WT respectively). In this analysis all EDL fibers are included, i.e. both fibers with multi-layered CRUs and those that contain CRUs formed by three elements. By contrast, in Soleus muscle the number of RyRs per unit area of section remains unchanged (Table 3, column II n=54 and n=74 for WT and CS1-*null* respectively). The increase in RyR content found in EDL fibers was confirmed by an increase in B_{max} of ^{3}H-ryanodine binding (see Fig. 7). Calculations based on morphometric analysis (Loud *et al.*, 1965; Mobley & Eisenberg, 1975) show that the total SR volume relative to the total fiber volume is virtually unchanged in CS1-*null* EDL fibers compared to WT fibers (Table 3, column III): 5.25 ± 1.9 % in CS1-*null* fibers vs. 5.66 ± 1.8 % in WT (n. of micrographs; n=97 and n=93 respectively). The surprisingly unvaried total SR volume is the final result of two significant structural alterations: a) shrinkage of the SR terminal cisternae (Table 3, column I), which alone would lead to a decrease in SR volume; and b) proliferation of the junctional SR vesicles (Fig. 5 C) that alone would lead to an increase in SR volume. The compounded effect of

these two structural changes seems to result in an approximately unchanged total SR volume.

The final ultrastructural alteration in CS1-*null* muscles is that mitochondria are significantly more abundant in EDL fibers of CS1-*null* mice when compared to WT EDL fibers (62.1 vs. 36.3 mitochondria/100μm^2 of thin section area. In contrast, no change is detected in Soleus fibers (Table 3, column IV). On the whole, in agreement with the more pronounced lack of total CS, the re-organization of the SR, of the T-tubule/SR junctions, and of the mitochondrial apparatus is much more evident in CS1-*null* EDL than in CS1-*null* Soleus. Only the reduction in size of the SR terminal cisternae is similar in both muscles.

Expression levels of RyR, CS2, SERCA1, and triadin in EDL muscle. Since EDL muscles are more affected by the lack of CS1 both functionally and structurally, we limited this analysis to the EDL. A quantitative estimate of the RyR content is given by ^{3}H-ryanodine binding of total membranes isolated from either WT or CS1-*null* EDL. As can be seen in Fig. 7 $B_{max}/\mu g$ protein is approximately doubled in CS1-*null* samples as compared to WT samples, whereas K_d is virtually unchanged. The ^{3}H-ryanodine binding experiments confirm the ultrastructural results reported in Table 3, column II of an increase in the amount of RyR expression in EDL fibers. Densitometric analysis of total homogenates from WT and CS1-*null* EDL muscles was used to quantify the expression levels of CS2, SERCA1 and 95kDa triadin. This quantitative analysis confirmed that there is no compensatory expression of CS2 in CS1-*null* muscle. Expression of CS2 in CS1-*null* EDLs seems actually slightly decreased, whereas SERCA1 and 95kDa triadin contents are not significantly changed. Data plotted in the bar graphs of Fig 7 are expressed as means ± SD for n=4 WT EDL and n=4 CS1-*null* EDL. Although the time to ½ relaxation is increased in CS1-*null* EDL, SERCA1 content is unchanged compared to WT (Fig. 7 B and C) suggesting that the reduction in Ca^{2+} uptake must be due to the absence of CS1 buffering ability. The 95kDa triadin isoform (Brandt *et al.*, 1990; Kim *et al.*, 1990; Caswell *et al.*, 1991) is thought to be a CS1 binding protein. However, as can be seen from the average of 4 different experiments, there is no statistically significant difference in Triadin-95 expression between CS1-*null* and WT EDL muscles (Fig. 7 D).

Ca^{2+} kinetics in single muscle fibers. Intracellular free Ca^{2+} concentrations and Ca^{2+} transients in response to electrical stimulation were measured in single FDB fibers loaded with fura 2 AM. Each fiber was later individually characterized by Western blot for their CS1 and CS2 content. Data obtained from WT fibers lacking CS2 and *null* fibers lacking both CS1 and CS2 are compared in Fig. 8, A and D. Basal calcium levels at rest are not significantly different in CS1-*null* compared to WT fibers, but the amplitude of the transient induced by a single electrical stimulation is strongly and significantly reduced in the CS1-*null* group. Caffeine contractures of saponin skinned fast muscle fibers from the tibialis muscle, loaded with calcium confirm that the amount of releasable calcium at maximal doses of caffeine is significantly reduced in *null* versus WT fibers (an example is given in Fig. 8 B, caffeine 20 mM). The caffeine concentrations at which one-half of the maximal response is achieved (EC50) is not different in fibers lacking CS (Fig. 8 E), so that when the dose-response curves are normalized to the maximal response they are virtually superimposable (Fig. 8 F). These findings strongly support the view that, in spite of the ultrastructural re-organization of the CRUs and the increased density of RyR1, the absence of calsequestrin reduces the amount of releasable Ca^{2+} and this in turn is responsible for the smaller amplitude of cytosolic Ca^{2+} transients.

DISCUSSION

The contribution of calsequestrin (CS) to the capacity of the SR to sequester and hold a large Ca^{2+} load and its specific location next to Ca^{2+} release channels are usually considered essential to support the massive Ca^{2+} release that occurs during normal activation of a muscle fiber (Somlyo *et al.*, 1981; Hollingworth *et al.*, 1996). In addition, it has been suggested that CS, which is held in proximity of the RyRs and presumably connected to them via triadin (Caswell *et al.*, 1991; Liu & Pessah, 1994; Guo & Campbell, 1995), may have a direct regulatory role on the SR release channels, perhaps helping to shape the release event. However, available evidence are controversial pointing either to an activation (Kawasaki & Kasai, 1994; Ohkura *et al.*, 1995; Szegedi *et al.*, 1999; Herzog *et al.*, 2000) or to an inhibition by CS of Ca^{2+} release through RyR1

(Beard *et al.*, 2002). In addition, in SR vesicles that have been stripped of CS, the rate of ATP hydrolysis, indicative of active Ca^{2+} transport, falls off rapidly during the first seconds of uptake, due to back inhibition by accumulated Ca^{2+} (Weber, 1971; Inesi & de Meis, 1989), whereas SR Ca^{2+} capacity is increased by Ca^{2+} chelating agents, or Ca^{2+} buffering molecules such as CS (Makinose & Hasselbach, 1965).

Based on the above reasoning, the ablation of CS1 was expected to deeply impair contractile function. In this view, the small effect of the ablation of CS1 on the contractile response of skeletal muscles was totally unexpected, particularly in the case of the fast twitch muscles in which the amount of Ca^{2+} cycled during a single twitch is about three times greater than in slow twitch fibers (Baylor & Hollingworth, 2003). The knock-out of CS1 gene in our mice results in muscles containing a large number of fibers virtually devoid of any CS (Fig. 3 and 8). Nevertheless, their ability to generate a contractile response is maintained (Fig. 4). A careful investigation of the CRU's ultrastructure (and of the mitochondrial apparatus) in these CS-*null* muscles reveals significant adaptations that may to some extent compensate for the lack of CS1, particularly in fast twitch muscles (i.e. EDL, FDB, tibialis anterior). These changes in CS1-*null* animals include multiple junctions presenting a wider profile and an almost doubled amount of Ca^{2+} release channels, compared to junctions in WT animals (Fig. 5 and Table 3). The proliferation of the SR junctional domains, i.e. the re-organization in multilayers of the Ca^{2+} release units, likely represent a compensation for the reduction in storage volume caused by the shrinkage of the terminal cisternae, since there is no variation in the relative SR volume (Table 3) and no variation in the relative amount of longitudinal SR (not shown). The increased number of release sites can also be ascribed to the compensatory changes, but it is important to underline that the striking proliferation of SR junctional domains and the increased abundance of RyR1 is not sufficient to completely compensate for the lack of CS1, as demonstrated by the lower amount of SR Ca^{2+} content and the reduced amplitude of the Ca^{2+} transients (Fig. 8). Nevertheless, the occurrence of compensatory changes of the SR/T-tubule junctional domains should be taken into consideration when comparing the contractile responses of WT and CS1-

null muscles, since the structural re-arrangement of the Ca^{2+} handling apparatus may likely reduce the functional impairment of the contractile response caused by the absence of CS1. The search for compensatory adaptations, however, has not been successful in all cases. Similarly, no apparent upregulation of Ca^{2+} binding proteins has been found in the hearts of CS2-*null* mice (Knollmann *et al.*, 2006). Fibers lacking completely CS show a clear decrease in the amount of calcium release as shown by the reduced tension-time area of the response to maximal doses of caffeine and by the reduced amplitude of the Ca^{2+} transient measured with Fura-2 (Fig. 8). This means that, as mentioned above, the large increase in junctional domains (Fig. 5) and number of the RyRs (Table 3 and Fig. 7) are not sufficient to completely compensate for the lack of CS1 in the SR lumen. It is important, however, to observe that in spite of the lower amount of Ca^{2+} released, tension developed by a twitch induced by electrical stimulation is not reduced (Fig. 4). The preservation of the peak tension reached during the twitch points to a second important effect of the lack of CS1, i.e. the prolongation of the twitch time course. The likely cause of the prolonged time-to-peak tension and half relaxation time is the impairment of Ca^{2+} re-uptake by the SR. In the absence of CS1, the increase of intraluminal Ca^{2+} concentration inhibits Ca^{2+} sequestration into SR (Weber, 1971; Inesi & de Meis, 1989). The delayed Ca^{2+} re-uptake allows a prolonged activation of the myofibrils in CS1-*null* fibers and this, in turn, gives the necessary time to develop tension up or even slightly above the peak value reached in WT fibers.

Taken together the functional alterations demonstrate that two distinct effects follow the lack of CS1, on one hand the impaired Ca^{2+} release and on the other hand the impaired Ca^{2+} re-uptake (see cartoon in Fig. 9). The impaired Ca^{2+} release can be attributed to the role played by CS in proximity to junctional membrane (Jorgensen *et al.*, 1983; Franzini-Armstrong *et al.*, 1987), to control either Ca^{2+} availability or opening kinetics of RyR (Ikemoto *et al.*, 1989; Kawasaki & Kasai, 1994; Beard *et al.*, 2002). The reason for the delayed Ca^{2+} re-uptake can be found in the reduced Ca^{2+} buffering capacity of the SR. The re-uptake rate is limited by intra-SR free [Ca^{2+}] by back-inhibition on the Ca^{2+} pump as discussed above (Fryer & Stephenson, 1996). Fast-twitch fibers (superficial layers of

Tibialis anterior and FDB) and predominantly fast muscles (EDL) are particularly sensitive to the lack of CS1, because the amount of Ca^{2+} released and taken up is greater than in slow fibers (Fryer & Stephenson, 1996) and because CS1 is in most cases the only isoform present. The only effective, although partial, compensation for the delayed removal of Ca^{2+} from the cytosol is likely given by the proliferation of the mitochondria in EDL fibers (see below).

The structural reactions to lack of CS are quite interesting and may considered a combination of compensatory adaptations and developmental effects, in addition to some obvious geometrical alterations. A large decrease in size of the jSR cisternae is detected both in the EDL and soleus and is particularly prominent in the former, where very little CS2 is present. It is logical to assume that this volume decrease is directly due the lack of the luminal CS polymer that usually fills the junctional SR. In support of this hypothesis, other studies indicate that CS2 over-expression in murine myocardium induced the opposite effects, i.e., drastic swelling of SR terminal cisternae (Jones *et al.*, 1998), whereas CS2 knock out in cardiomyocytes also caused significant alterations of the SR terminal cisternae, which were either slightly narrower or noticeably wider than in wild-type myocardium (Knollmann *et al.*, 2006).

Interestingly, two changes that may seem to be direct compensatory responses to the reduced SR capacity for calcium, are seen only in the EDL and are quite undistinguishable from the response of this muscle to other physio-pathological stimuli (Franzini-Armstrong, 1991; Takekura *et al.*, 1993; Takekura & Kasuga, 1999; Takekura *et al.*, 2001; Boncompagni *et al.*, 2006). The complex proliferation of the junctional SR and the convoluted (and often longitudinal) T tubule path has the effect of increasing the density of Ca^{2+} release channels while maintaining the total SR volume constant (despite the fact that the cisternae are smaller in size, see above). The same abundance, and interestingly, also the same change in orientation of the junctional SR is seen in the EDL, but not in soleus, as a swift response to short-term denervation that rapidly returns to normal when the muscle is innervated again (Takekura & Kasuga, 1999). Thus, the formation of complex junctions and the increased density

of RyRs may be in response to complex stimuli rather than simply as a compensation for the lowered calcium content of the SR.

It is interesting that CS1-*null* EDL shows a doubling of mitochondria content, with the resulting increase in fatigue resistance. In contrast, mitochondria content is unchanged in CS1-*null* Soleus or CS2-*null* cardiomyocytes (Knollmann *et al.*, 2006). Skeletal muscle mitochondria take up calcium during a single twitch (Rudolf *et al.*, 2004) and can affect the time course of relaxation if sufficiently abundant, e.g. in mitochondria-rich slow-twitch fibers (Gillis, 1997). Mitochondrial biogenesis in fast-twitch fibers has previously been shown to be stimulated by of the absence of the cyoplasmic calcium buffering protein parvalbumin (Racay *et al.*, 2006) and in junctate overexpressing mice (Divet *et al.*, 2007). Conceivably, prolonged presence of Ca^{2+} in the cytosol, even if only slight, induces mitochondrial proliferation as suggested by (Rohas *et al.*, 2007). However an increased mitochondrial volume, while perhaps helpful in accelerating relaxation, does not fully solve the problem due to reduced SR capacity for calcium, since the ions need to be sequestered in the SR, not the mitochondria to be available for subsequent release.

The preserved ability to develop tension even in fibers completely devoid of CS is, in our view, one of the most remarkable findings stemming from the analysis of CS1-*null* mice. The reduced Ca^{2+} release and the decreased cytosolic Ca^{2+} transient support the view that the Ca^{2+} storage capacity of the SR is impaired, whereas the prolongation of the contractile response is consistent with a defective Ca^{2+} re-uptake. Such functional alterations are present in spite of the re-organization of the CRUs, the large increase in RyR content and the increased abundance of mitochondria. Thus, Ca^{2+} buffer in the SR is unequivocally one of the essential functions of CS1 in skeletal muscles, in agreement with the very recent study by Pape *et al.* (2007). The evidence pointing to an impaired Ca^{2+} release is not sufficient to conclude about the modulatory function of CS1 on RyR kinetics. The dissection of the Ca^{2+} release and uptake on single muscle fibers or myotubes in culture and a detailed analysis of compensatory mechanisms at transcriptomic and proteomic level will be the goal of future studies on the CS1-*null* model.

REFERENCES

Appelt D, Buenviaje B, Champ C & Franzini-Armstrong C. (1989). Quantitation of 'junctional feet' content in two types of muscle fiber from hind limb muscles of the rat. *Tissue Cell* **21,** 783-794.

Baylor SM & Hollingworth S. (2003). Sarcoplasmic reticulum calcium release compared in slow-twitch and fast-twitch fibres of mouse muscle. *J Physiol* **551,** 125-138.

Beard NA, Sakowska MM, Dulhunty AF & Laver DR. (2002). Calsequestrin is an inhibitor of skeletal muscle ryanodine receptor calcium release channels. *Biophys J* **82,** 310-320.

Beard NA, Casarotto MG, Wei L, Varsanyi M, Laver DR & Dulhunty AF. (2005). Regulation of ryanodine receptors by calsequestrin: effect of high luminal Ca2+ and phosphorylation. *Biophys J* **88,** 3444-3454.

Block BA, Imagawa T, Campbell KP & Franzini-Armstrong C. (1988). Structural evidence for direct interaction between the molecular components of the transverse tubule/sarcoplasmic reticulum junction in skeletal muscle. *J Cell Biol* **107,** 2587-2600.

Boncompagni S, d'Amelio L, Fulle S, Fano G & Protasi F. (2006). Progressive disorganization of the excitation-contraction coupling apparatus in aging human skeletal muscle as revealed by electron microscopy: a possible role in the decline of muscle performance. *J Gerontol A Biol Sci Med Sci* **61,** 995-1008.

Brandt NR, Caswell AH, Wen SR & Talvenheimo JA. (1990). Molecular interactions of the junctional foot protein and dihydropyridine receptor in skeletal muscle triads. *J Membr Biol* **113,** 237-251.

Campbell KP, MacLennan DH, Jorgensen AO & Mintzer MC. (1983). Purification and characterization of calsequestrin from canine cardiac sarcoplasmic reticulum and identification of the 53,000 dalton glycoprotein. *J Biol Chem* **258,** 1197-1204.

Caswell AH, Brandt NR, Brunschwig JP & Purkerson S. (1991). Localization and partial characterization of the oligomeric disulfide-linked molecular weight 95,000 protein (triadin) which binds the ryanodine and dihydropyridine receptors in skeletal muscle triadic vesicles. *Biochemistry* **30,** 7507-7513.

Cho JH, Oh YS, Park KW, Yu J, Choi KY, Shin JY, Kim DH, Park WJ, Hamada T, Kagawa H, Maryon EB, Bandyopadhyay J & Ahnn J. (2000). Calsequestrin, a calcium sequestering protein localized at the sarcoplasmic reticulum, is not essential for body-wall muscle function in Caenorhabditis elegans. *J Cell Sci* **113 (Pt 22),** 3947-3958.

Damiani E, Volpe P & Margreth A. (1990). Coexpression of two isoforms of calsequestrin in rabbit slow-twitch muscle. *J Muscle Res Cell Motil* **11,** 522-530.

Damiani E, Tobaldin G, Volpe P & Margreth A. (1991). Quantitation of ryanodine receptor of rabbit skeletal muscle, heart and brain. *Biochem Biophys Res Commun* **175,** 858-865.

Defranchi E, Bonaccurso E, Tedesco M, Canato M, Pavan E, Raiteri R & Reggiani C. (2005). Imaging and elasticity measurements of the sarcolemma of fully differentiated skeletal muscle fibres. *Microsc Res Tech* **67,** 27-35.

Divet A, Paesante S, Grasso C, Cavagna D, Tiveron C, Protasi F, Huchet-Cadiou C, Treves S & Zorzato F. (2007). Increased Ca2+ storage capacity of the skeletal muscle sarcoplasmaic reticulum of transgenic mice over-expressing membrane bound calcium binding protein junctate. *J Cell Physiol* **DOI: JCP-07-0045.R1(21121)**.

Dolmetsch R. (2003). Excitation-transcription coupling: signaling by ion channels to the nucleus. *Sci STKE* **2003,** PE4.

Dulhunty AF, Beard NA, Pouliquin P & Kimura T. (2006). Novel regulators of RyR Ca2+ release channels: insight into molecular changes in genetically-linked myopathies. *J Muscle Res Cell Motil* **27,** 351-365.

Endo M & Iino M. (1988). Measurement of Ca2+ release in skinned fibers from skeletal muscle. *Methods Enzymol* **157,** 12-26.

Fliegel L, Ohnishi M, Carpenter MR, Khanna VK, Reithmeier RA & MacLennan DH. (1987). Amino acid sequence of rabbit fast-twitch skeletal muscle calsequestrin deduced from cDNA and peptide sequencing. *Proc Natl Acad Sci U S A* **84,** 1167-1171.

Franzini-Armstrong C. (1970). Studies of the triad. *J Cell Biol* **47,** 488-499.

Franzini-Armstrong C, Kenney LJ & Varriano-Marston E. (1987). The structure of calsequestrin in triads of vertebrate skeletal muscle: a deep-etch study. *J Cell Biol* **105,** 49-56.

Franzini-Armstrong C. (1991). Simultaneous maturation of transverse tubules and sarcoplasmic reticulum during muscle differentiation in the mouse. *Dev Biol* **146,** 353-363.

Franzini-Armstrong C, Protasi F & Ramesh V. (1999). Shape, size, and distribution of Ca(2+) release units and couplons in skeletal and cardiac muscles. *Biophys J* **77,** 1528-1539.

Fryer MW & Stephenson DG. (1996). Total and sarcoplasmic reticulum calcium contents of skinned fibres from rat skeletal muscle. *J Physiol* **493 (Pt 2),** 357-370.

Gerke V, Creutz CE & Moss SE. (2005). Annexins: linking Ca2+ signalling to membrane dynamics. *Nat Rev Mol Cell Biol* **6,** 449-461.

Gilchrist JS, Belcastro AN & Katz S. (1992). Intraluminal Ca2+ dependence of Ca2+ and ryanodine-mediated regulation of skeletal muscle sarcoplasmic reticulum Ca2+ release. *J Biol Chem* **267,** 20850-20856.

Gillis JM. (1997). Inhibition of mitochondrial calcium uptake slows down relaxation in mitochondria-rich skeletal muscles. *J Muscle Res Cell Motil* **18,** 473-483.

Guo W & Campbell KP. (1995). Association of triadin with the ryanodine receptor and calsequestrin in the lumen of the sarcoplasmic reticulum. *J Biol Chem* **270,** 9027-9030.

Herzog A, Szegedi C, Jona I, Herberg FW & Varsanyi M. (2000). Surface plasmon resonance studies prove the interaction of skeletal muscle sarcoplasmic reticular Ca(2+) release channel/ryanodine receptor with calsequestrin. *FEBS Lett* **472,** 73-77.

Hollingworth S, Zhao M & Baylor SM. (1996). The amplitude and time course of the myoplasmic free [Ca2+] transient in fast-twitch fibers of mouse muscle. *J Gen Physiol* **108,** 455-469.

Ikemoto N, Ronjat M, Meszaros LG & Koshita M. (1989). Postulated role of calsequestrin in the regulation of calcium release from sarcoplasmic reticulum. *Biochemistry* **28,** 6764-6771.

Inesi G & de Meis L. (1989). Regulation of steady state filling in sarcoplasmic reticulum. Roles of back-inhibition, leakage, and slippage of the calcium pump. *J Biol Chem* **264,** 5929-5936.

Jones LR, Suzuki YJ, Wang W, Kobayashi YM, Ramesh V, Franzini-Armstrong C, Cleemann L & Morad M. (1998). Regulation of Ca2+ signaling in transgenic mouse cardiac myocytes overexpressing calsequestrin. *J Clin Invest* **101,** 1385-1393.

Jorgensen AO, Shen AC, Campbell KP & MacLennan DH. (1983). Ultrastructural localization of calsequestrin in rat skeletal muscle by immunoferritin labeling of ultrathin frozen sections. *J Cell Biol* **97,** 1573-1581.

Jorgensen AO, Shen AC, Arnold W, Leung AT & Campbell KP. (1989). Subcellular distribution of the 1,4-dihydropyridine receptor in rabbit skeletal muscle in situ: an immunofluorescence and immunocolloidal gold-labeling study. *J Cell Biol* **109,** 135-147.

Kawasaki T & Kasai M. (1994). Regulation of calcium channel in sarcoplasmic reticulum by calsequestrin. *Biochem Biophys Res Commun* **199,** 1120-1127.

Kim KC, Caswell AH, Talvenheimo JA & Brandt NR. (1990). Isolation of a terminal cisterna protein which may link the dihydropyridine receptor to the junctional foot protein in skeletal muscle. *Biochemistry* **29,** 9281-9289.

Knollmann BC, Chopra N, Hlaing T, Akin B, Yang T, Ettensohn K, Knollmann BE, Horton KD, Weissman NJ, Holinstat I, Zhang W, Roden DM, Jones LR, Franzini-Armstrong C & Pfeifer K. (2006). Casq2 deletion causes sarcoplasmic reticulum volume increase, premature Ca2+ release, and catecholaminergic polymorphic ventricular tachycardia. *J Clin Invest* **116,** 2510-2520.

Lai FA, Erickson HP, Rousseau E, Liu QY & Meissner G. (1988). Purification and reconstitution of the calcium release channel from skeletal muscle. *Nature* **331,** 315-319.

Launikonis BS & Stephenson DG. (1997). Effect of saponin treatment on the sarcoplasmic reticulum of rat, cane toad and crustacean (yabby) skeletal muscle. *J Physiol* **504 (Pt 2),** 425-437.

Leberer E & Pette D. (1986). Immunochemical quantification of sarcoplasmic reticulum Ca-ATPase, of calsequestrin and of parvalbumin in rabbit skeletal muscles of defined fiber composition. *Eur J Biochem* **156,** 489-496.

Leberer E, Hartner KT & Pette D. (1988). Postnatal development of Ca2+-sequestration by the sarcoplasmic reticulum of fast and slow muscles in normal and dystrophic mice. *Eur J Biochem* **174,** 247-253.

Liu G & Pessah IN. (1994). Molecular interaction between ryanodine receptor and glycoprotein triadin involves redox cycling of functionally important hyperreactive sulfhydryls. *J Biol Chem* **269,** 33028-33034.

Loud AV, Barany WC & Pack BA. (1965). Quantitative Evaluation of Cytoplasmic Structures in Electron Micrographs. *Lab Invest* **14,** 996-1008.

Lowry OH, Rosebrough NJ, Farr AL & Randall RJ. (1951). Protein measurement with the Folin phenol reagent. *J Biol Chem* **193,** 265-275.

MacLennan DH & Wong PT. (1971). Isolation of a calcium-sequestering protein from sarcoplasmic reticulum. *Proc Natl Acad Sci U S A* **68,** 1231-1235.

Makinose M & Hasselbach W. (1965). [The influence of oxalate on calcium transport of isolated sarcoplasmic reticular vesicles]. *Biochem Z* **343,** 360-382.

Mobley BA & Eisenberg BR. (1975). Sizes of components in frog skeletal muscle measured by methods of stereology. *J Gen Physiol* **66,** 31-45.

Ohkura M, Ide T, Furukawa K, Kawasaki T, Kasai M & Ohizumi Y. (1995). Calsequestrin is essential for the Ca2+ release induced by myotoxin alpha in skeletal muscle sarcoplasmic reticulum. *Can J Physiol Pharmacol* **73,** 1181-1185.

Pape PC, Fenelon K, Lamboley CR & Stachura D. (2007). Role of calsequestrin evaluated from changes in free and total calcium concentrations in the sarcoplasmic reticulum of frog cut skeletal muscle fibres. *J Physiol* **581,** 319-367.

Pellegrino MA, Canepari M, Rossi R, D'Antona G, Reggiani C & Bottinelli R. (2003). Orthologous myosin isoforms and scaling of shortening velocity with body size in mouse, rat, rabbit and human muscles. *J Physiol* **546,** 677-689.

Protasi F, Franzini-Armstrong C & Flucher BE. (1997). Coordinated incorporation of skeletal muscle dihydropyridine receptors and ryanodine receptors in peripheral couplings of BC3H1 cells. *J Cell Biol* **137,** 859-870.

Protasi F, Franzini-Armstrong C & Allen PD. (1998). Role of ryanodine receptors in the assembly of calcium release units in skeletal muscle. *J Cell Biol* **140,** 831-842.

Protasi F, Takekura H, Wang Y, Chen SR, Meissner G, Allen PD & Franzini-Armstrong C. (2000). RYR1 and RYR3 have different roles in the assembly of calcium release units of skeletal muscle. *Biophys J* **79,** 2494-2508.

Protasi F. (2002). Structural interaction between RYRs and DHPRs in calcium release units of cardiac and skeletal muscle cells. *Front Biosci* **7,** d650-658.

Racay P, Gregory P & Schwaller B. (2006). Parvalbumin deficiency in fast-twitch muscles leads to increased 'slow-twitch type' mitochondria, but does not affect the expression of fiber specific proteins. *Febs J* **273,** 96-108.

Rios E, Ma JJ & Gonzalez A. (1991). The mechanical hypothesis of excitation-contraction (EC) coupling in skeletal muscle. *J Muscle Res Cell Motil* **12,** 127-135.

Rohas LM, St-Pierre J, Uldry M, Jager S, Handschin C & Spiegelman BM. (2007). A fundamental system of cellular energy homeostasis regulated by PGC-1{alpha}. *Proc Natl Acad Sci U S A* **104,** 7933-7938.

Rossi R, Bottinelli R, Sorrentino V & Reggiani C. (2001). Response to caffeine and ryanodine receptor isoforms in mouse skeletal muscles. *Am J Physiol Cell Physiol* **281,** C585-594.

Rudolf R, Mongillo M, Magalhaes PJ & Pozzan T. (2004). In vivo monitoring of Ca(2+) uptake into mitochondria of mouse skeletal muscle during contraction. *J Cell Biol* **166,** 527-536.

Sacchetto R, Volpe P, Damiani E & Margreth A. (1993). Postnatal development of rabbit fast-twitch skeletal muscle: accumulation, isoform transition and fibre distribution of calsequestrin. *J Muscle Res Cell Motil* **14,** 646-653.

Saito A, Seiler S, Chu A & Fleischer S. (1984). Preparation and morphology of sarcoplasmic reticulum terminal cisternae from rabbit skeletal muscle. *J Cell Biol* **99,** 875-885.

Sandow A. (1965). Excitation-contraction coupling in skeletal muscle. *Pharmacol Rev* **17,** 265-320.

Schiaffino S, Gorza L, Sartore S, Saggin L, Ausoni S, Vianello M, Gundersen K & Lomo T. (1989). Three myosin heavy chain isoforms in type 2 skeletal muscle fibres. *J Muscle Res Cell Motil* **10,** 197-205.

Schneider MF & Chandler WK. (1973). Voltage dependent charge movement of skeletal muscle: a possible step in excitation-contraction coupling. *Nature* **242,** 244-246.

Schneider MF. (1994). Control of calcium release in functioning skeletal muscle fibers. *Annu Rev Physiol* **56,** 463-484.

Scott BT, Simmerman HK, Collins JH, Nadal-Ginard B & Jones LR. (1988). Complete amino acid sequence of canine cardiac calsequestrin deduced by cDNA cloning. *J Biol Chem* **263,** 8958-8964.

Silver J & Keerikatte V. (1989). Novel use of polymerase chain reaction to amplify cellular DNA adjacent to an integrated provirus. *J Virol* **63,** 1924-1928.

Somlyo AV, Gonzalez-Serratos HG, Shuman H, McClellan G & Somlyo AP. (1981). Calcium release and ionic changes in the sarcoplasmic reticulum of tetanized muscle: an electron-probe study. *J Cell Biol* **90,** 577-594.

Szegedi C, Sarkozi S, Herzog A, Jona I & Varsanyi M. (1999). Calsequestrin: more than 'only' a luminal Ca2+ buffer inside the sarcoplasmic reticulum. *Biochem J* **337 (Pt 1),** 19-22.

Takekura H, Shuman H & Franzini-Armstrong C. (1993). Differentiation of membrane systems during development of slow and fast skeletal muscle fibres in chicken. *J Muscle Res Cell Motil* **14,** 633-645.

Takekura H & Kasuga N. (1999). Differential response of the membrane systems involved in excitation-contraction coupling to early and later postnatal denervation in rat skeletal muscle. *J Muscle Res Cell Motil* **20,** 279-289.

Takekura H, Fujinami N, Nishizawa T, Ogasawara H & Kasuga N. (2001). Eccentric exercise-induced morphological changes in the membrane systems involved in excitation-contraction coupling in rat skeletal muscle. *J Physiol* **533,** 571-583.

Terentyev D, Viatchenko-Karpinski S, Gyorke I, Volpe P, Williams SC & Gyorke S. (2003). Calsequestrin determines the functional size and

stability of cardiac intracellular calcium stores: Mechanism for hereditary arrhythmia. *Proc Natl Acad Sci U S A* **100,** 11759-11764.

Wang Y, Xu L, Duan H, Pasek DA, Eu JP & Meissner G. (2006). Knocking down type 2 but not type 1 calsequestrin reduces calcium sequestration and release in C2C12 skeletal muscle myotubes. *J Biol Chem* **281,** 15572-15581.

Weber A, Herz P & Reiss I. (1966). Study on the kinetics of calcium transport by isolated sarcoplasmic reticulum. *Biochem Z* **345,** 329-369.

Weber A. (1971). Regulatory mechanisms of the calcium transport system of fragmented rabbit sarcoplasmic rticulum. I. The effect of accumulated calcium on transport and adenosine triphosphate hydrolysis. *J Gen Physiol* **57,** 50-63.

Zambrowicz BP, Friedrich GA, Buxton EC, Lilleberg SL, Person C & Sands AT. (1998). Disruption and sequence identification of 2,000 genes in mouse embryonic stem cells. *Nature* **392,** 608-611.

Zorzato F, Volpe P, Damiani E, Quaglino D, Jr. & Margreth A. (1989). Terminal cisternae of denervated rabbit skeletal muscle: alterations of functional properties of Ca2+ release channels. *Am J Physiol* **257,** C504-511.

ACKNOWLEDGEMENTS

We thank the Charles River Laboratories (Boston, MA), Ronit Hirsch and Santwana Mukherjee (P. D. Allen laboratory) for the technical support in managing the mice colony and the genotyping. We also thank L. R. Jones (Indiana University) and S. Schiaffino (University of Padova) for the generous gift of antibodies used to mark CS, triadin, and MHC in our experiments; Luana Toniolo for the help with single fiber experiments; Giorgio Fanò for the lab space and financial support that have allowed us to start working at the University of Chieti; Dante Tatone for his technical help in setting up our new laboratory in the CeSI bldg. This study was supported by: a) Research Grant # GGP030289 from the Italian Telethon Foundation and Research Funds from the University G. d'Annunzio of

Chieti to Feliciano Protasi; b) FIRB to Pompeo Volpe; c) NIH P01AR AR17605-05 to Paul D. Allen.

TABLE LEGENDS

TABLES

Table 1. ***Average muscle of EDL and Soleus muscle in WT and CS1-null mice.***

	I	II	III	IV	V
Group	***Body weight, g***	***EDL weight, mg***	***Relative EDL muscle weight, %***	***Soleus weight, mg***	***Relative Soleus muscle weight, %***
Wild type	30.1 ± 2.9	9.3 ± 1.4	0.036 ± 0.02	8.8 ± 0.8	0.034 ± 0.02
CS1-null	27.3 ± 2.0‡	7.5 ± 1.2‡	0.028 ± 0.03‡	8.6 ± 1.2	0.033 ± 0.03

Values are shown as Mean ± SD.

‡ Significantly different from Wild type group at P<0.0001.

Table 1. Average muscle of EDL and Soleus muscle in WT and CS1-null mice. *Column I)* CS1-*null* mice show a lower body weight than WT mice of same sex (male) and age (4-6 months, CS1-*null*, n = 211; WT, n = 150; n, number of animals). *Columns II-V)* The weight of EDL and Soleus muscles are shown as absolute value (mg, columns II and IV) and relative to body weight (mg/g, columns III and V). EDL muscles in CS1-*null* mice are on the average 20% smaller than in WT (columns II and III): this difference is highly significant (P < 0.0001). Soleus muscles on the other hand, do not show a significant difference between the two groups (columns IV and V). Data are means and standard deviations of 35 muscles in CS1-*null* mice and 25 muscles in wild type mice.

Table 2. ***Tension development of EDL and Soleus muscles of WT and CS1-null mice.***

		I	II	III
		Twitch tension, mN/mm^2	***Tetanus tension, mN/mm^2***	***Twitch/ Tetanus, ratio***
EDL	***Wild type n=12***	43.5 ± 3.9	168.1 ± 14.3	0.263 ± 0.016
	CS1-null n=14	53.6 ± 6.1	153.3 ± 15.7	0.373 ± 0.020‡
Soleus	***Wild type n=13***	25.1 ± 6.3	169.4 ± 28.7	0.147 ± 0.023
	CS1-null n=17	29.9 ± 4.5	190.6 ± 22.1	0.141 ± 0.009

Values are shown as Means ± SD,

‡ Significantly different at $P<0.05$.

Table 2. Tension development of EDL and Soleus muscles of WT and CS1-null mice. Tension developed during isometric tetanus is not significantly different in the two muscles (column II), whereas twitch tension tends to be higher in CS1-*null* EDL than in WT EDL (column I) and twitch/tetanus ratio is significantly greater (column 3). Means and Standard Errors, ‡$P<0.05$.

Table 3. ***Ultrastructural morphometry of CRUs and mitochondria in EDL and Soleus muscles.***

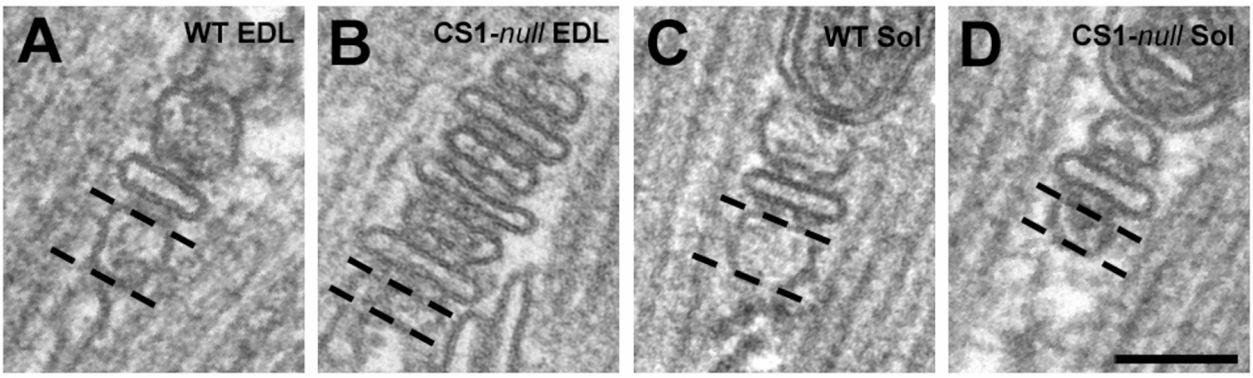

I I I I I I I IV

		Junctional SR width, nm	*No. RyR/ 10μm^2 of sectional area*	*Total SR volume, %*	*No. mitochondria profiles/ 100μm^2 of sectional area*
EDL	***Wild type n=3***	62.4±10.5 (n=716)	39.2±16.7 (n=143)	5.66 ± 1.80 (n=93)	36.3±14.2 (n=98)
	CS1-null n=3	25.0±4.5‡ (n=487)	71.8±26.3‡ (n=111)	5.25 ± 1.95 (n=97)	62.1±21.7‡ (n=125)
Sol	***Wild type n=3***	62.5±11.7 (n=308)	36.0±15.3 (n=54)	/	80.0±18.8 (n=85)
	CS1-null n=3	30.0±5.9‡ (n=404)	32.7±13.9 (n=74)	/	81.4±9.2 (n=132)

Values are shown as Mean ± SD.

‡ Significantly different from Wild type group at P<0.0001.

Table 3. Ultrastructural morphometry of CRUs and mitochondria in EDL and Soleus muscles. *Column I)* The profile of the SR terminal cisternae appear different and its width, measured as shown in the panels

A-D, is much smaller in CS1-*null* than in WT fibers of both EDL and Soleus. In Soleus muscle CRUs are still formed by three elements, whereas junctions in EDL fibers are often formed by multiple elements (panel B). *Column II)* This re-organization of CRUs results in a large increase of RyR content in EDL fibers. *Column III)* On the other hand, the total SR volume (in relation to the total fiber volume) in CS1-*null* fibers is still very similar to that of WT fibers. *Column IV)* CS1-*null* EDLs present also a large increase in the average density of mitochondria, that may be related to the decreased fatigability of these muscles (see Fig. 4). Values are mean ± SD number of RyRs/mitochondria per μm^2 of sectional area (respectively columns II and IV). Bar: A-D, 0.1 μm.

FIGURE LEGENDS

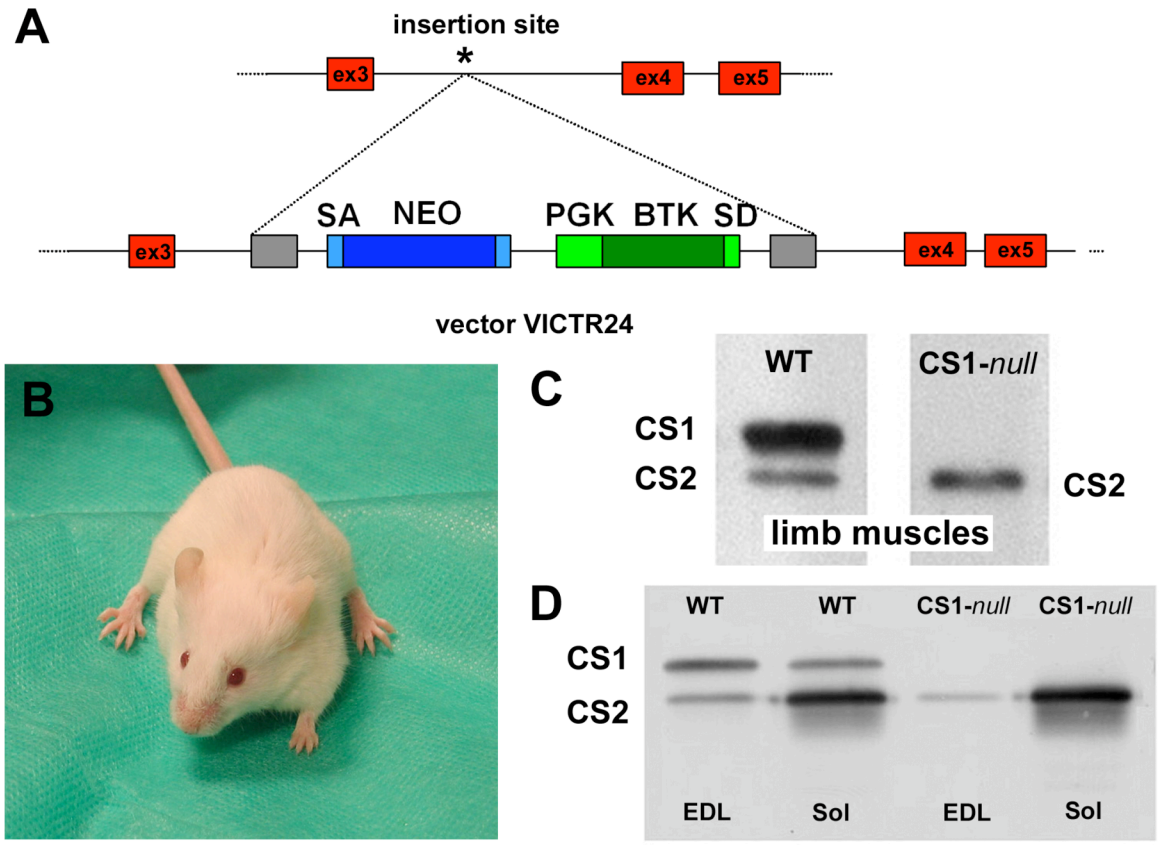

Figure 1. CS1-null mutation is not lethal and no compensatory increase of CS2 is detectable. *A)* The SMCALSE1 gene trap allele was generated, using random insertional mutagenesis with retroviral vector VICTR24. The precise genomic insertion site of the gene-trap vector (asterisk) was determined by inverse genomic PCR. *B)* The CS1-*null* mice do not shown any significant behavioral alteration under standard housing conditions. *C)* Western blot analysis of total homogenates prepared from limb muscles shows that CS1 is missing in CS1-*null* muscle (right lane). *D)* Representative western blots of EDL and Soleus homogenates from WT and CS1-*null* mice: lack of CS1 is confirmed and no sign of compensatory increase of CS2 expression is detectable.

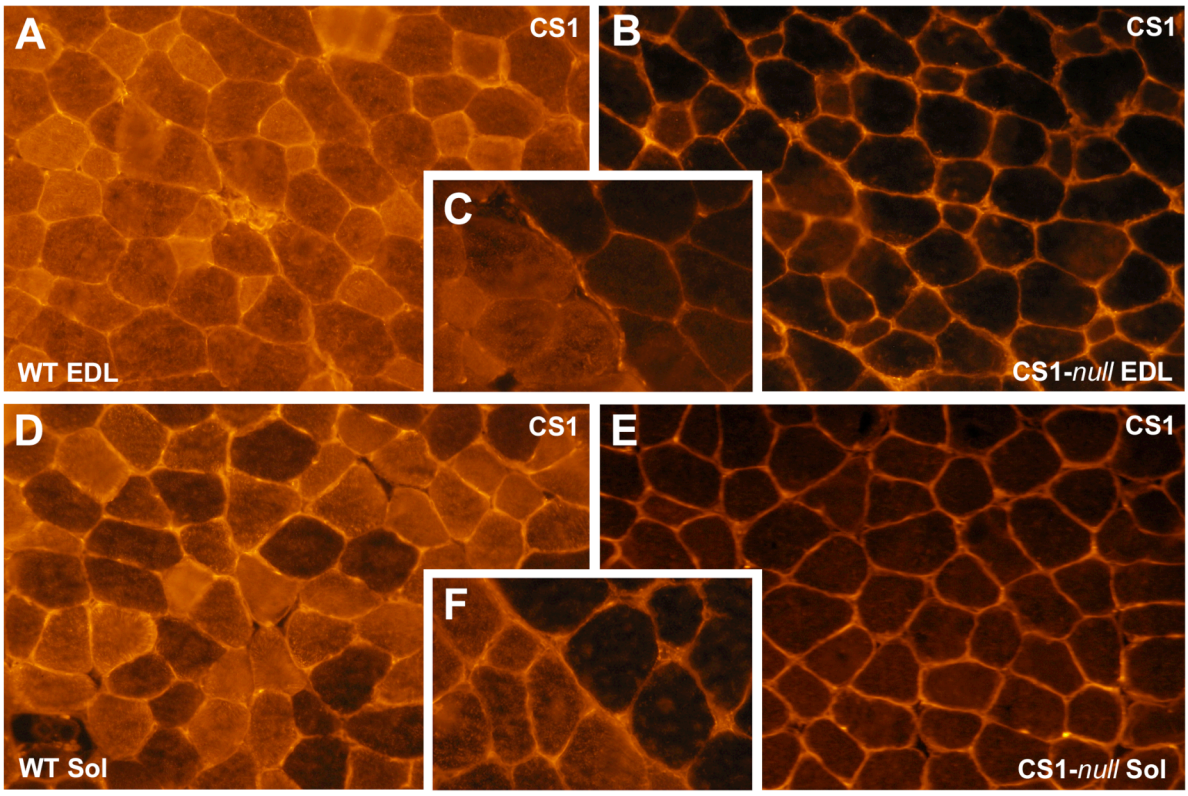

Figure 2. Immunohistochemistry of CS1-null and WT muscles confirms the lack of CS1 in knockout muscles. *A and D)* Immunohistochemistry of transverse sections stained with the antibody specific for CS1 shows that all muscle fibers in WT EDL and Soleus express CS1, even if the levels of expression are variable. *B and E)* Muscle fibers of CS1-*null* EDL and Soleus muscles do not express any CS1. *C and F)* CS1-*null* and WT muscles frozen next to one another and visible within the same sections.

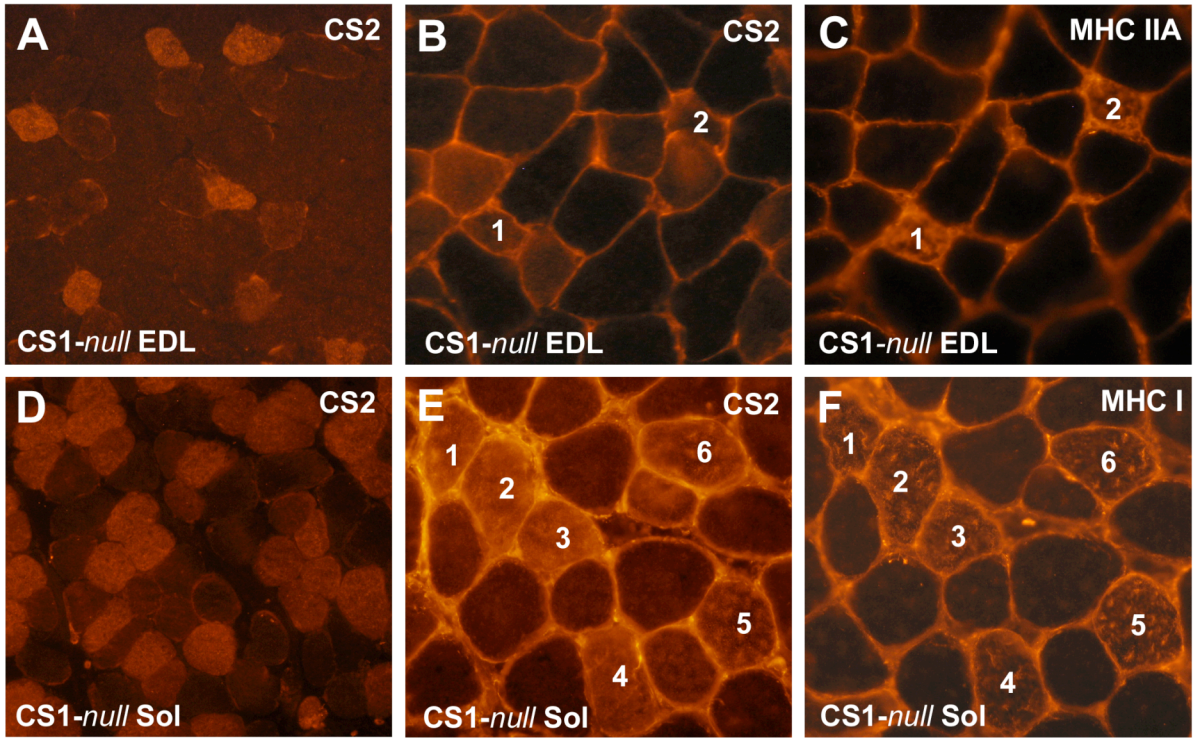

Figure 3. CS2 is confined to a subpopulation of fibers, some of which are type IIA in EDL and mostly type I in Soleus. *A and D)* CS2 is not expressed in all fibers, but confined to a subpopulation of them, rare in EDL (5 to 20%), but abundant in Soleus (40-50%). *B-C and E-F)* In Soleus muscle, CS2 is mostly expressed in type I fibers, whereas in the EDL CS2 appears to be confined mostly to smaller fibers, some of which are type IIA. Corresponding fibers in the different sections are marked with the same numbers in paired panels.

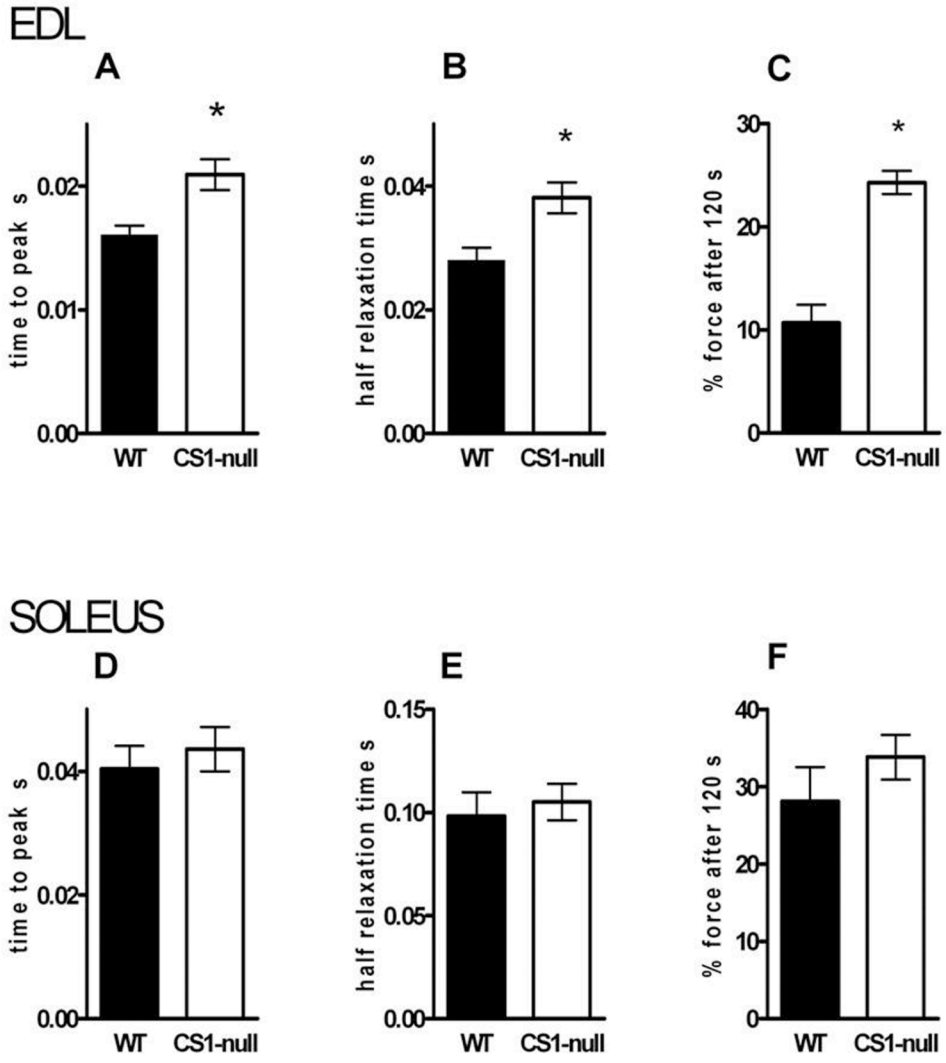

Figure 4. CS1-null EDL, but not Soleus, muscles show slower contraction kinetics and higher resistance to fatigue. Time to peak tension and half relaxation time are prolonged in CS1-*null* EDL (A and B), but not in Soleus (D and E) compared to WT. Force still developed after 120s of stimulation with the fatigue protocol is much greater in CS1-*null* EDL but not in Soleus (C and F) compared to WT. Values are Means ± Standard Errors. * $p<0.05$.

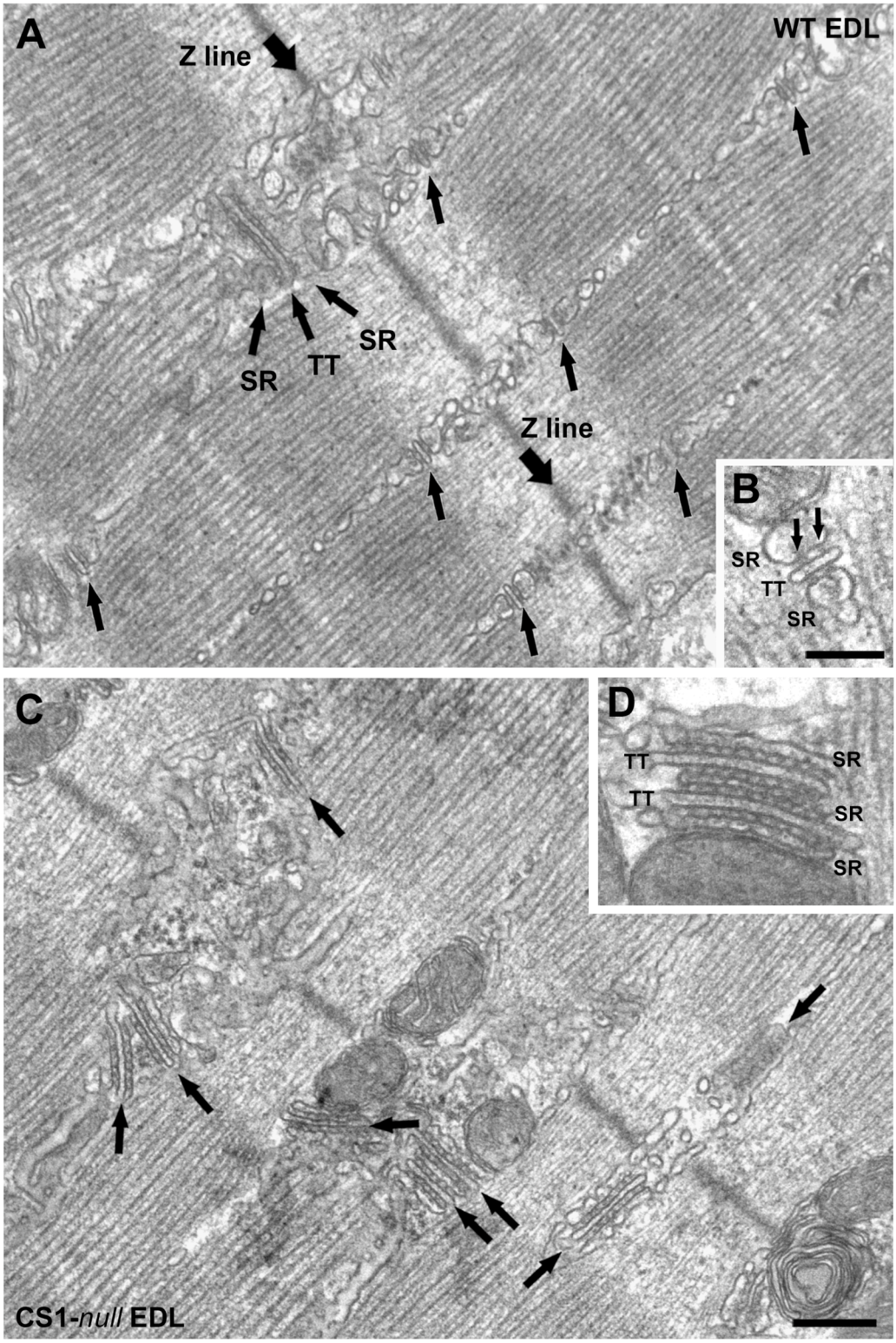

Figure 5. CRUs in CS1-null EDL muscle are usually formed by multiple elements, which often contain multiple rows of RyRs. *A)* CRUs in WT EDL are usually transversally oriented, evenly distributed within the fibers, and formed by three elements, i.e. triads (arrows). *B)* RyRs, the Ca^{2+} release channels of the SR, in WT muscle usually form two rows (small arrows). *C)* In CS1-*null* fibers the T-tubules often change

direction forming CRUs that are more variably oriented (arrows). *D)* CRUs are often formed by multiple elements and couplons usually contain more than two rows of RyRs. The lumen of the SR terminal cisternae appears significantly narrower than in controls (compare panels B and D). Bars: A and C, 0.25 um; B and D, 0.1 um.

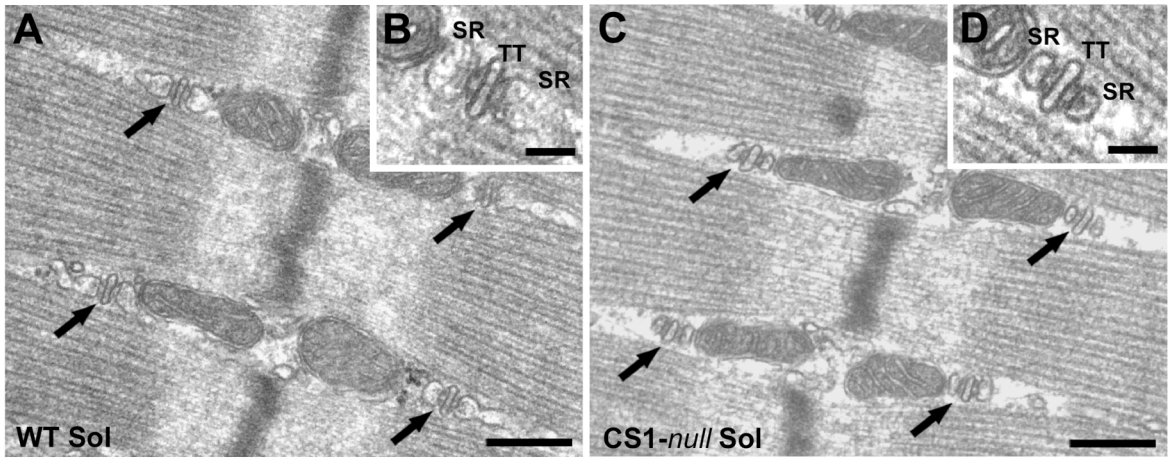

Figure 6. CRUs in CS1-null Soleus muscle maintain the triadic structure, but the terminal cisternae appear much smaller. In CS1-*null* fibers from Soleus muscle (C and D), CRUs are mostly in the form of triads, as in WT Soleus muscle (A and B), and maintain their normal location and orientation at the edges of the sarcomeric A band. The width of the SR terminal cisternae is, though, visibly smaller than in CS1-*null* fibers (B and D). Bars: A and C, 0.25 um; B and D, 0.05 um.

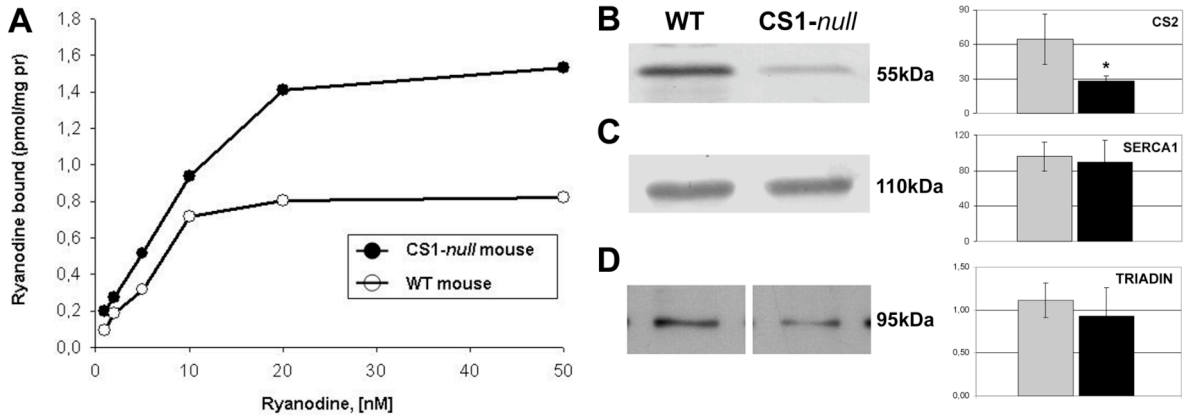

Figure 7. RyR expression, but not CS2, SERCA1, and triadin, is upregulated in EDL muscle. Binding of ^{3}H-ryanodine shows that the B_{max} is approximately doubled in CS1-*null* mice samples as compared to WT

samples, whereas the K_d is virtually unchanged. Each data point represents the average of duplicate determinations. B_{max} and K_d values are calculated by Scatchard plot analysis with Enzifitter version 1.03 Elsevier Biosoft program. *B-D)* Quantitative analysis of total homogenates from WT and CS1-*null* EDL muscles (left panels) and graphical representation of the mean values of densitometric signals (right panels, arbitrary units). Data plotted in the bar graph are expressed as means ± SD for n=4 WT EDL and n=4 CS1-*null* EDL. Densitometric analysis shows a decrease of expression of CS2 in CS1-*null* EDLs, whereas SERCA1 and 95kDa triadin contents are not significantly changed.

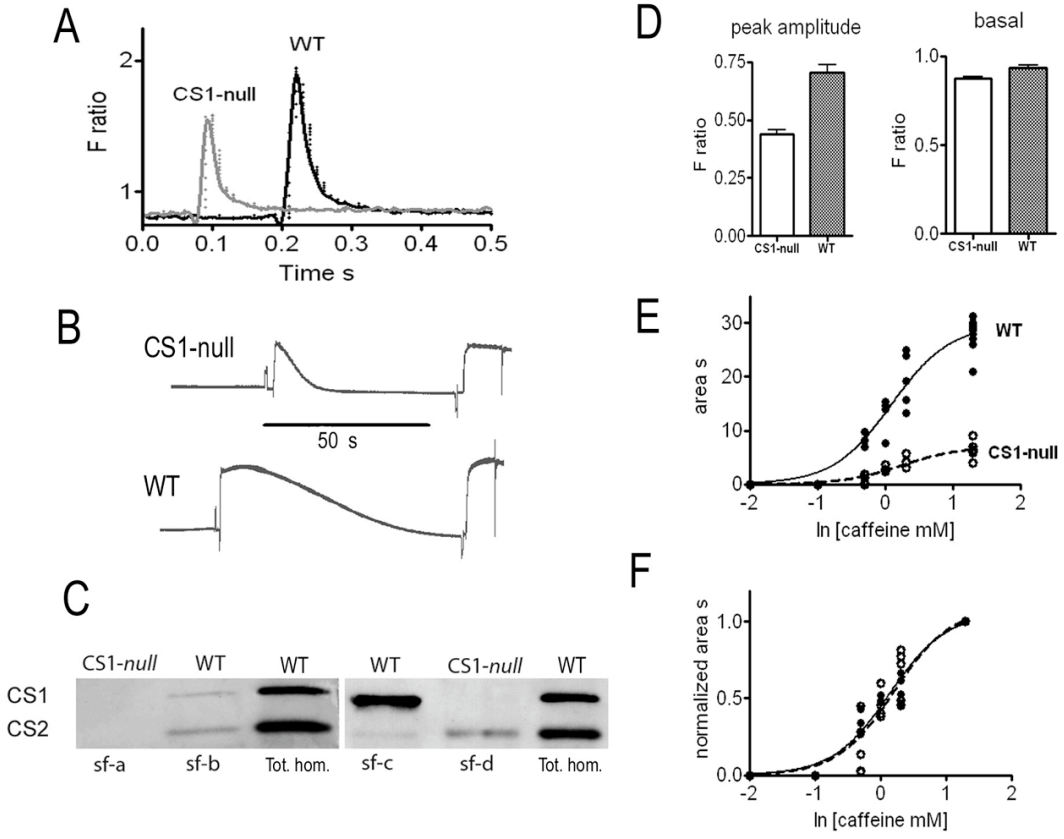

Figure 8. Calcium transient amplitude and calcium release in response to caffeine in single muscle fibers. A and D) CS1-*null* single muscle fibers display similar basal cytosolic free Ca^{2+} concentrations, but significantly smaller Ca^{2+} transients induced by electrical stimulation compared to WT fibers. Fura 2AM is used as cell permeant free Ca^{2+} indicator (see Methods). B) The amount of Ca^{2+} released by caffeine (20 mM) from the SR of single fibers permeabilized with saponin is

significantly smaller in CS1-*null* than in WT. The amount of Ca^{2+} released is evaluated by the tension-time area of the response to caffeine (see dose-response curve in E and F). E) The curves in panel E correspond to the equation Y=T/(1+10^(logEC50-X)) where T=7.06±0.41 and logEC50=0.24±0.08 for CS1-*null* and T=29.71±1.19 and logEC50=0.09±0.06 for WT: the difference between the T values of CS1-*null* and WT is statistically significant. F) The dose response curve for tension-time area normalized to the highest value reached with maximal caffeine concentration indicates no difference between CS1-*null* and WT. C) After all single fiber experiments, the presence of CS isoforms has been verified in each fiber with Western blot. Examples of Western blot on single fibers (sf) are shown in comparison with total homogenate from WT FDB muscles. Only fibers lacking both CS1 and CS2 (as sf-a) have been used for comparison with WT fibers.

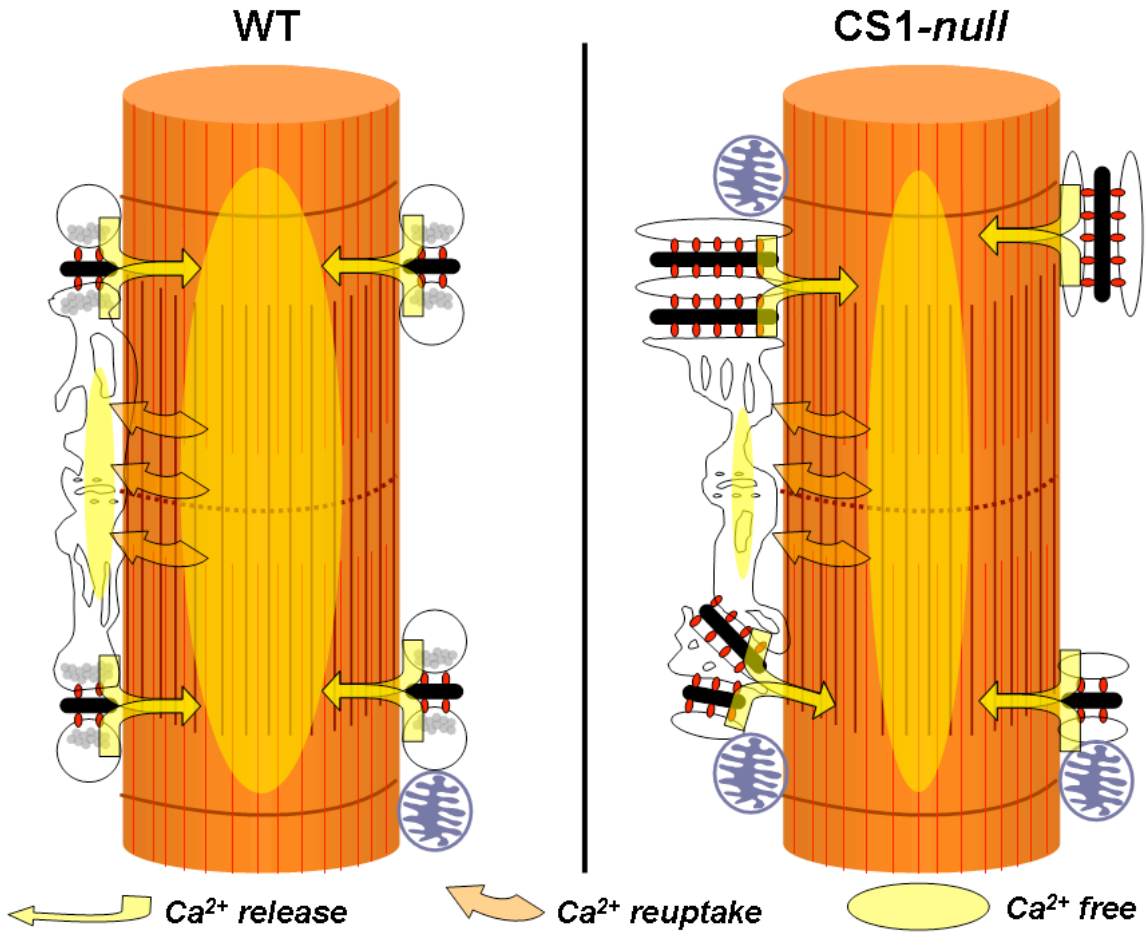

Figure 9. Cartoon showing the structural and functional modifications occurring in fast twitch muscle fibers following the

removal of CS1. Ultrastructural features of CRUs in CS1-*null* EDL fibers differ from those of WT muscle: junctions are often multilayered and longitudinal. RyR-feet and mitochondria are also increased in number (see also Fig. 5 and Table 3). Mitochondrial proliferation likely explains the surprising increase in fatigue resistance in CS1-*null* EDL (Fig. 4). Experiments in single fibers and in skinned fibers suggests that Ca^{2+} transient and total SR Ca^{2+} content (see ovals) are reduced in CS1-*null* muscle (see also Fig. 8). Abbreviations used: CS, calsequestrin; CRUs, calcium release units; SR, sarcoplasmic reticulum; RyRs, ryanodine receptors.

CHAPTER 2

CALSEQUESTRIN-1: A NEW ACTOR IN MALIGNANT HYPERTHERMIA-LIKE EPISODES UNDER CHALLENGING ENVIRONMENTAL AND ANESTHETICS CONDITIONS

Authors:

[2]**Marco Quarta** and, [1]Marco Dainese , [1]Cecilia Paolini, , [2]Marta Canato, [4]Paul D. Allen, [3]Robert T. Dirksen, [2]Carlo Reggiani, and [1]Feliciano Protasi.

Affiliations:

[1&2]IIM Interuniversity Institute of Myology; [1]Ce.S.I. Centro Scienze dell'Invecchiamento, University G. d'Annunzio, I-66013 Chieti Italy; [2]Dept. of Anatomy and Physiology, University of Padova, I-35131 Padova, Italy; [3]School of Medicine and Dentistry, University of Rochester, NY 1464 [4]Dept. of Anaesthesia Research, Brigham and Women's Hospital, 02115 Boston MA.

ABSTRACT

Our recently published results in mice lacking skeletal calsequestrin (Paolini et al. 2007, *J. Physiol.* 583:767) indicates that, in fast twitch fibers, CS1 is important for SR structure, Ca^{2+} storage and possibly to facilitate Ca^{2+} release. Because mutations/ablation in CS2 result in a phenotype reminiscent of that caused by mutations of RyR2 in cardiac muscle (CPVT), it is possible to hypothesise that mutations in CS1 may result in a similar myopathy as mutations in RyR1 in skeletal muscle (*MH and/or CCD*). We tested *in vivo* the sensitivity of CS1-*null* mice to heat-stress and to exposure to halothane. Surprisingly, both treatments were lethal in the majority of CS1 null mice, whereas identical treatments were well-tolerated by WT mice. The symptoms were remarkably similar to those described as *fulminant malignant hyperthermia (MH) episodes* in knock-in mice carrying RyR1-MH mutations (Chelu et al. 2006, *Faseb J.* 20:329; Yang et al. 2006, Anesthesiology 105:1164), suggesting that ablation of CS1 could indeed cause a syndrome similar to MH. To determine if these crisis were associated with functional alteration of skeletal muscle similar to MH muscle, we performed *in vitro* studies of adult EDL muscles and FDB fibers over a temperature range of 25-45°C. Whereas in CS1-*null* specimens, there was a balance between Ca^{2+} release and uptake at low temperatures, above 37°C Ca^{2+} accumulates in the cytosol causing progressive contracture while in *Wt* the balance between uptake and release was maintained for a wider range of temperature. These results may advance our understanding of the molecular mechanisms leading to malignant hyperthermia (MH) in humans and possibly provide an alternative genetic locus for linkage studies.

INTRODUCTION

In muscle, rapid changes in intracellular Ca concentration [Ca], or Ca transients, control the contraction and relaxation of myofibrils. However, prolonged elevation of intracellular [Ca] above 10 microM is deleterious to the cell life and can activate apoptosis. There is thus a narrow window of Ca dysregulation that can cause muscle disease rather then apoptosis. It is well recognized, in fact, that pathological conditions affecting cardiac muscle (i.e. cardiac arrhythmias, heart failure, etc.) or skeletal muscle (i.e. malignant hyperthermia, MH, central core and multi-minicore diseases, CCD and MmD, etc.) result from altered intracellular Ca levels and have been associated with expression abnormalities, or mutations, of proteins involved in excitation-contraction (EC) coupling (9-11), the mechanism that controls the release and re-uptake of Ca from the internal stores. An extremely well organized system of tubules and vesicles, collectively named sarcotubular system, is able to finely control the cytoplasmic calcium (Ca) concentration (1, 2) and relies on a macromolecular complex containing numerous proteins. Ryanodine receptors (RyRs) and calsequestrin (CS) are two of the major players involved in this mechanism: the RyRs are the release channels located in the junctional domains of the SR terminal cisternae (5, 6) which in turn contains CS, a Ca binding protein (7, 8) that increases the capability of the SR to store the Ca needed to activate muscle contraction. CS location indicates a close proximity with RyRs and many studies suggest that CS is likely involved in modulating the activity of the Ca release channels (42-44).

It has been found that abnormalities in the skeletal muscle Ca release channel, RyR1, play a key role in MH, a toxic response to anesthetics (9-13), and in CCD, a skeletal myopathy characterized by hypotonia and proximal muscle weakness (14-16). Whereas various other diseases have been also associated to proteins involved in EC coupling and Ca handling, so far no specific skeletal myopathy has been associated with CS mutations and/or deletions.

MH, a clinical syndrome in which genetically susceptible individuals respond to inhalation of anesthetics (e.g. halothane) and muscle relaxants (e.g. succinylcholine) with attacks of extreme elevations in body

temperature, skeletal muscle rigidity, hypermetabolism, lactic acidosis, hypoxia and tachycardia (12-14). MH episodes are life threatening if not corrected immediately by suspension of triggering agent, hyperventilation, and treatment with dantrolene.

However, only ~50-80% of MH families can be linked to the RyR1 gene (11). Consequently, alternative candidate genes for MH have been proposed. A second MH locus has been mapped to the gene encoding for the skeletal alpha$_1$ subunit of the DHPR, a protein which interacts both functionally and structurally with the RyR1 during skeletal EC coupling. It is extremely interesting that mutations in both alpha$_{1S}$ DHPR and RyR1 generate a similar phenotype (24).

Taking this into consideration, it is possible to hypothesise that mutations and/or alteration in expression level of other proteins that interact with RyR1 during EC coupling, and that modulate its activity, could give rise to a MH phenotype. In this view, Calsequestrin is one of the most interesting candidates. Other significant findings in literature actually support this hypothesis. In cardiac muscle, for example, catecholaminergic polymorphic ventricular tachycardia (CPVT) - a rare arrhythmogenic disorder characterized by syncopal events and sudden cardiac death at a young age during either physical stress or emotion - has been associated with mutations or ablation of genes encoding for both the cardiac RyR and CS (RyR2 and CS2) (60-64). These results, showing how mutations in RyR2 and mutation/ablation of CS2 give rise to the same phenotype (CPVT), suggest the possibility that mutation of RyR1 and ablation of CS could indeed generate a similar myopathy (MH).

In the present study we show that deletion of CS1 results in an increased susceptibility of null-mice to lethal MH-like episodes in response to challenging environmental conditions and to anesthesia. These results may advance our understanding of the molecular mechanisms leading to malignant hyperthermia (MH) in humans and possibly provide an alternative genetic locus for linkage studies.

Materials and METHODS

A – In vivo experiments

Animals

Mice carrying null mutation of CS1 gene were obtained as described in Paolini et al 2007. C57BL/6J mice were obtained from the Charles River Laboratories Boston, MA. The animal were housed in single cages at 20 °C with 12 light hours. They were allowed to eat and drink ad libitum. All experiments involving animals were conducted according to the National Institutes of Health Guide for the Care and Use of Laboratory Animals and were approved by the animal welfare coordinator of our institution.

Halotane Exposition

Mice were exposed to air mixed with 3% Halotane(Sigma Aldrich, Italy). This air mixture had been obtained through an evaporator Isotec 3 (Datex-Ohmeda, GE Healthcare, Wauwatosa, Wisconsin, USA), and is sufficient to induce stage 3 anesthesia. The anesthesia chamber was warmed to 31°C to maintain normal body temperature in anesthetized mice. Each experiment was carried out simultaneously on WT and CS1 mice in adjacent chambers. The respiratory rate and behaviour were monitored visually during anesthesia. The mice were exposed for 1 hour and then the mice who survived were brought back in the normal conditions of stabulation. The rigidity was manually tested by limb resistance after the animal death.

We tested 14 male CS1-Null mice versus 9 male WT mice, and 13 female CS1-Null mice versus 12 female WT mice.

Heat stress

WT mice and CS1-null mice were exposed to thermal stress in a test chamber equilibrated at 41°C. The exposure was prolonged until start of

the crisis in the CS1-null animals and in all cases not longer than 60 minutes; then the survived animals were brought back to the normal conditions of stabulation and monitored for 24 hours. The rigidity was manually tested by limb resistance after the animal death.

We tested 12 male CS1-Null mice versus 12 male WT mice, and 8 female CS1-Null mice versus 6 female WT mice.

Inner Temperature

Mice's inner temperature was monitored using a rectal thermocouple, type K, connected to a digital thermometer (Tm-946). Mice were anesthetized with Ketamine, which does not trigger MH episodes. Two minutes following ketamine injection, mice were placed in an environmental chamber at 41°C. The initial core body temperature was recorded, and the temperature was monitored over all exposition every minute thereafter.

Dantrolene

In a small group of male CS1-null mice 4 mg/kg dantrolene was intraperitoneally administered to test the preventive activity.

Blood Analysis

Blood for baseline was collected from WT and CS1-null mice immediately after cervical dislocation by guillotine. The blood for tested animals was collected *via* cardiac puncture after the first signs of MH-like crisis.

B – Histology and Electron Microscopy

An MH-like episode shows up as an extremely fast chain of events. During the crisis, the CS1-*null* mouse starts getting stiff while the WT mouse is still moving normally. By the end of the episode, when the CS1-*null* mouse dies and the WT is still alive, the morphology analysis was performed on dissected muscles of both mice at the same time. EDL and Soleus

muscles were carefully dissected and fixed at room temperature in 3.5% glutaraldehyde in 0.1M Na cacodylate buffer, pH 7.2 for at least 2 h. Small bundles of fixed fibres were washed overnight in 0.1M Na cacodylate buffer and then postfixed in 2% OsO4 in the same buffer for 2 h, and block-stained in aqueous saturated uranyl acetate. After dehydration, specimens were embedded in epoxy resin (Epon 812). For histological analysis semithin sections were cut with a Leica Ultracut R microtome (Leica Microsystem, Vienna, Austria) using a Diatome diamond knife (DiatomeLtd. CH-2501 Biel, Switzerland). After staining with Toluidine Blue dye, the sections were viewed on a fluorescence microscope Leica DMLB (Leica Microsystem, Vienna, Austria). For electron microscopy, ultrathin sections were cut and then, after staining in 4% uranyl acetate and lead citrate, examined with a Morgagni Series 268D electron microscope (FEI Company, Brno, Czech Republic), equipped with Megaview III digital camera.

C - Ex vivo and in vitro experiments

Force and contraction kinetics of isolated intact Soleus and EDL. Soleus and EDL muscles were dissected from hind limb of WT and CS1-*null* mice in warm oxygenated Krebs solution and mounted between a force transducer (AME-801 SensorOne, Sausalito, California) and micro-manipulator controlled shaft in a small chamber where oxygenated Krebs solution was continuously circulated. Temperature was kept constant at 25°C. The stimulation conditions were optimized and muscle length was increased until force development during tetanus was maximal. Then, the responses to a single stimulus (twitch) or to a series of stimuli at various rates producing unfused or fused tetani were recorded. Time to peak tension, time to half relaxation and peak tension were measured and first derivative of tension was calculated in single twitches. Tension was measured in completely fused maximal tetani and twitch/tetanus ratio was determined. The resistance to fatigue was tested by stimulating the muscles with a fatiguing protocol based on 0.5s fused tetani with 1:4 duty ratio (low frequency fatigue). To assess the response to high temperature, muscles were exposed to stepwise increasing temperature by 2 degree

every 5 minutes keeping muscle paced at low frequency. For caffeine contracture, muscles were regularly paced at low frequency at 25° and exposed to caffeine concentrations progressively increasing with steps of 3 minutes.

Primary cultures of myoblasts and myotubes. Primary myoblast cultures were derived from hind limb muscles of a 1-5 days old WT and CS1-*null* mice. Muscle cells were dissociated by enzimatic digestion with trypsin (Sigma Aldrich, Italy) and of collagenase type I (Sigma Aldrich, Italy) solution at 37°C until the mixture is a melted slurry. Cells were grown on collagen type I-coated chip in Ham's nutrient mixture F-10 (Gibco BRL, Life Technologies, Germany) supplemented with 20 % horse serum (Gibco BRL, Life Technologies , Germany) and penicillin-streptomycin (100 U and 100 µg ml^{-1}, respectively; Sigma, Italy). To induce cells differentiation and myotube fusion the medium was replaced, 1 day after the plating, with DMEM (Sigma Aldrich, Italy) fusion medium supplemented with 2% heat-inactivated bovine serum (Gibco BRL, Life Technologies , Germany), 2mM L-glutamine, 100U/ml penicillin, 100µg/ml streptomycin, and 100µg/ml gentamycin (Sigma Aldrich, Italy). Cells were maintained at 37°C in a humidified atmosphere with 5% CO_2.

[Ca^{2+}] Imaging. $[Ca^{2+}]_i$ was measured in primary myotubes loaded with the Ca^{2+} -sensitive intracellular probe fluo-4 (Molecular Probes, Invitrogen). Briefly, cells were loaded with 3µM fluo-4 in incubation buffer (125mM NaCl, 5mM KCl, 1mM $MgSO_4$, 1mM KH_2PO_4, 5.5mM glucose, 1mM $CaCl_2$, 20mM Hepes and 1% bovine serum albumine, pH 7.4 with NaOH) for 30 min at 37°C. After loading with Fluo-4, cells were washed twice for 10 minutes with incubation buffer without BSA at 37°C to retain the indicator in the cytosol. After a minimum of 30 minutes calcium signals were recorded.

Cells were then moved to the experimental set up. For calcium imaging recording we used an upright Olympus BX51W and water immersion objectives (LumPlanFI 40x/0.8 water and LumPlanFI 10x/0.3 water) with large numerical aperture. Excitation light intensity was minimized via

neutral density filters, according to required time sampling, to reduce fluorophore's photobleaching. Data were collected with a cooled CCD camera (Leica DFC 350FX).

For basal calcium measurements at increasing temperature, an incubator cell chamber (Nikon Instruments, USA) equipped with a peltier temperature controller was used. Myotubes were studied at 8 days after starting differentiation. For Caffeine induced [Ca^{2+}] release, caffeine concentrations were increased every 2 minutes by circulating the cell culture medium. To compare calcium transients in different cells time sequences were normalized to first frame acquired (F0), in order to get rid off of photobleaching and F0 was subctracted from sequence by means of Image-Pro 6.0 (MediaCybernetics, USA) to measure only intensity increase. Then a ROI was selected in nuclear, perinuclear and cytoplasmatic regions and time measurement analysis was carried out with NIS-Elements A.R. 2.30 (Nikon Instruments, USA).

Western blot analysis of differentiated myotubes. Cells were washed in PBS at 37°C, then they were left in lysis buffer (1% SDS, 100mM beta mercaptoethanol, 10 mM Tris, pH 8) for 30 min. The lysate was collected and boiled for 5 min. The lysate was resuspended through a 20-gauge and 26-gauge needles repeatedly. It was then centrifuged at 10000 g for 10 min and the supernatant was collected. For each sample, 20 ug of total protein were loaded on a 8% SDS-polyacrylamide gel, electrophoresed and transferred to nitrocellulose. Immunostaining of blots was performed using the following primary antibody: rabbit polyclonal antibody reactive with both isoforms of CS (Affinity Bioreagents, USA); secondary antibody was antirabbit AP-conjugated antibodies (SIGMA, Italia). Densitometric scans were analysed with Scion Image Software to quantify protein band intensities. Normalization was performed with the total protein concentration for CS or to Ponceau Red staining, using QuantityOne Software from Bio-Rad Laboratories (Hercules, CA, USA).

RESULTS

A – ANIMAL MODEL

CS1-NULL MICE DO NOT OVEREXPRESS CS2). The time-course of disappearance of cardiac CS and that of appearance of the skeletal CS isoform has been already investigated by Sacchetto et al. (1993) in developing fast-twitch fibers from rabbit (Fig. 1 A). We performed a similar analysis in fast twitch-fibers from WT and CS1-*null* mice (Fig. 1 B and C). Decrease in the expression of cardiac CS (CS2) in EDL fibers in mice takes place at a critical period (within the first month of age) during post-natal maturation in both WT and CS1-*null* muscles. In WT fibers, CS2, very abundant in neonatal stages, is almost completely replaced by the skeletal isoform during post-natal maturation. Meanwhile, the accumulation of CS1 to reach adult levels around two months of age. In CS1-*null* muscles, the expression pattern for CS2 is very similar and no signs of compensatory increase are detected.

UNUSUALLY HIGH INCIDENCE OF SPONTANEOUS MORTALITY IN CS1-NULL MICE. We initially noted that the average life expectation of CS1-null mice is reduced compared to WT mice, due to sudden death of up to 50% of male mice in the colony between the age of 3 and 12 months. We have then closely monitored the incidence of spontaneous mortality and noted these deaths are mostly observed between 3 and 10 months of age with the highest rate after 6 months of age (see Fig. 2). Interestingly, most deaths were observed in male CS1-null mice while in reproductive cages.

B – INCREASED SUSCEPTIBILITY OF CS1-NULL MICE TO MH AND EHS EPISODES.

CS1-NULL MICE UNDERGOES MH/EHS-LIKE EPISODES FOLLOWED BY SUDDEN DEATH WHEN EXPOSED TO CHALLENGING ENVIRONMENTAL CONDITIONS (41^{o}C) OR TO AN HALOGENATED ANESTHETIC (HALOTHANE).

Heat stress. The sudden deaths observed under standard housing conditions bore some resemblance to the spontaneous triggering of MH/EHS episodes in animal models of this disease (Gallant and Lentz, 1992; Chelu et al. 1006; Yang et al., 2006). Thus, to search for the cause of these events, we initially selected a heat sensitivity test following the experimental approach described in Chelu et al. (2006) (66). We compared the effects of warming on WT and CS1-null mice, placed in parallel inside a heating chamber in which temperature was constantly kept at 41°C. In 8 out 12 CS1-null male mice heat-stress triggered lethal EHS-like episodes characterized by gasping, impaired movement, spasmodic contractions of the whole body, arched back followed by death (Figs. 3 and 4). The EHS-like lethal crisis lasted no longer than few minutes (5-10) and were usually triggered within 30 minutes from beginning of exposure to heat. During and after the crisis CS1-null mice presented a diffuse muscle rigidity. Identical heat challenge was well-tolerated in WT mice (Fig. 4).

Other observations: a) before the episodes, CS1-null mice always displayed an abnormal behaviour compared to controls (i.e. extremely restless); b) females were more resistant that males; c) after bringing back mice to room temperature, some delayed death (within 24 hours) was observed (2 males, 2 females – Fig. 4). These lethal episodes were remarkably similar to those described as fulminant MH episodes by Chelu et al., 2006 (66). In those experiments, heterozygous knock-in mice carrying a specific MH mutation in the RyR1 gene exhibited increased susceptibility to heat- and anesthetic-induced fulminant MH episodes characterized by full body contractions, hyperthermia, agonal breathing, and rhabdomyolysis (Fig. 3).

Halothane sensitivity and effect of pre-treatment with dantrolene

The sensitivity of CS1-null mice to a halogenated anesthetic (halothane), which is known as a *triggering agent* in human subject which are MH susceptible, was also tested. Also in this case, CS1-null animals (mostly males) showed a very high mortality rate during the treatment (Fig. 5): halothane exposure (2% for 1 hr) was lethal in 85% of CS1-null male mice (12 out of 14). Temperature of the chamber was kept at 31^{o}C during the

anaesthesia to avoid any drop in body temperature. Same treatment was well tolerated by WT animals.

Other observation: those CS1-null animals which did not die during treatment (mostly females), awakened from anaesthesia in a considerably longer time compared WT animals (about 15 vs. 5 min).

Preliminary data were collected to determine if pre-treatment with dantrolene (4 mg/kg) - used in humans to treat MH episodes - is protective against the MH-like crisis (Fig. 5): 5 out of 5 CS1 null male mice survived the to halothane anaesthesia (2% for 1 hr).

SKELETAL MUSCLE FIBERS OF CS1-NULL MICE ARE SEVERELY DAMAGED DURING LETHAL CRISIS INDUCED BY HEAT STRESS. During the EHS-like crisis, the CS1-null mice showed impaired movement, and spasmodic contractions, whereas WT animals kept in the same chamber were still moving normally. At the end of the lethal episode, both EDL and Soleus muscles from CS1-null mice which just died (3 animals) and from WT controls (3 animals), after sacrificing them by cervical dislocation, were quickly dissected. The samples were examined both at the light - and electron-microscopy and about 50% of the fibers in the sample were found severely damaged (asterisks in Fig. 6 A). The EM analysis revealed severe structural alterations, including disarrangement of the myofibrils, misalignment of the Z lines, zones of over-stretched myofilaments accompanied with complete loss of the M line, swelling of the sarcoplasmic reticulum, etc. In Fig. 6 B a regions showing areas of excessive contractures (grey arrows) and areas of over-stretched sarcomeres (red arrows). These alterations were never present in WT mice exposed to the same treatment and sacrificed immediately after Heat-stress treatment.

DISSECTED EDL MUSCLES AND CULTURED PRIMARY MYOTUBES FROM CS1-NULL MICE ARE MORE SENSITIVE THAN WT MUSCLES AND MYOTUBES TO INCREASING TEMPERATURES Both fast and slow muscles (EDL and Soleus) were dissected from 4 month old CS1-null mice and exposed to increasing temperatures while recording tension. EDL muscles from knockout animals started developing tension - which finally resulted in a contracture

- at lower temperature (30°C) than WT EDL muscles, which never showed contractures at temperature lower than 40°C (Fig. 7, left panel). Also CS1-null Soleus showed a higher sensitivity to temperature than WT, but lower sensitivity than EDLs. This is in accord with previous data showing EDL being more affected than Soleus by the knockout, both structurally and functionally (see above and Paolini et al., 2007 for more detail). We also performed preliminary experiments on cultured primary myotubes (8 days of differentiation). CS1-null myotubes displayed a progressive increase in intracellular [Ca] with increasing temperatures (Fig. 7, right panel), whereas in WT myotubes the increase in intracellular Ca levels only started at temperature higher than 40°C.

Other observations: a) at high temperature CS1 myotubes started to contract and to develop striking morphological alterations as effect of the heat-stress challenge (data not shown); b) similar but smaller effects were also observed in WT myotubes, but at significantly higher temperature (starting from 50°C).

C –EVIDENCE IN FAVOUR OF A SKELETAL MUSCLE MYOPAPHY IN CS1-NULL MICE.

CS1- NULL MICE DISPLAYED MUSCLE ATROPHY AND WEAKNESS.

Muscle atrophy. CS1-null mice were on the average slightly smaller than age-matched Wt animals (Fig. 8 A): in fact, the average body weight of CS1-*null* mice was about 10% lower when compared to the WT group: 27.3 g *versus* 30.1 g (male animals, age 4–6 months, *n*, number of animals: CS1-null, *n* =211; WT, *n* =150; *P* <0.0001). The smaller overall weight of the null mice was the result of a reduced mass of fast-twitch muscles (Fig. 8 B) which, in the mouse represent the majority of skeletal muscles: the average muscle/body weight ratio of the fast-twitch muscle

EDL in CS1-*null* mice was significantly lower than in WT mice of same sex and age: 0.036 ± 0.02 mg/g of WT mice compared to 0.028 ± 0.03 mg/g of CS1-*null* mice (*P* <0.0001). See Paolini et al., 2007 for more detail. The muscle atrophy was likely the direct result of a reduced cross sectional area of the fibers (Fig. 8 C): the average cross sectional area for CS1-*null* fibers of EDL was significantly lower when compared to the WT: 18018 ± 8264 pixels^2 of WT *versus* 11091 ± 5573‡ pixels^2 of CS1-*null* fibers (CS1-*null*, *n* = 1684; WT, *n* = 1279; *n*, number of measurements).

Muscle weakness. Grip test is a simple and non invasive method to test the mice muscle strength by sensing the peak force that animals apply in grasping an especially designed pull bar. A reduction in grip test performance is an indication of a general functional impairment of muscle performance. CS1-null mice showed a significant hypotonia when compared to age-matched WT animals: 0.042±0.011 volt/weight for CS1-*null* mice, versus 0.056±0.013 volt/weight for WT mice (*n*, number of animals: CS1-*null*, *n* =8; WT, *n* =11; *P* <0.0001; Table I, column D).

AFTER 1 YEAR OF AGE, SEVERAL EDL FIBERS DISPLAYS ABNORMAL ALTERATIONS, WHICH RESEMBLES ABNORMALITIES DESCRIBED IN HUMAN MYOPHATIES. Preliminary analysis of EDL fibers of 1.2 and 1.7 years old mice, revealed morphological alterations, which may be early signs of a developing myopathy. These alterations were not found in muscles from age-matched controls. Preliminary EM examination (Fig. 10) revealed various abnormalities: swollen/disrupted mitochondria (C); convoluted nuclei, with dispersion of chromatin, and lysosome vacuoles; areas with abnormal clustering of mitochondria and disrupted myofibrils, etc.

DISCUSSION

Calcium release from SR and subsequent reuptake is perfectly controlled and balanced to allow calcium-induced force generation but also to avoid the development of deterious calcium-mediated processes, such as excessive activation of calcium-stimuated proteolys or mitochondrial calcium overload.

Calcium dysregulation in skeletal muscle cells leads to apotosis and muscle disease and is often causally related with mutations of calcium related proteins. Mutations of the calcium release channel, RyR1, play a key role in Malignant Hypertermia (MH), a toxic response to anesthetics (9-13), and in Central Core Desease (CCD), a skeletal myopathy characterized by hypotonia and proximal muscle weakness (14-16). However, whereas CCD is primarily associated with mutations in RyR1, only ~50-80% of MH families can be linked to the RyR1 gene (11). Consequently, alternate candidate genes for MH have been proposed. Analysis of the human DNA sequence has allowed to associate families affected by MH with nearly 70 distinct mutations of the gene encoding for RyR1, located on the chromosome 19q (11). Interestingly, a second MH locus has been mapped to the gene encoding for the alpha$_1$ subunit of the DHPR, the L-type Ca channel, that in skeletal muscle triggers release of Ca from the RyR.

The novel finding of the present study points to CS1 as a new candidate protein for calcium-related disease in skeletal muscles. Our results clearly show MH-like effects in Cs1 null mice under thermic and anesthetics stress.

MALIGNANT HYPERTHERMIA (MH) AND CENTRAL CORE DISEASE (CCD). Diagnosis of CCD is confirmed by histological examination of muscle tissue in which skeletal fibers exhibit amorphous central areas (cores) that are characterized by the lack of both mitochondria and oxidative enzyme activity (21). Electron microscopic analysis of the central cores have shown disintegration of the contractile apparatus and alterations/proliferation of SR and T-tubule membranes (22). We observed these conditions in muscle fibers of the CS1 null mice aninals, in agreement with the MH-like episodes

observed in the same animals when stressed with high temperature and anesthetics.

CALSEQUESTRIN (CS): A POSSIBLE MODULATOR OF RYANODINE RECEPTORS. CS is an extremely acidic protein that binds Ca within the SR and concentrates it at the junctional face of the terminal cisternae, near the sites of Ca release, i.e. RyRs (7, 8, 25). Two isoforms of mammalian CS, which are products of two different genes, have been identified and characterized: a skeletal and a cardiac isoform, respectively CS1 and CS2 (26-29). Cardiac muscle expresses exclusively the cardiac isoform, independent of the developmental stage. In skeletal muscle, on the other hand, both cardiac and skeletal CS can be found, transcribed at different rates during development of fast twitch and slow-twitch skeletal fibers. In slow twitch muscle, the CS2 is the most abundant isoform in fetal and neonatal stages, whereas in adults it accounts for only 25% of the total CS present (30). In fast twitch fibers, on the other hand, CS2 disappears at a critical period between two and four weeks postnatally in rabbit muscle (present study and ref. (31)).

Although the deletion of the only gene coding for CS in C. Elegans (32) has suggested that CS may not be necessary for muscle function, there is a general consensus that CS is not only important for the SR's ability to store Ca, but also for modulating the activity of the SR Ca release channels, i.e. RyRs (33, 34). However, its specific regulatory function on the activity of RyRs is still debated: in fact, some authors have presented data showing that RyRs can be activated by CS (34, 35), whereas others have reported that CS inhibits RyRs (36). Studies in mice overexpressing CS2 in myocardium seem to indicate an inhibitory effect of CS2 (37, 38). On the contrary, the results of Terentyev et al. (2003) (39) have shown that, in rat heart cells, CS2 overexpression in vitro not only increases the SR storage capacity, but also controls the amount of Ca released during EC coupling. In further support of a specific role for CS in controlling Ca release, a recently published study shows that downregulation of CS2, but not of CS1, in C2C12 myotubes leads to an impaired Ca storage and release by the SR (40). In addition, recent studies in mice lacking CS2 have shown that adaptive responses to the lack of CS2 allows normal

cardiac function, although the increase diastolic leakage of Ca makes the heart susceptible to severe arrhythmias under certain conditions (41).
Nonetheless, a direct link between the CS1 and RyRs has not been demonstrated. CS is probably connected to RyRs through accessory proteins such as triadin and junctin, proteins that could indeed represent the anchoring filaments described in EM (45, 46). It is possible that triadin and junctin represent also the functional link between CS and RyR1, a link that would allow the modulation of the Ca channel activity (see Fig. 1).
The data presented here describe a newly identified pathological condition where CS1, mutated or lacking, leads to altered calcium storage, release and reuptake (73) which affect the muscle sensitivity to temperature and caffeine.
Moreover, CS1 mutations might also play a possible role in the origin of a myophathy during skeletal muscle development, with atrophy and morphological defects observed in CS1 null mice model.

In summary, mice homozygous for the CS1 null mutation are MH susceptible, exhibiting both in vivo sensitivity to halogenated anesthetics and positive in vitro contracture test (IVCT), both signatures characteristic of the human MH phenotype. Calcium measurements in myotubes from these mice support the conclusion that these responses are due to an overall accumulation of cytosolic [Ca2+]i possibly related to increased release or to impaired re-uptake.

REFERENCES

1. Franzini-Armstrong, C. (1970) Studies of the triad. *J. Cell Biol.* 47, 488-499

2. Protasi, F. (2002) Structural interaction between RYRs and DHPRs in calcium release units of cardiac and skeletal muscle cells. *Front Biosci* 7, d650-658

3. Schneider, M. F. (1994) Control of calcium release in functioning skeletal muscle fibers. *Annu Rev Physiol* 56, 463-484

4. Rios, E., Ma, J. J., and Gonzalez, A. (1991) The mechanical hypothesis of excitation-contraction (EC) coupling in skeletal muscle. *J Muscle Res Cell Motil* 12, 127-135

5. Rios, E., and Brum, G. (1987) Involvement of dihydropyridine receptors in excitation-contraction coupling in skeletal muscle. *Nature* 325, 717-720

6. Franzini-Armstrong, C., and Protasi, F. (1997) Ryanodine receptors of striated muscles: a complex channel capable of multiple interactions. *Physiol Rev* 77, 699-729

7. MacLennan, D. H., Campbell, K. P., and Reithmeier, R. A. F. (1983) Calsequestrin. In: Calcium and Cell function. *New York: Academic Press, Inc* Vol. IV, 152-173

8. Meissner, G. (1975) Isolation and characterization of two types of sarcoplasmic reticulum vesicles. *Biochim Biophys Acta* 389, 51-68

9. Mickelson, J. R., and Louis, C. F. (1996) Malignant hyperthermia: excitation-contraction coupling, Ca2+ release channel, and cell Ca2+ regulation defects. *Physiol Rev* 76, 537-592

10. MacLennan, D. H. (2000) Ca2+ signalling and muscle disease. *Eur J Biochem* 267, 5291-5297

11. Dirksen, R. T., and Avila, G. (2004) Distinct effects on Ca2+ handling caused by malignant hyperthermia and central core disease mutations in RyR1. *Biophys J* 87, 3193-3204

12. Fujii, J., Otsu, K., Zorzato, F., de Leon, S., Khanna, V. K., Weiler, J. E., O'Brien, P. J., and MacLennan, D. H. (1991) Identification of a

mutation in porcine ryanodine receptor associated with malignant hyperthermia. *Science* 253, 448-451

13. MacLennan, D. H., and Phillips, M. S. (1992) Malignant hyperthermia. *Science* 256, 789-794

14. Loke, J., and MacLennan, D. H. (1998) Malignant hyperthermia and central core disease: disorders of Ca2+ release channels. *Am J Med* 104, 470-486

15. Lynch, P. J., Tong, J., Lehane, M., Mallet, A., Giblin, L., Heffron, J. J., Vaughan, P., Zafra, G., MacLennan, D. H., and McCarthy, T. V. (1999) A mutation in the transmembrane/luminal domain of the ryanodine receptor is associated with abnormal Ca2+ release channel function and severe central core disease. *Proc Natl Acad Sci U S A* 96, 4164-4169

16. Dirksen, R. T., and Avila, G. (2002) Altered ryanodine receptor function in central core disease: leaky or uncoupled Ca(2+) release channels? *Trends Cardiovasc Med* 12, 189-197

17. Odermatt, A., Taschner, P. E., Khanna, V. K., Busch, H. F., Karpati, G., Jablecki, C. K., Breuning, M. H., and MacLennan, D. H. (1996) Mutations in the gene-encoding SERCA1, the fast-twitch skeletal muscle sarcoplasmic reticulum Ca2+ ATPase, are associated with Brody disease. *Nat Genet* 14, 191-194

18. Houser, S. R., Piacentino, V., 3rd, and Weisser, J. (2000) Abnormalities of calcium cycling in the hypertrophied and failing heart. *J Mol Cell Cardiol* 32, 1595-1607

19. Magee, K. R., and Shy, G. M. (1956) A new congenital non-progressive myopathy. *Brain* 79, 610-621

20. Sewry, C. A., Muller, C., Davis, M., Dwyer, J. S., Dove, J., Evans, G., Schroder, R., Furst, D., Helliwell, T., Laing, N., and Quinlivan, R. C. (2002) The spectrum of pathology in central core disease. *Neuromuscul Disord* 12, 930-938

21. Banker, B. Q. (1986) The congenital myopathies. In *Myology* (Engel, A. G., and Banker, B. Q., eds) Vol. Vol. II pp. 1527-1581, McGraw-Hill, New York

22. Hayashi, K., Miller, R. G., and Brownell, A. K. (1989) Central core disease: ultrastructure of the sarcoplasmic reticulum and T-tubules. *Muscle Nerve* 12, 95-102

23. Levitt, R. C., Olckers, A., Meyers, S., Fletcher, J. E., Rosenberg, H., Isaacs, H., and Meyers, D. A. (1992) Evidence for the localization of a malignant hyperthermia susceptibility locus (MHS2) to human chromosome 17q. *Genomics* 14, 562-566

24. Monnier, N., Procaccio, V., Stieglitz, P., and Lunardi, J. (1997) Malignant-hyperthermia susceptibility is associated with a mutation of the alpha 1-subunit of the human dihydropyridine-sensitive L-type voltage-dependent calcium-channel receptor in skeletal muscle. *Am J Hum Genet* 60, 1316-1325

25. Yano, K., and Zarain-Herzberg, A. (1994) Sarcoplasmic reticulum calsequestrins: structural and functional properties. *Mol Cell Biochem* 135, 61-70

26. Scott, B. T., Simmerman, H. K., Collins, J. H., Nadal-Ginard, B., and Jones, L. R. (1988) Complete amino acid sequence of canine cardiac calsequestrin deduced by cDNA cloning. *J Biol Chem* 263, 8958-8964

27. Zarain-Herzberg, A., Fliegel, L., and MacLennan, D. H. (1988) Structure of the rabbit fast-twitch skeletal muscle calsequestrin gene. *J Biol Chem* 263, 4807-4812

28. Fujii, J., Willard, H. F., and MacLennan, D. H. (1990) Characterization and localization to human chromosome 1 of human fast-twitch skeletal muscle calsequestrin gene. *Somat Cell Mol Genet* 16, 185-189

29. Arai, M., Alpert, N. R., and Periasamy, M. (1991) Cloning and characterization of the gene encoding rabbit cardiac calsequestrin. *Gene* 109, 275-279

30. Damiani, E., Volpe, P., and Margreth, A. (1990) Coexpression of two isoforms of calsequestrin in rabbit slow-twitch muscle. *J Muscle Res Cell Motil* 11, 522-530

31. Sacchetto, R., Volpe, P., Damiani, E., and Margreth, A. (1993) Postnatal development of rabbit fast-twitch skeletal muscle: accumulation, isoform transition and fibre distribution of calsequestrin. *J Muscle Res Cell Motil* 14, 646-653

32. Cho, J. H., Oh, Y. S., Park, K. W., Yu, J., Choi, K. Y., Shin, J. Y., Kim, D. H., Park, W. J., Hamada, T., Kagawa, H., Maryon, E. B., Bandyopadhyay, J., and Ahnn, J. (2000) Calsequestrin, a calcium

sequestering protein localized at the sarcoplasmic reticulum, is not essential for body-wall muscle function in Caenorhabditis elegans. *J Cell Sci* 113 (Pt 22), 3947-3958

33. Gilchrist, J. S., Belcastro, A. N., and Katz, S. (1992) Intraluminal Ca2+ dependence of Ca2+ and ryanodine-mediated regulation of skeletal muscle sarcoplasmic reticulum Ca2+ release. *J Biol Chem* 267, 20850-20856

34. Kawasaki, T., and Kasai, M. (1994) Regulation of calcium channel in sarcoplasmic reticulum by calsequestrin. *Biochem Biophys Res Commun* 199, 1120-1127

35. Ohkura, M., Ide, T., Furukawa, K., Kawasaki, T., Kasai, M., and Ohizumi, Y. (1995) Calsequestrin is essential for the Ca2+ release induced by myotoxin alpha in skeletal muscle sarcoplasmic reticulum. *Can J Physiol Pharmacol* 73, 1181-1185

36. Beard, N. A., Sakowska, M. M., Dulhunty, A. F., and Laver, D. R. (2002) Calsequestrin is an inhibitor of skeletal muscle ryanodine receptor calcium release channels. *Biophys J* 82, 310-320

37. Jones, L. R., Suzuki, Y. J., Wang, W., Kobayashi, Y. M., Ramesh, V., Franzini-Armstrong, C., Cleemann, L., and Morad, M. (1998) Regulation of Ca2+ signaling in transgenic mouse cardiac myocytes overexpressing calsequestrin. *J Clin Invest* 101, 1385-1393

38. Sato, Y., Ferguson, D. G., Sako, H., Dorn, G. W., 2nd, Kadambi, V. J., Yatani, A., Hoit, B. D., Walsh, R. A., and Kranias, E. G. (1998) Cardiac-specific overexpression of mouse cardiac calsequestrin is associated with depressed cardiovascular function and hypertrophy in transgenic mice. *J Biol Chem* 273, 28470-28477

39. Terentyev, D., Viatchenko-Karpinski, S., Gyorke, I., Volpe, P., Williams, S. C., and Gyorke, S. (2003) Calsequestrin determines the functional size and stability of cardiac intracellular calcium stores: Mechanism for hereditary arrhythmia. *Proc Natl Acad Sci U S A* 100, 11759-11764

40. Wang, Y., Xu, L., Duan, H., Pasek, D. A., Eu, J. P., and Meissner, G. (2006) Knocking down type 2 but not type 1 calsequestrin reduces calcium sequestration and release in C2C12 skeletal muscle myotubes. *J Biol Chem* 281, 15572-15581

41. Knollmann, B. C., Chopra, N., Hlaing, T., Akin, B., Yang, T., Ettensohn, K., Knollmann, B. E., Horton, K. D., Weissman, N. J., Holinstat, I., Zhang, W., Roden, D. M., Jones, L. R., Franzini-Armstrong, C., and Pfeifer, K. (2006) Casq2 deletion causes sarcoplasmic reticulum volume increase, premature Ca2+ release, and catecholaminergic polymorphic ventricular tachycardia. *J Clin Invest* 116, 2510-2520

42. Campbell, K. P., MacLennan, D. H., Jorgensen, A. O., and Mintzer, M. C. (1983) Purification and characterization of calsequestrin from canine cardiac sarcoplasmic reticulum and identification of the 53,000 dalton glycoprotein. *J Biol Chem* 258, 1197-1204

43. Saito, A., Seiler, S., Chu, A., and Fleischer, S. (1984) Preparation and morphology of sarcoplasmic reticulum terminal cisternae from rabbit skeletal muscle. *J Cell Biol* 99, 875-885

44. Franzini-Armstrong, C., Kenney, L. J., and Varriano-Marston, E. (1987) The structure of calsequestrin in triads of vertebrate skeletal muscle: a deep-etch study. *J Cell Biol* 105, 49-56

45. Kobayashi, Y. M., Alseikhan, B. A., and Jones, L. R. (2000) Localization and characterization of the calsequestrin-binding domain of triadin 1. Evidence for a charged beta-strand in mediating the protein-protein interaction. *J Biol Chem* 275, 17639-17646

46. Shin, D. W., Ma, J., and Kim, D. H. (2000) The asp-rich region at the carboxyl-terminus of calsequestrin binds to Ca2+ and interacts with triadin. *FEBS Lett.* 486 178-182

47. Ikemoto, N., Ronjat, M., Meszaros, L. G., and Koshita, M. (1989) Postulated role of calsequestrin in the regulation of calcium release from sarcoplasmic reticulum. *Biochemistry* 28, 6764-6771

48. Szegedi, C., Sarkozi, S., Herzog, A., Jona, I., and Varsanyi, M. (1999) Calsequestrin: more than 'only' a luminal Ca2+ buffer inside the sarcoplasmic reticulum. *Biochem J* 337 (Pt 1), 19-22

49. Rossi, R., Bottinelli, R., Sorrentino, V., and Reggiani, C. (2001) Response to caffeine and ryanodine receptor isoforms in mouse skeletal muscles. *Am J Physiol Cell Physiol* 281, C585-594

50. Franzini-Armstrong, C., Pincon-Raymond, M., and Rieger, F. (1991) Muscle fibers from dysgenic mouse in vivo lack a surface component of peripheral couplings. *Dev Biol* 146, 364-376

51. Takekura, H., Nishi, M., Noda, T., Takeshima, H., and Franzini-Armstrong, C. (1995) Abnormal junctions between surface membrane and sarcoplasmic reticulum in skeletal muscle with a mutation targeted to the ryanodine receptor. *Proc Natl Acad Sci U S A* 92, 3381-3385

52. Lorenzon, P., Bernareggi, A., Degasperi, V., Nurowska, E., Wernig, A., and Ruzzier, F. (2002) Properties of primary mouse myoblasts expanded in culture. *Exp Cell Res* 278, 84-91

53. Buonanno, A., and Fields, R. D. (1999) Gene regulation by patterned electrical activity during neural and skeletal muscle development. *Curr Opin Neurobiol* 9, 110-120

54. Chin, E. R., Olson, E. N., Richardson, J. A., Yang, Q., Humphries, C., Shelton, J. M., Wu, H., Zhu, W., Bassel-Duby, R., and Williams, R. S. (1998) A calcineurin-dependent transcriptional pathway controls skeletal muscle fiber type. *Genes Dev* 12, 2499-2509

55. Flucher, B. E., Andrews, S. B., Fleischer, S., Marks, A. R., Caswell, A., and Powell, J. A. (1993) Triad formation: organization and function of the sarcoplasmic reticulum calcium release channel and triadin in normal and dysgenic muscle in vitro. *J Cell Biol* 123, 1161-1174

56. Nishi, M., Komazaki, S., Kurebayashi, N., Ogawa, Y., Noda, T., Iino, M., and Takeshima, H. (1999) Abnormal features in skeletal muscle from mice lacking mitsugumin29. *J Cell Biol* 147, 1473-1480

57. Takekura, H., and Kasuga, N. (1999) Differential response of the membrane systems involved in excitation-contraction coupling to early and later postnatal denervation in rat skeletal muscle. *J Muscle Res Cell Motil* 20, 279-289

58. Boncompagni, S., d'Amelio, L., Fulle, S., Fano, G., and Protasi, F. (2006) Progressive disorganization of the excitation-contraction coupling apparatus in aging human skeletal muscle as revealed by electron microscopy: a possible role in the decline of muscle performance. *J Gerontol A Biol Sci Med Sci* 61, 995-1008

59. Raichman, M., Panzeri, M. C., Clementi, E., Papazafiri, P., Eckley, M., Clegg, D. O., Villa, A., and Meldolesi, J. (1995) Differential localization and functional role of calsequestrin in growing and differentiated myoblasts. *J Cell Biol* 128, 341-354

60. Priori, S. G., Napolitano, C., Tiso, N., Memmi, M., Vignati, G., Bloise, R., Sorrentino, V., and Danieli, G. A. (2001) Mutations in the cardiac ryanodine receptor gene (hRyR2) underlie catecholaminergic polymorphic ventricular tachycardia. *Circulation* 103, 196-200

61. Lahat, H., Pras, E., Olender, T., Avidan, N., Ben-Asher, E., Man, O., Levy-Nissenbaum, E., Khoury, A., Lorber, A., Goldman, B., Lancet, D., and Eldar, M. (2001) A missense mutation in a highly conserved region of CASQ2 is associated with autosomal recessive catecholamine-induced polymorphic ventricular tachycardia in Bedouin families from Israel. *Am J Hum Genet* 69, 1378-1384

62. Postma, A. V., Denjoy, I., Hoorntje, T. M., Lupoglazoff, J. M., Da Costa, A., Sebillon, P., Mannens, M. M., Wilde, A. A., and Guicheney, P. (2002) Absence of calsequestrin 2 causes severe forms of catecholaminergic polymorphic ventricular tachycardia. *Circ Res* 91, e21-26

63. Terentyev, D., Nori, A., Santoro, M., Viatchenko-Karpinski, S., Kubalova, Z., Gyorke, I., Terentyeva, R., Vedamoorthyrao, S., Blom, N. A., Valle, G., Napolitano, C., Williams, S. C., Volpe, P., Priori, S. G., and Gyorke, S. (2006) Abnormal interactions of calsequestrin with the ryanodine receptor calcium release channel complex linked to exercise-induced sudden cardiac death. *Circ Res* 98, 1151-1158

64. di Barletta, M. R., Viatchenko-Karpinski, S., Nori, A., Memmi, M., Terentyev, D., Turcato, F., Valle, G., Rizzi, N., Napolitano, C., Gyorke, S., Volpe, P., and Priori, S. G. (2006) Clinical Phenotype and Functional Characterization of CASQ2 Mutations Associated With Catecholaminergic Polymorphic Ventricular Tachycardia. *Circulation* 114, 1012-1019

65. Gallant, E. M., and Lentz, L. R. (1992) Excitation-contraction coupling in pigs heterozygous for malignant hyperthermia. *Am J Physiol* 262, C422-426

66. Chelu, M. G., Goonasekera, S. A., Durham, W. J., Tang, W., Lueck, J. D., Riehl, J., Pessah, I. N., Zhang, P., Bhattacharjee, M. B., Dirksen, R. T., and Hamilton, S. L. (2006) Heat- and anesthesia-induced malignant hyperthermia in an RyR1 knock-in mouse. *Faseb J* 20, 329-330

67. Group, T. E. M. H. (1984) A protocol for the investigation of malignant hyperpyrexia (MH) susceptibility. The European Malignant Hyperpyrexia Group. *Br J Anaesth* 56, 1267-1269

68. Shtifman, A., Paolini, C., Lopez, J. R., Allen, P. D., and Protasi, F. (2004) Ca2+ influx through alpha1S DHPR may play a role in regulating Ca2+ release from RyR1 in skeletal muscle. *Am J Physiol Cell Physiol* 286, C73-78

69. Protasi, F., Franzini-Armstrong, C., and Flucher, B. E. (1997) Coordinated incorporation of skeletal muscle dihydropyridine receptors and ryanodine receptors in peripheral couplings of BC3H1 cells. *J Cell Biol* 137, 859-870

70. Head, S. I. (1993) Membrane potential, resting calcium and calcium transients in isolated muscle fibres from normal and dystrophic mice. *J Physiol* 469, 11-19

71. Defranchi, E., Bonaccurso, E., Tedesco, M., Canato, M., Pavan, E., Raiteri, R., and Reggiani, C. (2005) Imaging and elasticity measurements of the sarcolemma of fully differentiated skeletal muscle fibres. *Microsc Res Tech* 67, 27-35

72. Connolly, A. M., Keeling, R. M., Metha, S., Pestronk, A., and Sanes, J. R. (2001) Three mouse models of muscular dystrophy: the natural history of strength and fatigue in dystrophin- dystrophin/utrophin-, and laminin alpha2-deficient mice. *Neuromusc. Disord.* 11, 703-712

73. Paolini C, Quarta M, Nori A, Boncompagni S, Canato M, Volpe P, Allen PD, Reggiani C, Protasi F (2007) Reorganized stores and impaired calcium handling in skeletal muscle of mice lacking calsequestrin-1 *J Physiol (Lond)* vol. 583 (pt2) 267-84.

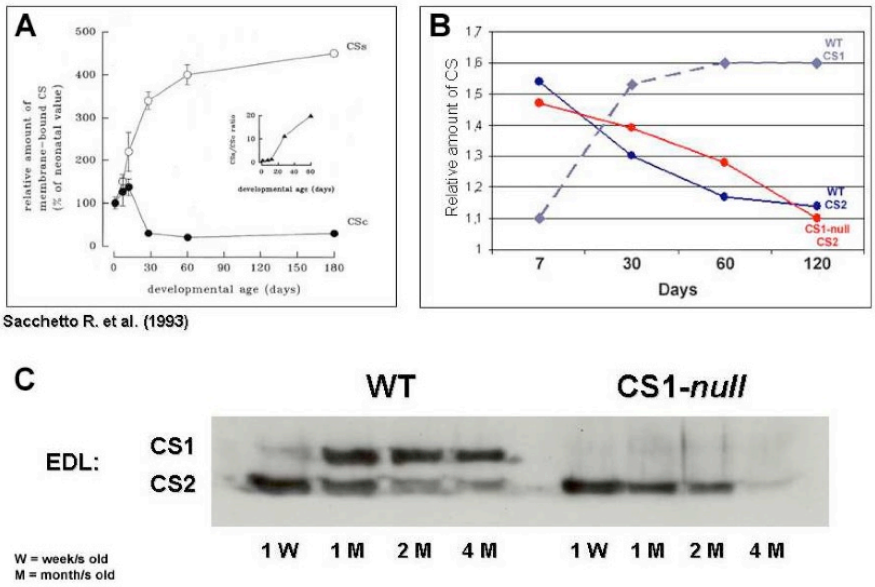

Figure 1. CS1-null EDL muscles do not display any compensatory increase of CS2 expression. A and B) Time course of expression of cardiac and skeletal CS during post-natal development in rabbit (Sacchetto et al., 1993) and mouse fast-twitch skeletal muscles (WT and CS1-null). C) Representative western blot of EDL homogenates from WT and CS1-*null* mice at four different post-natal time points: 1 week and 1, 2, and 4 months of age. In WT EDL muscle, cardiac CS (CS2, lower molecular weight) is very abundant immediately after birth, but is almost completely replaced by the skeletal isoform (CS1, higher molecular weight) during the first two months of post-natal maturation. The expression pattern of CS2 is very similar in CS1-*null* mice, in which CS2 is indeed down-regulated, even in absence of CS1.

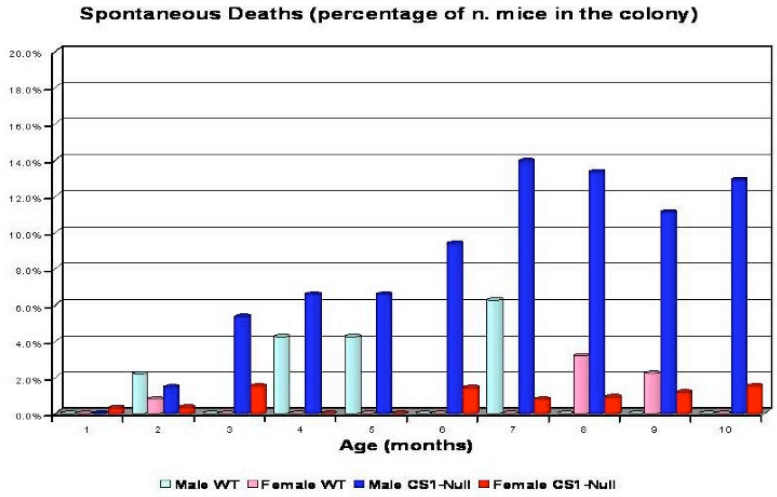

Figure 2. Unusually high incidence of spontaneous mortality in CS1-null male mice. Spontaneous deaths of CS1-null mice kept in standard housing condition are mostly observed between 3 and 10 months of age, the highest rate being between 6 and 10 months of age r. Interestingly, most deaths were registered in male mice while in reproductive cages.

Figure 3. Heat-stress triggers lethal MH-like episodes in CS1-null mice. A) CS1-null mice exposed to heat-stress (41^{o}C), triggered lethal MH-like episodes characterized by difficult in breathing, impaired movement, spasmodic contractions of the whole body, arched back followed by death. B) The lethal heat-induced episodes were remarkably similar to those described as fulminant MH episodes by Chelu et al. (2006) (66).

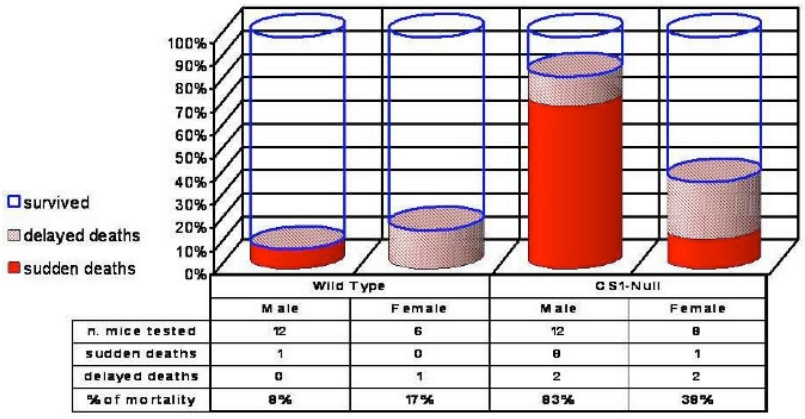

	Wild Type		CS1-Null	
	Male	Female	Male	Female
n. mice tested	12	6	12	8
sudden deaths	1	0	8	1
delayed deaths	0	1	2	2
% of mortality	8%	17%	83%	38%

Figure 4. A high percentage of CS1-null male undergoes EHS-like episodes followed by sudden death when exposed to heat stress (41°C). 8 out 12 CS1-null male mice exposed to heat-stress triggered lethal EHS-like episodes. Identical heat challenge was well-tolerated in WT mice. Female CS1-null mice are usually more resistant than males. Some delayed death (within 24 hours) were also registered (2 males, 2 females).

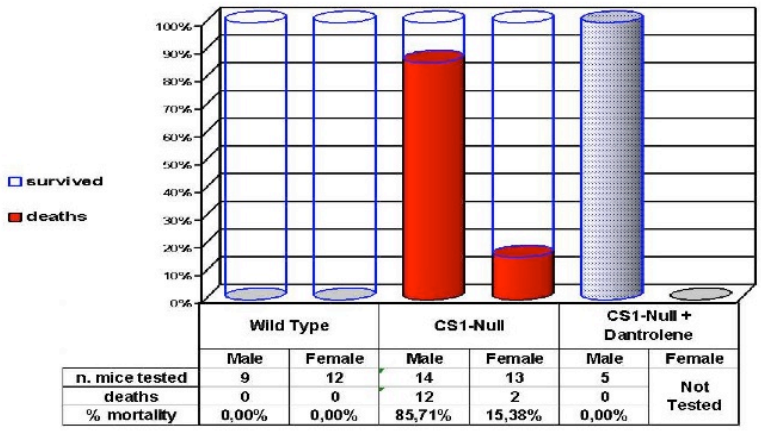

	Wild Type		CS1-Null		CS1-Null + Dantrolene	
	Male	Female	Male	Female	Male	Female
n. mice tested	9	12	14	13	5	Not Tested
deaths	0	0	12	2	0	
% mortality	0,00%	0,00%	85,71%	15,38%	0,00%	

Figure 5. CS1 null mice triggers MH-like lethal episodes if exposed to halothane. CS1-null animals showed an very high mortality rate during anesthesia with an halogenated anaesthetic halothane (2% for 1 hr) was lethal in 85% of CS1-null male mice (12 out of 14). Same treatment is well tolerated by WT animals anesthetized together (same chamber) with CS1-nulls. Preliminary results collected in mice pre-treated with dantrolene (4 mg/kg) - used in humans to treat MH episodes – suggests that this treatment is indeed effective also in CS1-null mice: 5 out of 5 CS1-null male mice survived the anaesthesia procedure.

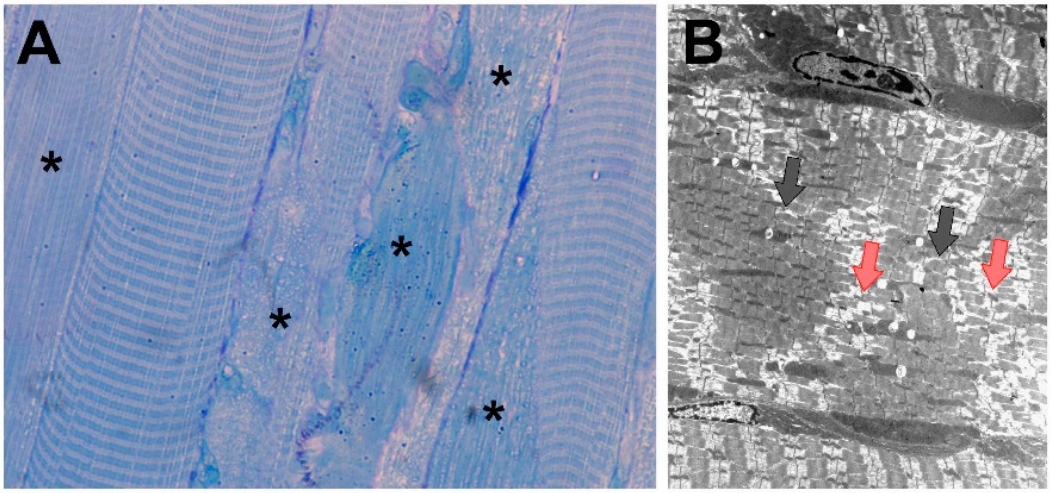

Figure 6. Skeletal muscle fibers of CS1-null mice are severely damaged during letha crisis. A) Histological and electron microscopical analysis of EDL muscles from CS1-*null* mice dissected and fixed immediately after a MH-like crisis induced by exposure to heat stress, shows a high percentage of fibers which are severely damaged (asterisks). B) EM analysis revealed that these fibers are indeed severely compromised: in B an areas of excessive contractures (grey arrows) and areas of over-stretched sarcomeres (red arrows). These alterations are not present in WT mice exposed to the same treatment.

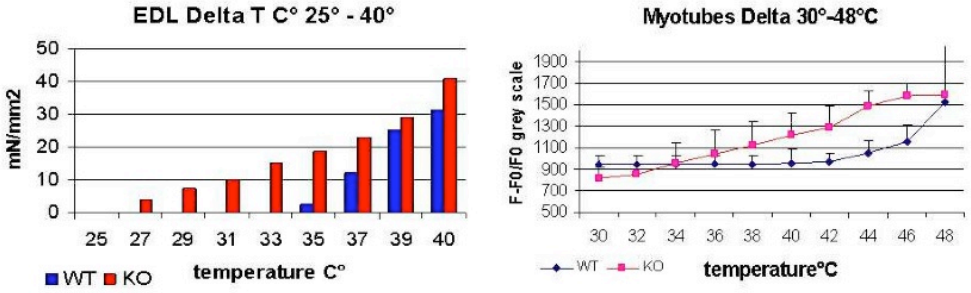

Figure 7. Dissected EDL muscles and cultured primary myotubes from CS1-null mice are more sensitive than WTs to increasing temperatures. Dissected EDL from knockout animals start developing tension (which finally results in a contracture) at lower temperature than WT EDLs (left panel). Cultured CS1-null myotubes displays a higher sensitivity to temperature, as shown by the progressive increase in intracellular [Ca] with increasing temperatures (right panels). WT specimens are also affected by temperature: however, dissected WT EDL muscles start to develop tension significantly later that CS1-nulls and WT myotubes displays an increase in intracellular Ca levels only at temperature higher than 41°C.

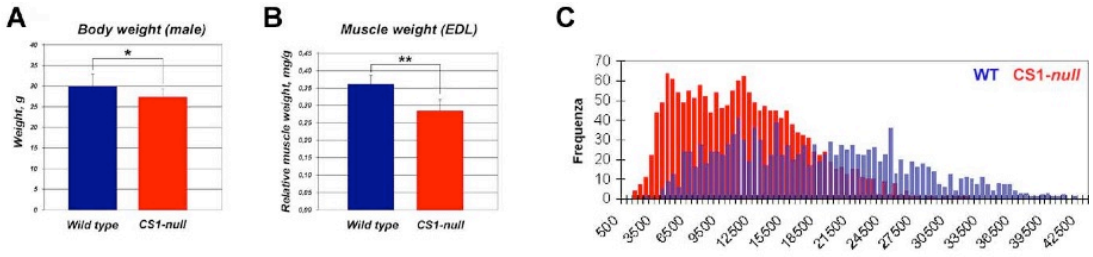

Figure 8. CS1-null mice display muscle atrophy. A) CS1-*null* mice show a lower body weight than WT mice of same sex (male) and age (4–6 months, CS1-*null*, *n* = 211; WT, *n* = 150; n, number of animals). B) Dissected fast-twitch muscles are smaller in mass: the normalized EDL muscle weight in CS1-*null* mice is on the average 20% smaller than in WT: this difference is highly significant ($P < 0.0001$). C) Cross sectional area of CS1-*null* EDL fibers is reduced when compared to WT fibers (CS1-*null*, *n* = 1684; WT, *n* = 1279).

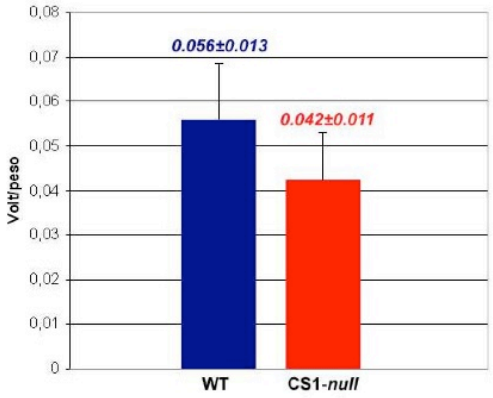

	Volt / weight (mean ± SD)
Wild type	0 056 ± 0 013 (n=11)
CS1-null	0 042 ± 0 011 (n=8)

Figure 9. CS1-null mice displays muscle weakness. Grip test is a simple and non invasive method to test the mice muscle strength by sensing the peak amount of force that animals apply in grasping an especially designed pull bar. Evaluation of the muscular strength using the grip test showed that CS1-*null* mice develop less strength when compared to WT mice of the same age (4–6 months, CS1-*null*, *n* = 8; WT, *n* = 11).

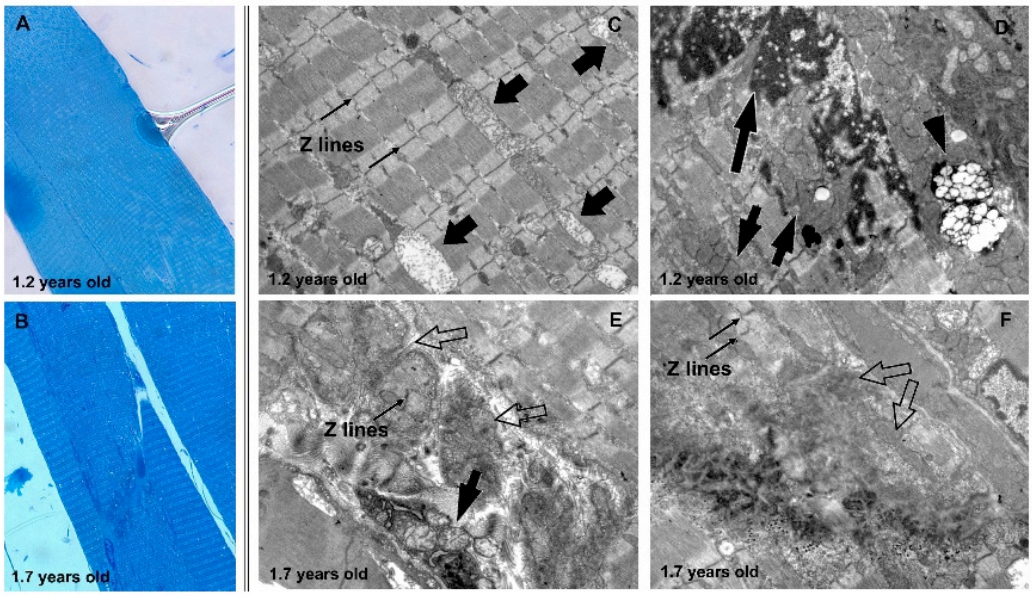

Figure 10. After 1 year of age, EDL fibers shows structural alterations. A and B) Preliminary analysis of EDL fibers of 1.2 and 1.7 years old mice have revealed morphological alterations, which may be early signs of a developing myopathy. C-F) Preliminary EM examination revealed various abnormalities: swollen/disrupted mitochondria (C); convoluted nuclei, with dispersion of chromatin, and lysosome vacuoles (D); areas with abnormal clustering of mitochondria and disrupted myofibrils (E and F).

CHAPTER 3:

CONTRACTILE RESPONSE IMPAIRMENT IN SKELETAL MUSCLES OF ANK1.5 DEFICENT MICE

Authors

M. Quarta[1], E. Giacomello[2], L. Toniolo[1], V. Cusimano[2], C. Birkenmeier[3], L. Peters[3], V. Sorrentino[2], C. Reggiani[1]

Affiliations

[1] Muscle Biophysics Lab, Dept. Anatomy and Physiology, University of Padova, Italy; [2] Molecular Medicine Section, Dept. of Neuroscience, University of Siena, Italy; [3] Jackson Labs, USA

ABSTRACT

Vertebrate genome contains three ankyrin genes (Ank1, Ank2, and Ank3) from which by differential splicing multiple transcripts originate resulting in a large number of expressed proteins that participate in the organization of specific membrane domains by linking specific membrane proteins with intracellular cytoskeleton. Recently, a muscle specific variant of Ank1, ank1.5 has been shown to link obscurin, a myofibrillar protein, with the sarcoplasmic reticulum in striated muscles. To clarify the role of Ank1.5 in skeletal muscles we generated mice carrying null mutations that selectively affect the expression of the ank1.5 mRNA. Homozygote Ank1.5 mice are vital and fertile. To further understand the role of ank1.5 protein, the structure of the SR and the contractile properties of skeletal muscles from ank1.5 KO mice were analysed. Although staining of SR proteins revealed no apparent alteration in the organization of SR proteins ank1.5 KO mice, the contractile performance of the diaphragm was however weaker than in wild type animals, fatigue resistance in an endurance test on the treadmill was reduced and gait analysis showed stride length and stride frequency differences. Moreover some Evans blue positive fibers indicated small necrosis in KO diaphragm muscles. These findings suggest that ank1.5 play an important, but yet not completely defined role, in muscle contraction.

INTRODUCTION

Reticular organization plays a special role in biology of striated muscle cells (Meldolesi and Pozzan, 1998; Petersen et al., 2001), in particular the sarcoplasmic reticulum (SR) presents a complex architecture (Franzini-Armstrong; Baumann and Walz, 2001) which is essential for the correct excitation-contraction coupling. In fact the SR forms a close link and a functional relationship wih respect to the contractile apparatus, forming a sleeve-like structure around myofibrils, distributed with a regular spatial distribution over specific sarcomere regions (Franzini-Armstrong, 1994). Considering that the SR is specialized in Ca2+ storage, relase and reuptake (Berridge et al., 2000) and develops the terminal cisternae which form together with T tubule/plasma membrane specific structure like diads, triads or peripheral couplings (Flucher and Franzini-Armstrong, 1996), the importance of intracellular organization at SR level become a key question to unlock molecular mechanism of EC coupling still poorly understood.

Ankyrins are multifunctional adaptor proteins of the plasma membrane and intracellular membranes (Bennet and Chen, 2001). They contribute to the formation and cytoskeletal anchoring of specialized membrane domains.

Three distinct genes have been identified to encode anyrins proteins, termed in the mouse *Ank1 (Ankyrin-R)*, mainly expressed in erythroid cells, *Ank2 (Ankyrin-B)*, in the brain, *Ank3* (Ankyrin-G) in epythelial cells. The same was confirmed also in human for ANK1, ANK2, ANK3 genes (Peters et al., 1995; reviewed by Peers nd Lux, 1993). All three genes face alternative spliced transcripts which develop different variants of Ankyrins proteins with different domains, from giant ankyrins to truncated small ankyrins (Birkenmeir et l., 1998; Kordeli et al., 1994; Peters et al., 1995). Others domains are on the other hand highly conserved. Ankyrins are in fact modular proteins, and their anatomy can be divided in three main major domains (fig 1; Bennet and Chien, 2001). They are: an amino-terminal membrane-binding domain comprised of ANK repeats; a spectrin-binding domain; a death domain located near the carboxy terminus. Carboxy-terminal domains generally diverge in

sequence and they present different functions. *Ank1* death domain is followed by a carboxy-terminal domain that regulates binding of both the anion exchanger and spectrin, subjected to alternative splicing (Lux et al., 1990).

Moreover, there are also particular Ankyrin proteins: *Ank2* and *Ank3* encode giant proteins that carry additional structural motifs (Kordeli and Bennet, 1991; Kunimoto, 1995; Zhang and Bennet, 1988) while *Ank1* and *Ank3* encode for small forms that lack domains of the canonical ankyrins (Peters et al., 1995; Birkenmeier et al., 1998; Gallagher and Forget, 1998).

Interestingly, ankyrin muscle-specific isoforms have been described. A group of striated muscle ankyrins proteins of *Ank1* gene in particular seem to interact specifically with SR (Kordeli et al., 1998; Gargelin et al., 2002). *Ank1* products are present in striated muscle, and include large, canonical (around 210 kDa) and small (around 17-19 kDa) ankyrins (Birkenmeier et al., 1998). The large ankyrin isoforms are concentrated at the sarcolemma of skeletal myofibers, whereas small Ank1 isoforms (Ank1.5, Ank1.6 and Ank1.7) are targeted to the SR, and specifically to the network SR, which is primarily responsible for Ca2+ uptake.

The small protein sAnk1 lacks of both membrane and spectrin-binding protein sequences, with the exception for a short sequence from the COOH-terminus. These srAnk1 isoforms present at NH_2-terminal portion a unique 73-amino acid segment, characterized by a first segment of hydrophobic 29 residues which anchor the protein to the SR membrane. Recently, a second small Ank1 isoforms, termed Ank1.9, has been reported to bind obscurin similarly to Ank1.5 (Armani et al. 2006).

One of these sAnk1 in particular, the sAnk1.5 but not the sAnk1.6 and sAnk1.7, presents a unique sequence at the COOH terminus which protrudes in the myoplasma and recognizes specific seuence of the giant citoplasmic protein obscurin in the nonmodular region at the COOH terminus following its last Ig-like domain (Bagnato et al., 2003; Kontrogianni-Konstantopoulos et al., 2003 and 2006). Obscuring is a very large muscle protein (around 800 kDa) known to bind titin and myomesin (Tuvia et al., 1999; Mohler et al, 2002, Kontrogianni-Konstantopoulos et al, 2006), and to act together with nebulin and M-protein in the organization of

A band, and M bands (Van der Ven et al, 1999; Agarkova et al, 2003 Kontrogianni-Konstantopoulos, 2006). In fact Ank1.5 appears to be located at the Z-disk and M-lines of the contractile apparatus, together with the obscurin and titin at myofibrils organized in the sarcomere (Bagno et al., 2003). This particular architecture suggested that Ank 1.5 plays a possibile structural and positioning role on the contractile and Ca2+ release apparatus.

The present data bring novel to specific role of Ank1.5 role in contrast with previous observations. To clarify the role of Ank1.5 in skeletal muscles we generated mice carrying null mutations that selectively affect the expression of the ank1.5 mRNA. Homozygote Ank1.5 mice are vital and fertile, and they do not present any structural or morphological alteration. On the other hand, they are characterized by a specific functional phenotype, with reduced force in fast muscle fibers and a reduced endurance in exhaustion test. Thus, sAnk1.5 may have a role not only in holding a stable connection between SR and myofibrils, but in the correct efficiency of EC coupling through still unclear molecular or mechanical interactions.

MATERIAL AND METHODS

- Animals. Mice carrying null mutation of Ank1.5 were generated at the Jackson Laboratory, AnnArbour. Using random insertional mutagenesis with retroviral vector (fig0) replacing the muscle specific exon 39° with a DNA segment containing a Neo gene, as described elsewhere (Paolini et al., 2007). Briefly, the *null* line was generated by microinjection of the OmniBank ES cell clone into host blastocysts, using standard methods. Chimeric mice resulting from the ES cell injections were bred to C57BL/6J mice for germline transmission of the mutation. Multiplex Quantitative real-time PCR was used to genotype knockout mice (Jackson Lab, USA). C57bll Were used as control mice. Mice were housed in individual with water and food ad libitumm, 12h light-dark cycle and temperature of 22°C.

- Immunostaining Ank1.5 +/+ and -/- muscles (soleus, extensor digitorum longus and diaphragm) were frozen in liquid nitrogen and sectioned longitudinally with a Leica cryostat. 8 μm sections were fixed with 3% paraformaldehyde in PBS for 7 minutes at room temperature and extensively washed with PBS with 0.2% BSA. Sections were blocked for two hours at 25°C in PBS containing O.2% BSA and 5% goat serum and then incubated overnight with the following antibodies: anti-ank1.5 (Armani et al, 2006), anti-obscurin (Bagnato et al, 2003), anti-α-actinin (purchased from Sigma) as marker of Z-disk, anti-RyR1 (Giannini et al), anti-ank1.5 (kindly provided by V. Bennett), anti-SERCA-1 (clone CaF2-5D2), anti-a1s-subunit-DHPR (purchased from ABR), anti-triadin (Trisk-95, kindly provided by I. Marty). The sections were extensively washed with PBS-BSA 0.2% and incubated with Cy2 or Cy3 conjugated secondary antibodies (Jackson Immunoresearch) for one hour, at the recommended concentration, at room temperature, washed with PBS-BSA 0.2% and mounted with mowiol added with 0.025% DABCO as antifading agent. The fluorescent specimes were analysed with a LSM 510-Meta confocal microscope (Zeiss).

- Western blot Ank1.5 +/+ and -/- muscles (soleus, edl and diaphragm) were dissected and homogenized in homogenization buffer (0.32 M sucrose, 5mM HEPES, protease inhibitors, pH 7.4), spun at 700rpm for 10 minutes, resuspended in homogenization buffer and quantified with the Bradford assay kit (BioRad). 10 mg of total proteins were loaded in each lane of SDS polyacrylamide gels (percentage depending on the protein tested) and transferred on nitrocellulosa membranes. The membranes were saturated in 50 mM Tris-HCl (pH 7.4), 150 mM NaCl, 0.2% tween 80 and 5% dry milk, incubated with the primary antibodies (anti-ank1.5, anti SERCA1, anti-a1s-subunit-DHPR, anti-RyR1, anti-triadin), extensively washed in 50 mM Tris-HCl (pH 7.4), 150 mM NaCl, 0.2% tween 80 and 0.5% dry milk, incubated with the appropriated HRP-conjugated antibodies, washed extensively and revealded with ECL western blotting detection kit (GE Healthcare).

- Blue Evans Ank1.5 +/+ and -/- mice were injected with Blue Evans into the peritoneal cavity as previously described (Straub et al, 1997), the following day mice were killed by cervical dislocation; soleus, edl and diaphragm muscles were frozen in liquid nitrogen and sectioned transversally with a Leica cryostat. 8 μm sections were collected and observed on an epifluorescent microscope. The percentage of positive fibers was established by calculating the ratio between blue Evans positive and total fibers.

- Force and contraction kinetics of isolated intact Diaphragm, Soleus and EDL. Thin strips extending from the tendineous center to the ribs were dissected from the costal portion of the diaphragm, soleus and EDL muscles were dissected from hind limb of WT and Ank1.5-*null* mice in warm oxygenated Krebs solution and mounted between a force transducer (AME-801 SensorOne, Sausalito, California) and micro-manipulator controlled shaft in a small chamber where oxygenated Krebs solution was continuously circulated. Temperature was kept constant at 25°C. The stimulation conditions were optimized and muscle length was increased until force development during tetanus was maximal. The responses to a single stimulus (twitch) or to a series of stimuli at various rates producing

unfused or fused tetani were recorded. Time to peak tension, time to half relaxation and peak tension were measured in single twitches. Tension was measured in completely fused maximal tetani and twitch/tetanus ratio was determined. The resistance to fatigue was tested by stimulating the muscles with a fatiguing protocol based on 0.5s fused tetani with 1:4 duty ratio (low frequency fatigue).

- Preparation of samples for Electron Microscopy (EM). Diaphragm strips**,** EDL and Soleus muscles were carefully dissected from Ank1.5-*null* and WT mice (4 to 9 months of age). Muscles were fixed at RT in 3.5% glutaraldehyde in 0.1 M Na cacodylate buffer, pH 7.2 for 2h. Small bundles of fixed fibers were then post-fixed in 2% OsO_4 in the same buffer for 2h and block-stained in aqueous saturated uranyl acetate. After dehydration, specimens were embedded in an epoxy resin (Epon 812). Ultra thin sections were cut in a Leica Ultracut R microtome (Leica Microsystem, Vienna, Austria) using a Diatome diamond knife (DiatomeLtd. CH-2501 Biel, Switzerland). Sections, after staining in 4% uranyl acetate and lead citrate, were examined with a Morgagni Series 268D electron microscope (FEI Company, Brno, Czech Republic), equipped with Megaview III digital camera.

- Calcium release in single permeabilized muscle fibers. Single fibers were manually dissected free from the superficial layers of Tibialis anterior muscle of Ank1.5-*null* and WT mice and segments of 1-1.5-mm length were mounted with small aluminum clips between a force transducer (AME-801 SensorOne, Sausalito, California) and an electro-magnetic puller to control fiber length. The force transducer and the electromagnetic puller were part of a set-up composed of an aluminum plate equipped with seven small pedestals where drops containing different solutions were accommodated. The aluminum plate was placed on the stage of an inverted microscope (Axiovert 10, Zeiss, Germany). The fiber segment could be quickly moved from one small pool to the other allowing a complete change of solution within 5s. Dissection was carried out in a high potassium solution containing EGTA and the fiber was mounted in the same solution (*drop n 1*) whereas the other six drops were respectively

composed of skinning solution containing 5 mg/ml saponin(*n 2*), relaxing solution (*n 3*), loading solution (*n 4*), washing solution (*n 5*), releasing solution (*n 6*), and maximal Ca^{2+} concentration activating solution (*n 7*). The compositions of the solutions were identical to those described in a previous paper (Rossi *et al.*, 2001). The floors of the pedestals were transparent so that specimens could be viewed at 320x through the eyepieces of the microscope and a video camera connected to a computer. Signals from the force and displacement transducer were displayed and recorded after A/D conversion (interface 1401 plus; CED) on a computer where the software Spike 2 (CED) was used for analysis.

For measuring Ca^{2+} release fibers were transferred from the first drop (high potassium solution) to the second drop to be permeabilized with saponin for 30 s. Fibers were then immersed in relaxing solution (*n 3*), and then SR was loaded by immersing the fibers in a solution (*n 4*) at pCa 6.45 in the presence of 5 mM ATP. After the fibers had been washed (*n 5*) to remove excess EGTA, Ca^{2+} release was induced by transferring the fiber to solution *n 6* with low EGTA content (0.1 mM) containing caffeine in one of X variable concentrations from 0.1 to 20 mM (pCa 8). The fiber was finally transferred to activating solution (*n 7*) to measure the ability to develop force during a maximal activation (pCa 4.7). The fiber was then brought back to relaxing solution (*n 3*) to start a new cycle of loading and release. The release of Ca^{2+} was inferred by the transient tension development and quantified by the tension-time area, according to a method, first developed by Endo (Endo & Lino, 1988) and widely used (Launikonis & Stephenson, 1997; Rossi *et al.*, 2001). As discussed in a previous study (Rossi *et al.*, 2001), experimental and model analyses point to the tension-time area as the best indicator of the amount of Ca^{2+} released from the SR and later removed by EGTA and diffusion. The tension-time area was normalized to the tension developed during maximal activation (pCa 4.7, *solution 7*) to account for the variability of the ability of the myofibrillar apparatus in each fiber to develop force. After normalization, the tension-time area was expressed in seconds. Dose-response curves were interpolated using the sigmoid curve Y=T/[1+10^(logEC50-X)] where Y is the normalized area, X the caffeine

concentration, T the maximal response amplitude, EC50 the concentration at which half-maximal response is achieved.

- ***Grip test***. Strength developed by WT and Ank1.5-*null* mice during instinctive grasp was measured with the protocol indicated as grip test (Connolly et al., 2001). The mouse was held by the tail in proximity to a trapeze bar connected with the shaft of a force transducer. Once the mouse had firmly grabbed the trapeze, a gentle pull was exerted on the tail. The measurement of the peak force generated by the mouse was repeated several times with appropriate intervals to avoid fatigue and average peak force values were expressed relative to body mass (Connolly et al., 2001).

- **Treadmill and Gait Analysis Device.** A system was designed to allow video capture of the paws of the mice during treadmill locomotion. Hardware consisted of a treadmill with a digital video camera (Basler A301fc, Basler, Inc., Exton, PA) mounted directly below a testing chamber that enclosed the mouse on the treadmill (Mouse Specifics, Inc., Boston, MA). The testing chamber was a rectangular plexiglass “corral” (20 × 4 × 16.5 cm) that ensured the mouse remained within view of the camera at all times. The digital camera operated at 80 fps with a resolution of 658 × 494 pixels and the camera output was fed directly to a computer. Treadmill speed could be varied from 0 to 1.2 m/s. The animal was placed into the testing chamber and the treadmill was turned on where it could be seen live on the computer screen. As soon as the mouse was walking somewhat consistently (i.e., straight line, fixed position relative to the camera) the animal was recorded for a fixed period (12 s, see below) after which the treadmill was stopped and the mouse was removed from the testing chamber.
A step cycle or stride consists of two consecutive contacts of a given paw. From this video clip, we selected a portion of the video in which the animal consistently stayed in the same position relative to the camera (i.e., maintained the selected treadmill speed) for at least five strides per paw (mean, 11 ± 3.6; minimum = 5, maximum = 20). Analysis software determines when individual paws are in contact with the treadmill and then

uses this determination to derive standard gait parameters. Stride time is the time between two initial paw contacts with the treadmill for the same paw. Stance time is the portion of the stride time that the paw is in contact with the treadmill, and the swing time is the portion of the stride time that the paw is not in contact with the treadmill surface. Representative values for each parameter were calculated using the average of consecutive strides (5–20) for each of the four paws. For group comparisons, the right and left paws were averaged to give representative values for the front and rear paws for each animal.

- Statistical analysis. Data were expressed as mean ± standard deviation (SD), unless differently stated. Student's unpaired *t* test was used for comparisons between Ank1.5-*null* and WT data and statistical significance was set at $p<0.05$. GraphPad Prism software (Site company and location) was used for curve fitting.

RESULTS

Ank1.5 knock out mice.

To study in vivo the role of the SR small Ankyrin 1.5 isoform and its role in EC coupling, Ank1.5 null mice were generated Specific knockout of the mouse Ank1.5 first exon by homologuous recombination The muscle-specific exon, 39°, is replaced by a DNA segment containing a Neo gene (fig 0A). On Nothern blots, all three small muscle transcripts are absent in -/- skeletal muscle mRNA (fig 0B). The a.5 kD isoform is missino on immunoblots of -/- skeletal muscle membrane proteins with p6 antibodies (fig 0C). Several other small ankyrins immuno-reactive proteins, once though to be alteatively spliced isoforms of Ank1.5 ankyrin, are unaffected in -/- aimals. In WT muscles, using specific antibodies to Ank1.5 isoform in immunostaining, Ank1.5 protein appeared to localize with banded patterns in parallel with sarcomeric patterning (fig. 3Aa-c). Transversal sections of WT myofibers present a diffuse cytoplasmic distribution of Ank1.5 which colocalizes with α-actinin (not shown). In KO muscles, on the other hand, no Ank1.5 protein was detectable as expected (fig. 3Ba-c).

Ank1.5 null mice muscles present no alterated morphology.

As previous studies suggested that Ank 1.5 has a structural role, in particular in positioning the SR relative to myofibrils through Obscurin specific binding (Bagnato et al., 2003), we investigated first the Obscurin localization and structure in KO muscle using an osbcurin specific antibody (Fig. 3Ad-c and 3Bd-c). No differences were observed between AnK 1.5 null and WT, obscuring showing the typical patterns and colocalization with α-actinin. To get a full picture of the EC coupling apparatus we monitored others key elements. We localized with immunostaining RyR1 co-labbelling it with SERCA1 (fig. 3Ag-i and 3Bg-1); with triadin (fig. 3 Aj-l and Bj-l) and with DHPR (fig. 3Am-o and 3Bm-o). The typical double banded pattern of RyR channels was always found in Ank1.5-null muscles and it colocalized with DHPR and Triadin, while kept its typical patterning with SERCA showing no significant differences with WT muscles organization. At ultrastructural level (fig. 4B) the sarcomeric

architecture was not altered in KO muscle; z-disk and M-line was similar to WT, triads were normally organized and mitochondria normally distributed. To conclude we can state that unexpectedly no structural alterations could be detected in Ank1.5 KO muscles.

Ank1.5-null muscle have unaltered level of ECC proteins

To investigate if possible compensations in ECC coupling elements occurred in Ank1.5-null muscles, we screened with Western Blotting for sarcoplasmic recticulum proteins of adult ank1.5 +/+ and -/-. Different muscle lysates (extensor digitorum longus, soleus and diaphragm) where analyzed with antibodies against α_1S-DHPR, SERCA1 and RyR1 antibodies, but apparently no alterations in these proteins levels occurred (fig. 4A).

Ank1.5 KO slow muscles do not show functional alterations.

Ex vivo characterization of contractile activity of Soleus muscles was carried out in Ank 1.5 KO. Two different group of animals of different ages were investigated to characterize functional differences in relation to age. Soleus, together with EDL and Diaphragm, was dissected and kept under organ culture while exposed to electrical stimuli and tension was recorded with a force transducer. Both twitch and tetanic force were not significantly different in young (4-6 month) and old (12-15 month) KO compared to WT mice (tab 1; fig 5A). Also time to peak and half relaxation times were not significantly different in KO and WT mice., even if a small trend in longer kinetics can be noted.

Ank1.5 KO fast muscles have slower kinetics.

EDL muscle mechanics was also studied (tab1; fig 5B). Both twitch and tetanic force of KO EDL mice were similar to WT both in young and old animals. However, the kinetics appeared to be slowered in aged mice, but not in young mice, as time to peak showed a trend to a prolongation (data not shown), and half relaxation time was significantly longer in KO compared to WT.

Ank1.5 KO Diaphragm is weaker but not slower than WT.

The mechanics of diaphragm strips appeared to be different than that of hind limb muscles (tab 1; Fig 5C). Time to peak (not shown) and half relaxation time of KO muscles were similar to WT in young and old groups. No significant differences were observed even if there is a clear trend in developping longer kinetics in old, but not in young animals. On the other hand tensions unexpectedly developed in twitch and tetanus were reduced in KO mice compared to WT. To further explore these functional differences of KO diaphragm, single fiber experiments were performed (fig 5D). Single fibers were mechanically dissected from the muscles, permeabilized with saponin and exposed to different concentration of calcium and caffeine. No differences in force developed by direct activation with calcium and the amount of calcium relased with caffeine were observed. This indicates that, in single muscle fibres, the SR and the myofibrillar structure were not affected by the lack of Ank1.5, as suggested by electron microscopy and immunoistochemistry.

Considering these data together, we can state that in Anl1.5-null mice, diaphragm muscle presents a reduced force along with age, even if the muscle morphology appears not to be affetcted.

Ank1.5 null diaphragm shows necrotic fibers

To further investigate the reasons of diaphragm disfunction, we injected Evans Blue dye in both KO and WT mice. Histological observations revealed a small number of Evans Blue positive fibers in the diaphragm of KO mice (3,7%±0,7 over 500 counted fibers in three KO animals versus 1,7±1,2 in WT), indicating the occurrence of damage and necrosis (Fig. 5E). No positive fibers were observed in Soleus and EDL muscles.

KO mice do not develop less force in hind limb but show less resistance to fatigue.

To study Ank1.5 KO mice force in vivo, grip test which measures instictive grasp force of both anterior and posterior limbs was used (Fig 6A). KO and WT animals gave similar perfomances, and force was not reduced in KO mice, as expected from ex vivo experiments on soleus and EDL.

Endurance test was performed by comparing Ank1.5 KO with WT mice in a treadmill test, where animals were left running until exhaustion, KO mice showed a significantly reduced performance, as they were able to run only for half the time compared to WT. The same test was repeated also with Ank1.5 heterozigotes mice (+/-). These mice were able to run for the about same time as WT, indicating that one allele was sufficent to compensate the loss of function of their homozigotes brothers.

Ank1.5 KO mice show altered locomotor behaviour

Skeletal muscle ankyrins localize not only at SR, like the small sr Ankyrins isoforms, but also at sarcoplasma level, like AnkB (Tuvia et al., 1999; Mohler et al., 2002), and at neuromuscular junction level, like AnkG (Flucher et al., 1990; Bennet and Baines, 2001). To investigate whether motor control was affected in Ank 1.5 mice, a gait analysis test was performed. Surprisingly, KO mice showed a reduced gait length and higher gait frequences (Fig 6C) compared to WT.

DISCUSSION

Ankyrins are multidomain proteins, expressed in the majority of tissues where they play different functions, from signaling to structural roles. There are three genes encoding ankyrins and all generate different isoforms through alternative splicing. Ankyrins were first described as a link between integral membrane proteins and underlying spectrin network in the human erytrocyte (Bennet and Stenbuck, 1979). After this first observation, a variety of different ankyrins have been described in a large number of vertebrate cells and tissues, such as brain (Davis and Bennet, 1994), epithelia (Kordeli and Bennet, 1991) and skeletal muscles (Nelson and Lazaridies, 1984). In skeletal muscles all three genes are expressed and ankyrin proteins are located at plasma membrane, in the Golgy membrane and in the SR (Gargelin et al., 2002; Zhou et al, 1997). The sAnk1.5 locates specifically at SR and binds Obscurin colocalizing together both at M-bands and Z-disks (Armani et al, 2006). However, the exact role of sAnk1.5 is not clear as it may not act only as a structural component of the SR-myofibril connection. To investigate the roles of sAnk1.5, we have realized and characterized an Ank1.5 null mouse model. The KO mice are vital and similar to WT. Surprisingly no morphological and structural or ultrastructural alterations can be found in muscle fibres. On the contrary, functional alterations are present in fast muscles and, particularly, in diaphragm, as these muscle are weaker and slower in KO mice. Blue Evans positive, necrotic fibres are present in the diaphram of KO mice. Moreover, KO mice show a reduced endurance perfomance and altered locomotor. Alltogether these data suggest an active role of Ank1.5.

Recently, the role of Obscurin in the assembling the sarcomeres during development, in particular the M band and A band, and also the Z disk has been studied (Kontrogianni-Konstantopoulos et al, 2006, Young et al, 2001).

Unlike other sarcomeric proteins, such as myosin and myomesin, which are lost when obscurin levels are reduced by siRNA in myotubes, sAnk1

remains stably associated with intracellular membranes, consistently with its identity as an integral protein of the SR. The SR, however, fails to organize around the contractile elements when obscurin is depleted, suggesting a role for sAnk1 in organizing the network SR in its stereotypical pattern around the the middle of the M-band of the sarcomere. (Kontrogianni-Konstantopoulos et al, 2004 and 2006).

Ankyrins partecipate also in signal trasduction and protein sorting trough their binding to ion pumps, Ca2+ release channels and cell adhesion molecules (De Matteis and Morrow, 1998). Recently, an ankyrin-B-based macromolecular complex of Na/K ATPase (alpha 1 and alpha 2 isoforms), Na/Ca exchanger 1, and InsP3 receptor has been identified in cardiomyocyte T-tubules. Such complex is organized in discrete microdomains distinct from classic dihydropyridine receptor/ryanodine receptor complexes, suggesting a role for cytosolic Ca2+ modulation (Mohler et al, 2005). Moreover, a the tissue-specific alternative splicing of Ank3 in skeletal muscle has been shown to point to novel functions of small ankyrins-G in organizing microdomains of the plasma membrane (Hopitzan et al., 2005). Further evidence about the role of ankyrins come from the studies on the diseases attributed to Ankyrins (Bennet and Chien, 2001), including hereditary anemias in mice (Bodine et al., 1994) and humans (Eber et al., 1996; Tse and Lux, 1999) and cardiomyopathies. In particular, Ankyrin-B mutations are important in causing type 4 long-QT cardiac arrhythmia and sudden cardiac death (Mohler et al. 2003 and 2007).

This scenario suggests a complex concertated network of all ankyrins in skeletal muscle, where the Ank1.5 could play a specific role not restricted to a correct positioning of the SR at specific sarcomere regions. Ank1.5 mutations may contribute to the generation of myopathies, and EC coupling dysfunctions. However, further studies are required to clarify the exact role and mechanism of Ank1.5 in physiology and the Ank.1.5 mutations in causing alterations in skeletal muscle performance.

REFERENCES

1. Aderto JM, Steihardt RA (2000) Calcium influx trough calcium leak channels is responsible for the elevated levels of calcium-dependent proteolysis in dystrophic myoubes. *J Biol Chem* 275:9452-60

2. Agarkova, I., Ehler, E., Lange, S., Schoenauer, R., and Perriard, J. C. (2003) M-band: a safeguard for sarcomere stability? J. Muscle Res. Cell Motil. 24, 191–203

3. Armani A, Galli S, Giacomello E, Bagnato P, Barone V, Rossi D, Sorrentino V (2006) Molecular interactions with obscurin are involved in the localization of muscle-specific small ankyrin1 isoforms to subcompartments of the sarcoplasmic reticulum. Exp Cell Res. vol. 312 (18) pp. 3546-58.

4. P. Bagnato, V. Barone, E. Giacomello, D. Rossi, V. Sorrentino, Binding of an Ankyrin-1 isoform to the C-terminus of Obscurin identifies a molecular link between the sarcoplasmic reticulum and myofibrils in striated muscles, *J. Cell Biol*. 160 (2003) 245 – 253

5. Bang M.L., T. Centner, F. Fornoff, A.J. Geach, M. Gotthardt, M. McNabb, C.C. Witt, D. Labeit, C.C. Gregorio, H. Granzier, S. Labeit, The complete gene sequence of titin, expression of an unusual c700- kDa titin isoform, and its interaction with obscurin identify a novel Z- line to I-band linking system, Circ. Res. 89 (2001) 1065 – 1072.

6. Baumann O., B. Walz, Endoplasmic reticulum of animal cells and its organization into structural and functional domains, Int. Rev. Cytol. 205 (2001) 149 – 214

7. Baylor SM and Hollingworth S (2000) Measurements and interpretationof cytoplasmic [Ca2+] signals from calcium-indicatoes dyes. *News Physiol. Sci*. 15:19-26.

8. Bennet V, Baines AJ (2001) Spectrin and ankyrin-based pathways: metozan invections for integratine cells tissues. *Physiol Rev* 81 1352-1292.

9. Bennett, V., and Chen, L., (2001). Ankyrins and cellular targeting of diverse membrane proteins to physiological sites. Curr. Opin. Cell Biol. *13*, 61– 67.

10. Bennett V, Stenbuck PJ (1979): The membrane attachment protein for spectrin is associated with band 3 in human erythrocyte membranes. Nature, 280:468-473.

11. Berridge M J, P Lipp, M D Bootman (2000) The versatility and universality of calcium signaling. Nat Rev Mol Cell Biol. vol. 1 (1) pp. 11-21

12. Blaustei and Lederer (1999) Sodium/Calcium Exchange: Its Physiological ImplicationsPhysiological Review 79 792

13. Birkenmeier C.S., J.J. Sharp, E.J. Gifford, S.A. Deveau, J.E. Barker (1998) An alternative first exon in the distal end of the erythroid ankyrin gene leads to production of a small isoform containing an NH2-terminal membrane anchor, Genomics 50 79 – 88.

14. Bodine DM IV, Birkenmeier CS, Barker JE (1984)Spectrin deficient inherited hemolytic anemias in the mouse: characterization by spectrin synthesis and mRNA activity in reticulocytes. Cell, 37:721-729.

15. Brandl CJ, deLeon S, Martin DR, MacLennan DH (1987) Adult forms of the Ca2+ ATPase os sarcoplasmic reticulum. Expression in developing skeletal muscle. *J Biol Chem* 262: 3768-74.

16. Chen W, Steenbergen C, Levy LA, Vance J, London RE, Murphy E. (1996) Measurements of free Ca2+ in sarcoplasmic reticulum in perused rabbit heartloaded with 1,2-bis(2-amino-5,6-difluorophenoxy)ethane-N,N,N',N'-tetraacetic acid by 19F NMR. *J Biol Chem* vol. 271 (13) pp7398-4.

17. Davis JQ, Bennett V (1994): Ankyrin binding activity shared by the neurofascin/L1/NrCAM family of nervous system cell adhesion molecules. J Biol Chem, 269:27163-27166.

18. De Matteis M A, J S Morrow (1998) The role of ankyrin and spectrin in membrane transport and domain formation. Curr Opin Cell Biol. vol. 10 (4) pp. 542-9.

19. Du A., J.M. Sanger, K.K. Linask, J.W. Sanger, (2003) Myofibrillogenesis in the first cardiomyocytes formed from isolated quail precardiac mesoderm, Dev. Biol. 257 382 – 394.

20. Eber SW, Gonzalez JM, Lux ML, Scarpa AL, Tse WT, Dornwell M, Herbers J, Kugler W, Ozcan R, Pekrun A et al (1996) Ankyrin-1 mutations are a major cause of dominant and recessive hereditary spherocytosis. Nat Genet,13:214-218

21. Flucher B E, C Franzini-Armstrong (1996) Formation of junctions involved in excitation-contraction coupling in skeletal and cardiac muscle. Proc Natl Acad Sci USA. vol. 93 (15) pp. 8101-6.

22. Franzini-Armstrong, C., Protasi, F., and Ramesh, V. (1998*). Ann N Y Acad Sci*. 853:20-30.

23. Franzini-Armstrong C., The sarcoplasmic reticulum and the transverse tubules, in: A.E. Engel, C. Franzini-Armstrong (Eds.), Myology, vol. 1, McGraw-Hill, New York, USA, 1994, pp. 176 – 199.

24. Fromherz P (2006) Three levels of neuroelectronic interfacing: silicon chips with ion channels, nerve cells, and brain tissue. *Ann N Y Acad Sci* vol. 1093 pp 143-60.

25. Fromherz P, Offenhäusser A, Vetter T, Weis J. (1991) A neuron-silicon junction: a Retzius cell of the leech on an insulated-gate field-effect transistor, Science May 31;252(5010):1290-3

26. Gallagher P.G., B.G. Forget, (1998) An alternate promoter directs expression of a truncated, muscle-specific isoform of the human ankyrin 1 gene, *J. Biol. Chem.* 273 1339-1348.

27. Gallagher P.G., W.T. Tse, A.L. Scarpa, S.E. Lux, B.G. (1997) Forget, Structure and organization of the human ankyrin-1 gene, *J. Biol. Chem*. 272 19220 – 19228.

28. Gagelin C., B. Constantin, C. Deprette, M.A. Ludosky, M. Recouv-reur, J. Cartaud, C. Cognard, G. Raymond, E. Kordeli (2002) Identification of AnkG107, a muscle-specific ankyrinG isoform, *J. Biol. Chem.* 277 12978 – 12987.

29. Gregorio C.C., H. Granzier, H. Sorimachi, S. (1999)Labeit, Muscle assembly: a titanic achievement? Curr. Opin. Cell Biol. 11 18 – 25.

30. Gonzalez A and Rios E (2003) Molecular Control Mechanism in Striated Muscle. Solaro and Moss ed.

31. Kamp F, Donoso P, Hidalgo C (1998) Changes in luminal pH caused by calcium release in sarcoplasmic reticulum vesicles *Biophys J* vol. 74 (1) pp.290-6

32. Kontrogianni-Konstantopoulos A, Catino DH, Strong JC, Sutter S, Borisov AB, Pumplin DW, Russell MW, Bloch RJ (2006) Obscurin modulates the assembly and organization of sarcomeres and the sarcoplasmic reticulum. FASEB J. vol. 20 (12) pp. 2102-11.

33. Kontrogianni-Konstantopoulos A., E.M. Jones, D.B. van Rossum, R.J. Bloch, Obscurin is a ligand for small ankyrin 1 in skeletal muscle, Mol. Biol. Cell 14 (2003) 1138 – 1148.

34. Kordeli, E., and Bennett, V. (1991). Distinct ankyrin isoforms at neuron cell bodies and nodes of Ranvier resolved using erythrocyte ankyrin-deficient mice. J. Cell Biol. *114*, 1243–1259.

35. Kordeli E., M.A. Ludosky, C. Deprette, T. Frappier, J. Cartaud, (1998) AnkyrinG is associated with the postsynaptic membrane and the sarcoplasmatic reticulum in the skeletal muscle fiber, *J. Cell Sci.* 111 2197 – 2207.

36. Kordeli E, Ludosky MA, Deprette C, Frappier T, Cartaud (1993) Ankyring is associated with the postsynaptic membrane and the 3' ends are found among transcripts of the erythroid ankyrin gene. *J. Biol. Chem* 268 (1993) 9533-9540.

37. Kunimoto, M. (1995). A neuron-specific isoform of brain ankyrin, 440-kD ankyrinB, is targeted to the axons of rat cerebellar neurons. J. Cell Biol. *131*, 1821–1829.

38. Hopitzan AA, A J Baines, M Ludosky, M Recouvreur, E Kordeli (2005) Ankyrin-G in skeletal muscle: tissue-specific alternative splicing contributes to the complexity of the sarcolemmal cytoskeleton. Exp Cell Res. vol. 309 (1) pp. 86-98.

39. Inesi G (1994) Teaching active transport at the run of the twenty-first century: recent discoversies and conceptual changes. *Biophys J*. 66:554-60.

40. Lux, S.E., John, K.M., and Bennett, V. (1990). Analysis of cDNA for human erythrocyte ankyrin indicates a repeated structure with ho- mology to tissue-differentiation and cell-cycle control proteins. Nature *344*, 36 – 42.

41. MacLennan D H, Wong P T (1971) Isolation of a calcium-sequestering protein from sarcoplasmic reticulum. Proc Natl Acad Sci USA. Vol. 68 (6) pp 1231-5.

42. Meldolesi J., T. Pozzan (1998), The heterogeneity of ER Ca2+ stores has a key role in nonmuscle cell signaling and function, *J. Cell Biol.* 142 1395 – 1398.

43. Meissner G., (1994). Ryanodine receptor/Ca++ release channels and their regulation by endogeneous effectors. *Annu Rev Physiol*. 56:485-508.

44. Meissner G (1975) Isolation and characterization of two types of sarcoplasmic reticulum vesicles. *Biochim Biophys Acta* vol 389 (1) pp 51-68.

45. MichaelP. Maher[a,] , Jerome Pine[b], John Wright[c] and Yu-Chong Tai[c] (1999) The neurochip: a new multielectrode device for stimulating and recording from cultured neurone, Journal of Neuroscience Methods V. 87 1 February 1999, P 45-56.

46. Mobley BA, Eisenberg BR (1975) Sizes of components in frog skeletal muscle measured by methods of stereology*. J Gen Physiol*, vol. 66(1) pp. 32-45.

47. Mohler PJ, S Le Scouarnec, I Denjoy, J S Lowe, P Guicheney, L Caron, I M Driskell, J Schott, K Norris, A Leenhardt, R B Kim, D Escande, D M Roden (2007) Defining the cellular phenotype of "ankyrin-B syndrome" variants: human ANK2 variants associated with clinical phenotypes display a spectrum of activities in cardiomyocytes. Circulation. vol. 115 (4) pp. 432-41.

48. Mohler PJ, J Q Davis, V Bennett (2005) Ankyrin-B coordinates the Na/K ATPase, Na/Ca exchanger, and InsP3 receptor in a cardiac T-tubule/SR microdomain. PLoS Biol. vol. 3 (12) pp. e423.

49. Mohler P.J., J.Q. Davis, L.H. Davis, J.A. Hoffman, P. Michaely, V. Bennett, (2004a) Inositol 1,4,5-Trisphosphate receptor localization and stability in neonatal cardiomyocytes requires interaction with ankyrin- *B, J. Biol. Chem*. 279 12980 – 12987.

50. Mohler P.J., J.A. Hoffman, J.Q. Davis, K.M. Abdi, C.-R. Kim, S.K. Jones, L.H. Davis, K.F. Roberts, V. Bennett, (2004b) Isoform specificity among ankyrins, *J. Biol. Chem*. 279 25798 – 25804.

51. Mohler P.J., J.-J. Schott, A.O. Gramolini, K.W. Dilly, S. Guatimosim, W.H. duBell, L.-S. Song, K. Haurogne´ , F. Kyndt, M.E. Alı `, T.B. Rogers, W.J. Lederer, D. Escande, H. Le Marec, V. Bennett, (2003) Ankyrin- B

mutation causes type 4 long-QT cardiac arrhythmia and sudden cardiac death, *Nature* 421 634 – 639.

52. Mohler, P.J., Gramolini, A.O., and Bennett, V. (2002). Ankyrins. J. Cell Sci. *115*, 1565–1566.

53. Nelson W J, E Lazarides (1984) Goblin (ankyrin) in striated muscle: identification of the potential membrane receptor for erythroid spectrin in muscle cells. Proc Natl Acad Sci USA. vol. 81 (11) pp. 3292-6.

54. Paolini C, Quarta M, Nori A, Boncompagni S, Canato M, Volpe P, Allen PD, Reggiani C, Protasi F (2007) Reorganized stores and impaired calcium handling in skeletal muscle of mice lacking calsequestrin-1 *J Physiol (Lond)* vol. 583 (pt2) 267-84.

55. Pape PC, Jong DS, Chandler WK (1995) Calcium release and its voltage dependance in frog cut muscle fibers equilibrated with 20 mM EGTAA, *J Gen Physiol*. 106:259-336.

56. Penniston J T, Enyedi A (1998) Modulation of the plasma membrane Ca2+ pump. *J Membr Biol.* Vol 165 (2) pp. 101– 9.

57. Pessah IN, Waterhouse AL, Casida JE. (1985) The calcium-ryanodine receptor complex of skeletal and cardiac muscle. *Biochem Biophys Res Commun*. Apr 16;128 (1)

58. Peters L.L., K.M. John, F.M. Lu, E.M. Eicher, A. Higgins, M. Yialamas, L.C. Turtzo, A.J. Otsuka, S.E. Lux, (1995) Ank3 (Epithelial Ankyrin), a widely distributed new member of the ankyrin gene family and the major ankyrin in kidney, is expressed in alternatively spliced forms, including forms that lack the repeat domain, *J. Cell Biol*. 130 313 – 330.

59. Prasad S, Yang M, Zhang X, Ozkan CS, Ozkan M (2003) Electricl Field assisted patterning of Neuronal Netorks for the Study of Brain Functions*. Biomedical Microdevices* 5:2, 125-137.

60. Rosenberg R L, P Hess, R W Tsien (1988) Cardiac calcium channels in planar lipid bilayers. L-type channels and calcium-permeable channels open at negative membrane potentials. *J. Gen. Physiol*. 1988 p2752

61. Russel M.W., M.O. Raeker, K.A. Korytkowski, K.J. Sonneman, (2002) Identification, tissue expression and chromosomal localization of human Obscurin-MLCK, a member of the titin and Ddl families of myosin light chain kinases, *Gene* 282 237 – 246.

62. Sandow A (1952). "Excitation-contraction coupling in muscular response.". *Yale J Biol Med* **25** (3)

63. J.W. Sanger, P. Chowrashi, N.C. Shaner, S. Spalthoff, J. Wang, N.L. Freeman, J.M. Sanger, (2002) Myofibrillogenesis in skeletal muscle cells*, Curr. Orthop. Relat. Res*. 403S S153 – S162.

64. Schatzmann H J (1989) Asymmetry of the magnesium sodium exchange across the human red cell membrane. *Biochim Biophys Acta*. 1993 p 2831.

65. Schneider MF, Chandler WK. (1973) Voltage dependent charge movement of skeletal muscle: a possible step in excitation-contraction coupling. *Nature*. Mar 23;242, 5395

66. Smith JS, McKenna EJ, Ma JJ, Vilven J, Vaghy PL, Schwartz A, Coronado R. (1987) Calcium channel activity in a purified dihydropyridine-receptor preparation of skeletal muscle Nov *Biochemistry*.3;26(22):7182-8.

67. Sorrentino V (2004) Molecular determinants of the structural and functional organization of the sacroplasmic reticulum. *Biochim Biophys Acta* vol. 1742 (1-3) pp-113-8 1585 – 1596.

68. Stromer M.H., (1998) The cytoskeleton in skeletal, cardiac and smooth muscle cells, *Histol. Histopathol*. 13 283 – 291.

69. Takeshima H, Yamazawa T, Ikemoto T, Takekura H, Nishi M, Noda T, Iino M. (1995) Ca(2+)-induced Ca2+ release in myocytes from dyspedic mice lacking the type-1 ryanodine receptor. *EMBO J*. Jul 3;14(13):2999-3006.

70. Trinick J., L. Tskhovrebova, (1999) Titin: a molecular control freak, *J. Cell Biol*. 9 377 – 380.

71. Tse WT, Lux SE (1999) Red blood cell membrane disorders. Br J Haematol, 104:2-13. 29

72. Tuvia S, Buhusi L, Davis M, Bennet V (1999) Ankyrin-B is reguired for intracellular sorting of structurally diverse Va2+ homeostasis proteins. *J Cell Biol* 147 995-1007.

73. Van der Ven, P. F., Ehler, E., Perriard, J. C., and Furst, D. O. (1999) Thick filament assembly occurs after the formation of a cytoskeletal scaffold. J. Muscle Res. Cell Motil. 20, 569 –579

74. Veratti E., Ricerche sulla fine struttura della fibra muscolare striata, Mem. Ist. Lomb. Cl. Di Sc. Matem. E Nat. 19 (1902) 87 – 133.
75. Young P., E. Ehler, M. Gautel, (2001) Obscurin, a giant sarcomeric Rho guanine nucleotide exchange factor protein involved in sarcomere assembly, J. Cell Biol. 154 123 – 136.
76. Zhang, X., and Bennett, V. (1998). Restriction of 480/270-kD Ankyrin G to axon proximal segments requires multiple ankyrin G-specific domains. J. Cell Biol. *142*, 1571–1581.
77. Zhou, C.S. Birkenmeier, M.W. Williams, J.J. Sharp, J.E. Barker, R.J. Bloch, (1997) Small, membrane-bound, alternatively spliced forms of ankyrin 1 associated with the sarcoplasmatic reticulum of mammalian skeletal muscle, *J. Cell Biol*. 136 621 – 631

TABLES

		Twitch Force mN/mm^2	Tetanus Force mN/mm^2	Time to Peak s	Half Relaxation Time s
SOLEUS	*Wild Type* n=8	30,51±14,50	179,45±55	0,04±0,014	0,105±0,048
	Ank1.5-null N=8	29,09±16,17	171,85±72	0,048±0,014	0,014±0,107
EDL	*Wild Type n=8*	45,86±16,81	151,35±43,44	0,019±0,025	0,031±0,003
	Ank1.5-null n=10	36,12±17,14	129,30±58,99	0,029±0,030	0,082±0,181‡
DIAPHRAGM	*Wild Type n=12*	41,53±17,52	131,52±28,43	0,0368±0,005	0,076±0,007
	Ank1.5-null n=13	23,39±10,87‡	78,56±30,81‡	0,0442±0,005	0,095±0,014

Tab. 1 ***Tension and time parameters of Soleus, EDL and Diaphragm muscles of WT and Ank1.5-null old mice (12-14 months).***

Values are shown as Means ± SD; ‡ Significantly different at $P<0.05$.

FIGURES

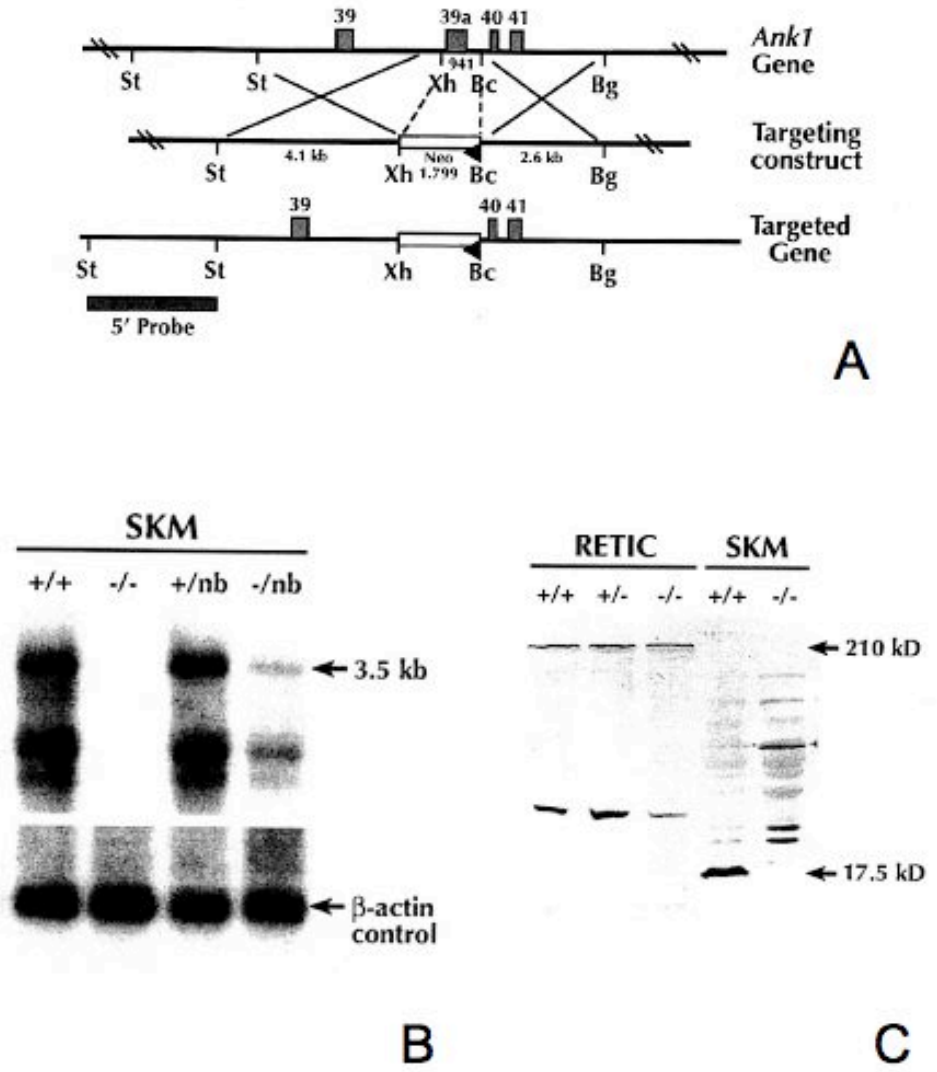

Figure 0 Specific knockout of the mouse Ank1.5 first exon by homologuous recombination. The muscle-specific exon, 39°, is replaced by a DNA segment containing a Neo gene (A). On Nothern blots, all three small muscle transcripts are absent in -/- skeletal muscle mRNA (B). The a.5 kD isoform is missino on immunoblots of -/- skeletal muscle membrane proteins with p6 antibodies (C).

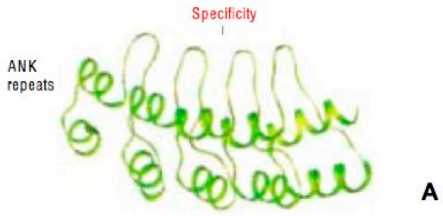

A

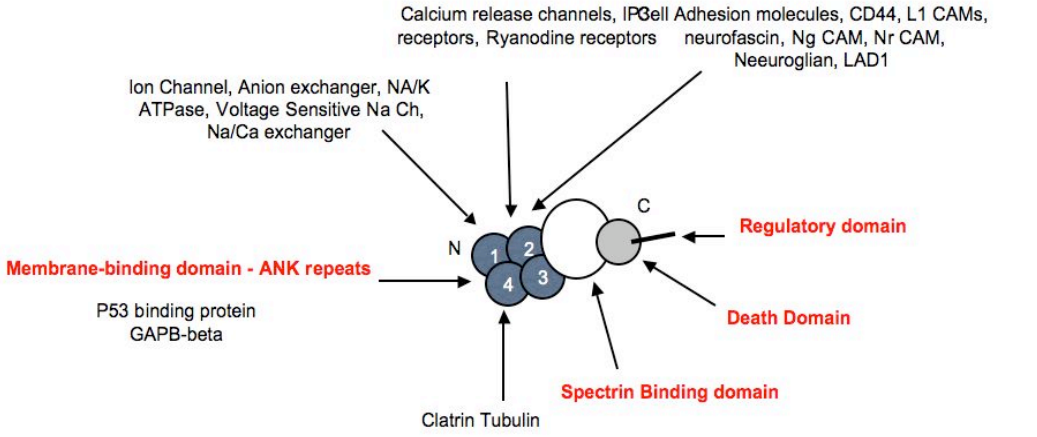

B

FIGURES AND LEG

Figure 1. Schematic view of ankyrin domains and their protein interactions. Ankyrins are modular proteins comprising three conserved domains
as well as specialized domains in alternatively spliced isoforms. The three conserved domains are the ANK repeats, the spectrin- binding domain and the death domain. The amino-terminal membrane-binding domain of ankyrins is composed of 24 ANKrepeats folded into six-repeat subdomains. These domains associate with a variety of membrane proteins including ion channels/pumps, calcium-release channels and cell adhesion molecules, as well as tubulin and clathrin. The bottom figure shows a stack of four ANKrepeats in the protein GABP-β. The sites of protein interactions are likely to be the loops of the ANKrepeats, on the basis of structures of complexes of GABP-βand several otherANK-repeat proteins with their protein partners [adapted from Bennet and Chienn, 2001].

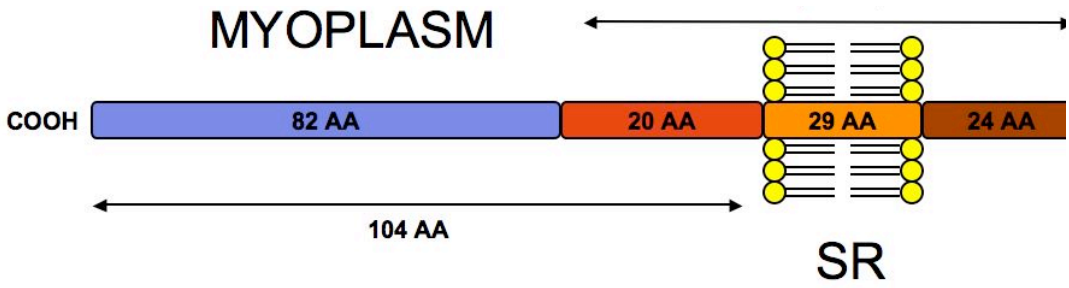

Figure 2. Ank1.5 sequence structure. The 73 unique aminoacid sequence at NH2 terminal is common for all the three SR Ank1 isoforms targets and a 29 AA sequence, in the picture colored orange, anchors with the proteins at the SR level. At COOH, colored in blue, a sequence present only in Ank1.5 reconginzes specific seuence of the giant citoplasmic protein obscurin in the nonmodular region at the COOH terminus following its last Ig-like domain.

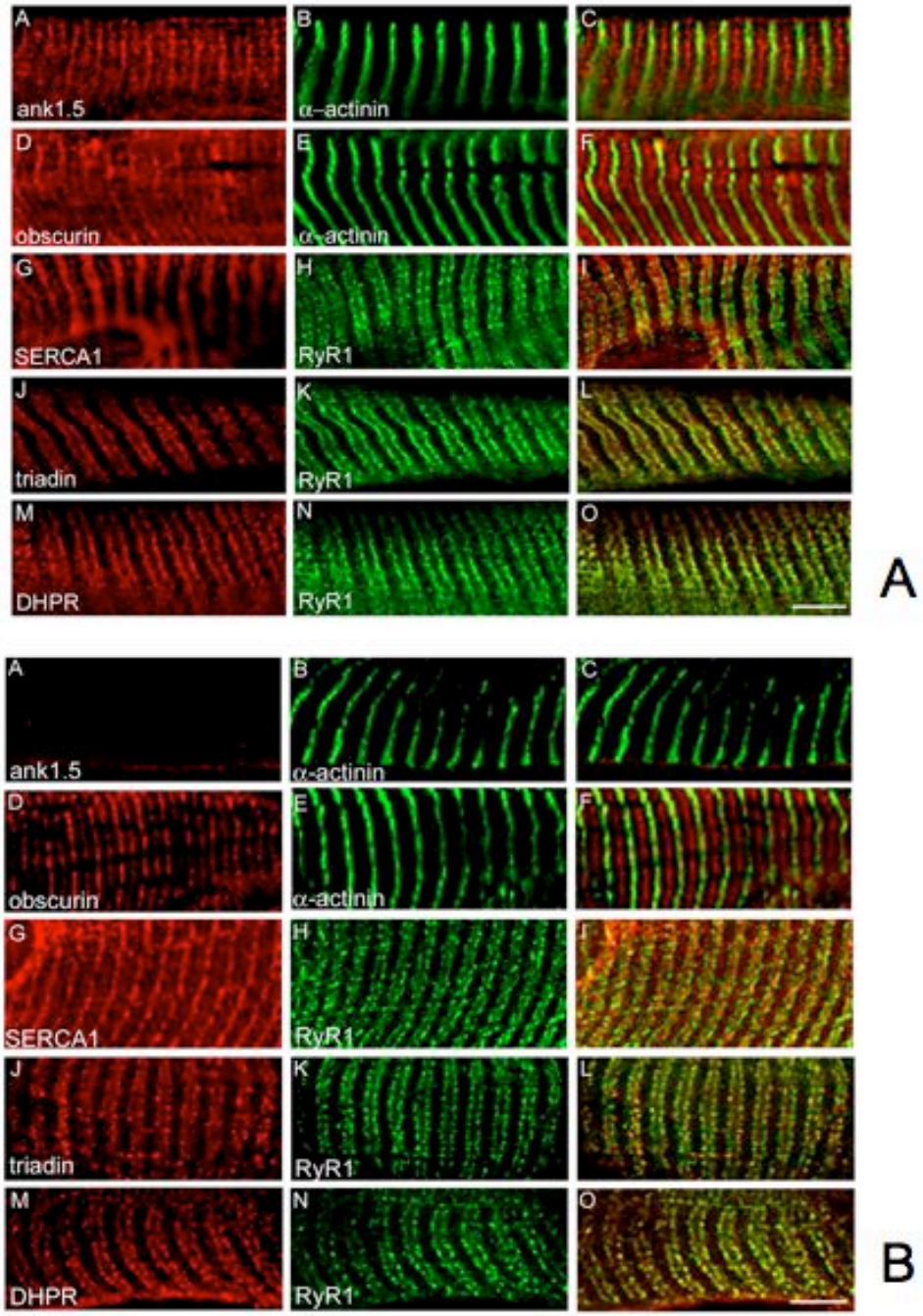

Figure 3. Ank1.5 null mice muscle morphology. To characterize the role of Ank1.5 as a structural intramembrane protein, immunostaining for Obscurin, RyR and SERCA have been processed for diaphragm muscle However, no differences between KO and WT have been observed, and all the sarcomeric and myofibrillar proteins present the typical patern. Longitudinal cryosections of adult ank1.5+/+ and ank1-5-/- EDL fibers were labelled with antibodies against ank1.5 (A and C), α-actinin (B, C, E and F), obscurin (D and F), SERCA1 (G and I), RyR1 (H, I, K, L, N and O), triadin (J and L) and α_1S-DHPR (M and O). Bar 5 μm.

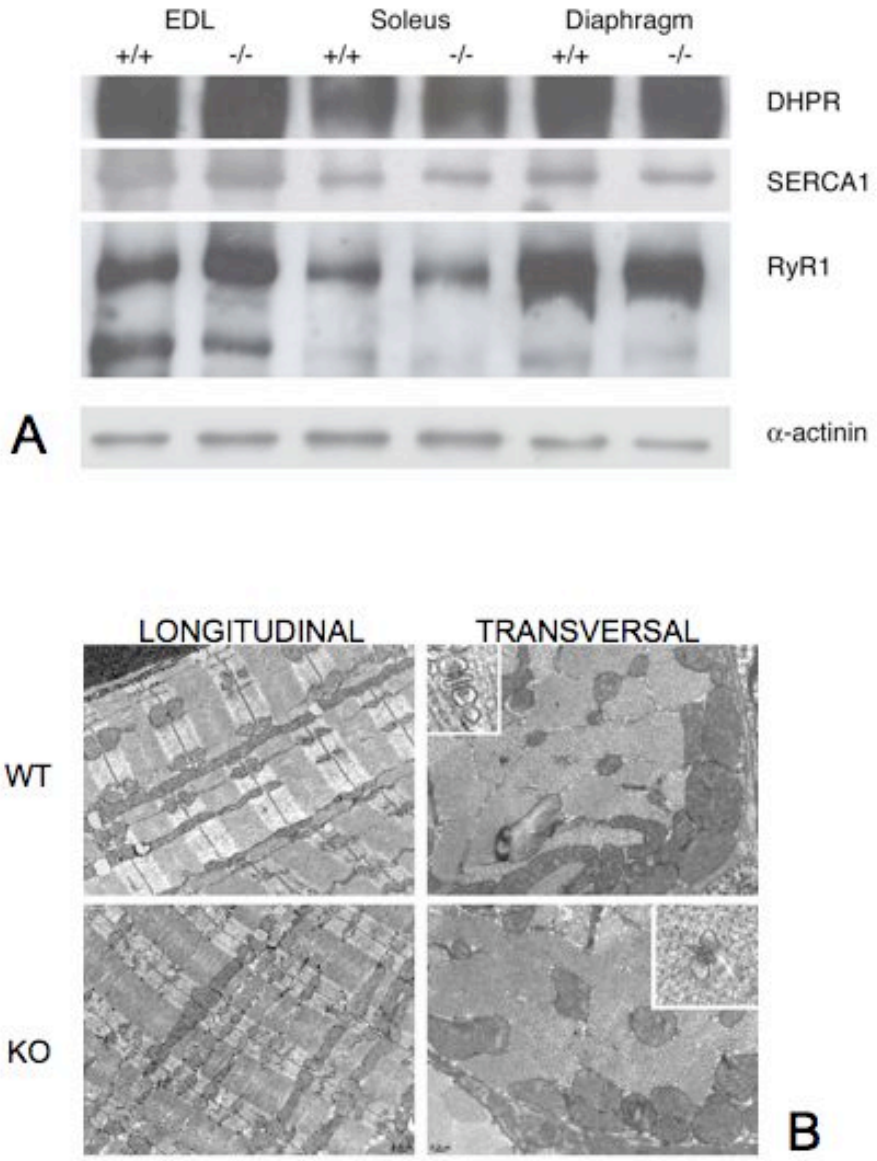

Figure 4. Ank1.5-null muscle ultrastructure and ECC proteins are unchanged. All ECC proteins considered in immunohistochemistry were analyzed with antibodies against α_1S-DHPR, SERCA1 and RyR1 antibodies in different muscle lysates (extensor digitorum longus, soleus and diaphragm). As control an antibody against a-actinin was used (A). Ultrastructure examined by electron microscopy does not display any difference in sarcomeric architecture and mitochondrial organization (B). Triads also are normal (small boxes).

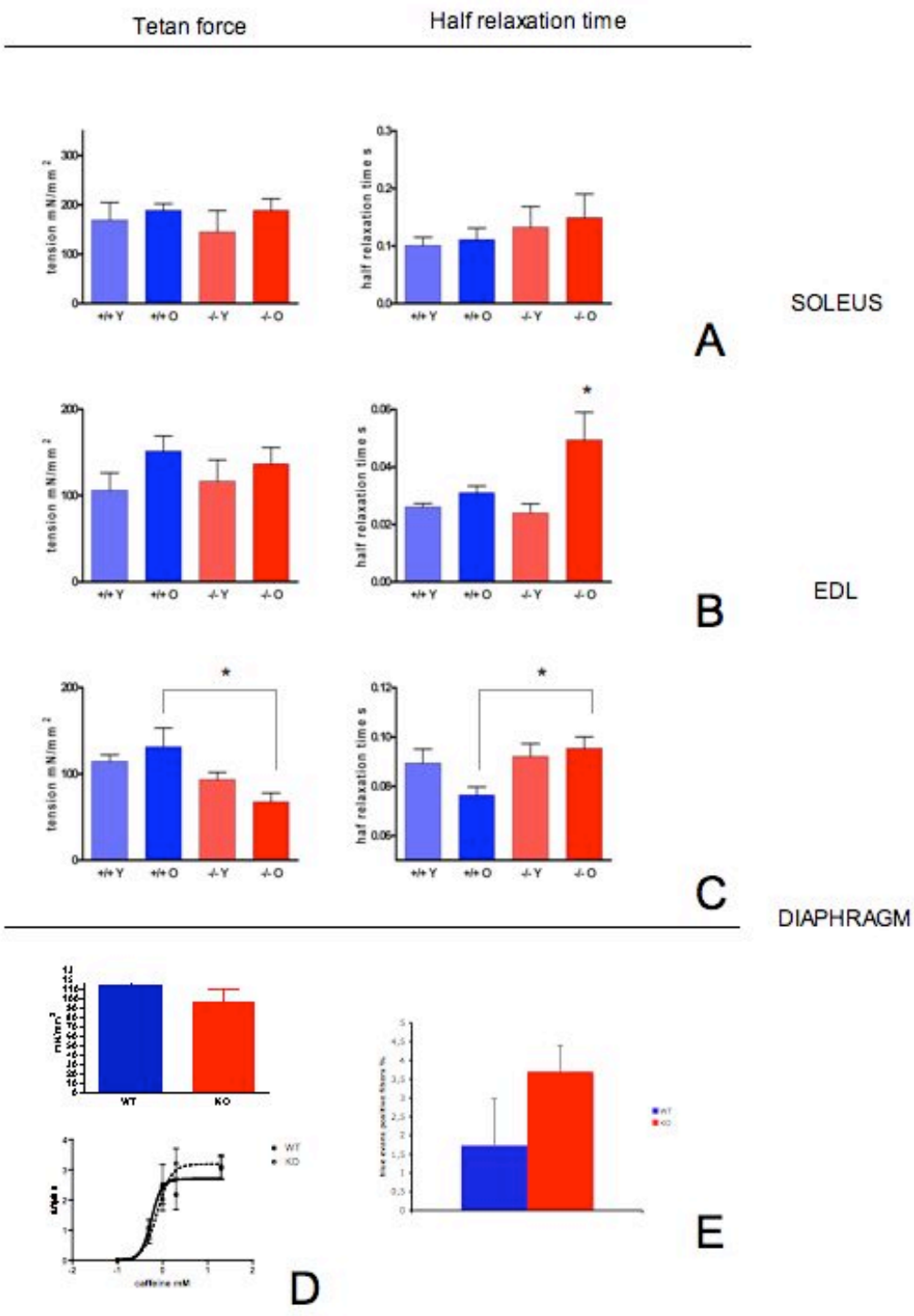

Figure 5. Ex vivo functional characterization of Ank1.5 null mice muscles. Muscle force generation and kinetics were analyzed during animal aging. Two groups were analyzed: mice 3-4 and 12-14 months age old. Our results show that Akn1.5-null mice present major differences along aging.
Slow muscles (A) do not show significant differences in tension generation and kinetics. On the other side, fast muscles (B) appear to be slower in KO than in WT but they generate similar forces. On the other side, Diaphragm KO muscles (C) are weaker than WT. However, single diaphragm KO fibers do not show reduced force or altered calcium release (D), but there is a small higher percentage (n=500) of necrotic fibers, positive to blue evans (E). Values are shown as Means ± SD; * Significantly different at $P<0.05$.

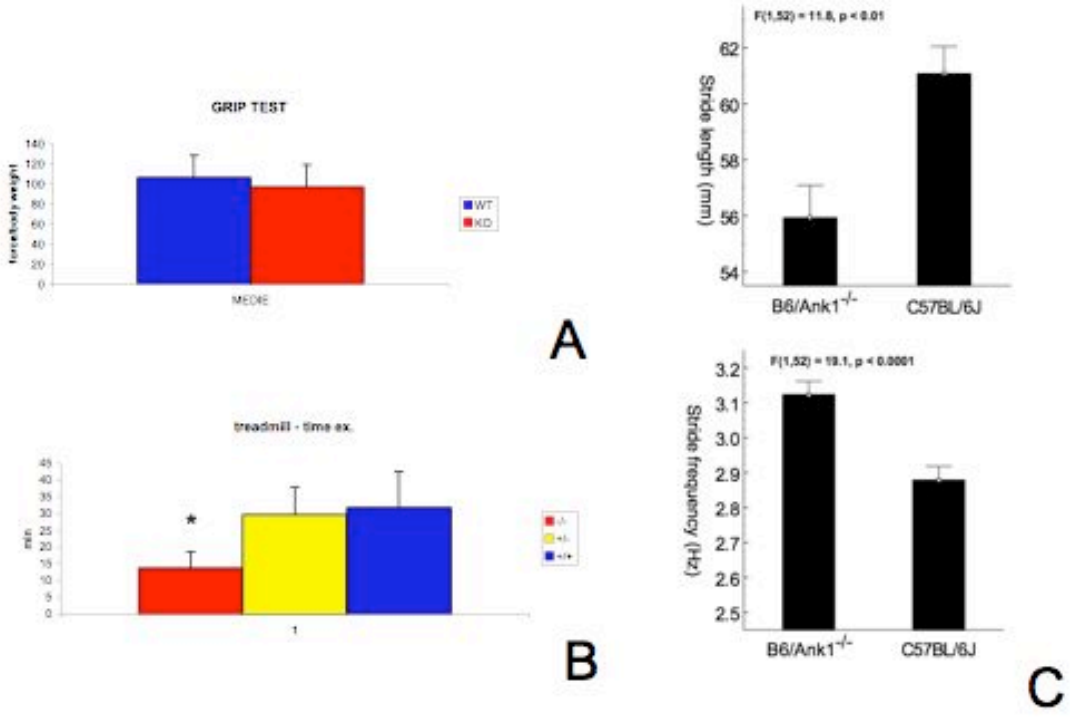

Figure 7. In vivo functional characterization of ANk1.5 null mice. Although KO mice generate similar force at limbs level in grip test (A), they show a drastic reduction of endurance performance in exhaustion tests (B), in accordance with the reduced force observed in diaphragm muscles and slower kinetics in fast muscle. KO mice present also alteration in locomotor behaviour; as indicated by the gait analysis (C) they have a reduced gait length but higher gait frequency. In all experiments n=10; age 12-14 months. Values are shown as Means ± SD; * Significantly different at P<0.05.

CHAPTER 4

A NOVEL MYO-SYLICON JUNCTION ACHIEVES SINGLE CELL ELECTRIC CAPACITIVIE STIMULATION AND MODULATES PLASTICITY AND IFFERENTIATION OF MYOGENIC

Authors

Marco Quarta[1], Michele Scorzeto[2], Marta Canato[1], Marco Dal Maschio[2], Bert Blaauw[3], Stefano Vassanelli[2], Carlo Reggiani[1]

Affiliations

[1] Muscle Biophysics Lab, Dept. of Anatomy and Physiology, University of Padova, Italy; [2] NaChip Lab, , Dept. of Anatomy and Physiology, University of Padova, Italy; [3] Venetian Institute of Molecular Medicine

ABSTRACT

We employed semiconductor bioelectronics to design an artificial neuromuscular junction prototype which achieves focal electric capacitive stimulation (ECS) of muscle fibres and myogenic cells at single cell level. Coupling without electrochemical process ion-conducing cells and electron-conducing semiconductors relies on a close contact of cell membrane and oxidised silicon with a high resistance of the junction and a high conductance of the attached membrane. Changing voltage applied to a stimulation spot beneath an electrogenic cell leads to a capacitive current through the insulating oxide. As a result voltage-gated ion channels may open in the membrane and an action potential may arise.

For this purpose we set up a model of electrical interfacing of individual muscle cells and silicon microstructures, as well as the assembly of elementary hybrid systems made by myotubes networks and semiconductor microelectronics.

The hybrid interface develops close contacts with single myoblasts, myotubes or dissociated muscle fibers offering a spatial resolution up to single cells separated by few micrometers from each other.

The myo-electronic junction was employed to stimulate muscle cells via ECS at different development stages and induced cytosolic calcium transients. Slow calcium waves were evoked in myoblasts while fast [Ca2+]i transients were induced in myotubes and muscle fibers.

The hybrid junction elicited via chronic ECS a programming of muscle cells by inducing muscle contraction maturation and muscle plasticity effects, such as NFAT-C3 nuclear translocation. In addition, in the presence of agrin, chronic ECS induced a modulation of AchR clustering which simulates an in vitro synaptogenesis .

INTRODUCTION

Neuro-electronics offers new avenues to biological investigation and application to excitable tissues, both in vitro and in vivo. In particular the studies, initiated at the beginnings of '90s (Fromherz at al., 1991) on interfacing neurons with semiconductors, have offered a new bio-electronics approach characterized by a spatial resolution down to nanometers and non-invasive two way interactions with cells.

Coupling without electrochemical process ion-conducing cells and electron-conducing semiconductor relies on a close contact of cell membrane and oxidised silicon with a high resistance of the junction and a high conductance of the attached membrane. Studies in this direction have progressed towards a neuron-semiconductor hybrid junction (REF) where neuronal excitation can be elicited and recorded from the chip by capacitive contacts and by field-effect transistors with an open gate (REF.).
In this model to obtain a perfect coupling between the two dielectrics, the lipid core of a cell membrane and the silicon dioxide should be fully attached (Fromherz, 2002). However, in practical terms they are never in close contact, but a distance in between is created by dangling polymer molecules that protrude from the membrane (glycocalix) and that are deposited on the chip (Gleizner and Fromherz, 2006). They give rise to repulsive entropic forces that balance the attractive forces of cell adhesion between the integrins in the membrane and collagen, laminin and other molecules deposited on the silicon surface and a cleft is formed in the junction.

According to an accepted model (Fromherz et al, 1991), changing voltage (V_S) applied to a stimulation spot beneath an electrogenic cell leads to a capacitive current through the insulating oxide (fig.1a). The concomitant current along the cleft between cell and chip gives rise to a *Transductive Extracellular Potential (TEP, V_J)* beneath the cell. As a result voltage-gated ion channels may open in the membrane and change the

membrane potential (V_M) until an action potential is triggered. The combination of transistor recording with whole-cell patch-clamp has confirmed that functional ion channels exist in the area of cell adhesion (Straub et al., 2001; Vassanelli and Fromherz, 1999) and their activation is the final result of the voltage applied to the stimulation spot.

Even if extensive studies have been performed in this direction using neurons and immortalized cells (Fromherz et al., 1991; Straub et al. 2001; Zeck and Fromherz, 2001), such an approach was never applied to skeletal muscle cells. Skeletal muscle cells, like neurons, are electrogenic cells, which have a plasma membrane, termed sarcolemma, characterized by Na+ Voltage gated ion channels to propagate action potentials and AchR, i.e. chemically gated ion channels to induce post synaptic excitatory potentials. Voltage-gated and chemically gated ion channels are organized together with the ending of innervating axon of a motor neuron in specific architectures defined Neuro Muscle Junction (NMJ).

Based on the above mentioned results in neurons, a bio-electronic interface might aim to become an artificial NMJ prototype. In this study we applied semiconductor bioelectronics to achieve focal electric stimulation together with chemical stimulation as a model to study muscle plasticity and synaptogenesis. For this purpose we set up a model of electrical interface of individual muscle cells and silicon microstructures, where single proliferating myoblasts or developing myotubes grow over semiconductor circuits with close junctions adhesion regions; as well as the assembly of elementary hybrid systems made by myotube networks, developed by myotubes fusing each other in several point or in communication each via gap junctions, and semiconductor microelectronics. The set-up was employed to investigate the response to ECS in terms of contraction and intracellular calcium waves and to follow the effects of long term stimulation on NFAT nuclear translocation as an example of activity-dependent plasticity and on AchR clustering as an example of activity dependent differentiation. In this respect we collected novel and surprising evidence in favour of the interaction between activity and agrin-signalling in NMJ formation.

MATERIALS AND METHODS

Animals

Muscles for preparation of primary cultures of myogenic cells were dissected from newborn mice, whereas FDB for preparation of adult muscle fibres were isolated from young (30-40 day old) mice. Mice were purchased from Charles Rivers Laboratory (Como, Italy) and killed by cervical dislocation. The experimental protocol was approved by the department Ethical Committee for Animal studies and by the Italian Health Ministry.

Semiconductor Chips

We used electrolyte/oxide/silicon capacitors as described in a previous study (Wallrap and Fromherz, 2006). As a substrate, we used p+-doped silicon 100 4 in. wafers, 400 m thick, polished one side, 0.006 – 0.01 cm. After a standard RCA Radio Corporation of America clean, a 1 m thick SiO2 field oxide was grown by wet oxidation. Circular capacitors with a diameter of 2 mm were etched. We created a thin buffer layer of silicon nitride that was reported to suppress the formation of an interfacial layer of SiO2 for HfO2 and TiO2 on silicon.10–12 After dipping the wafers into HF, the nitride buffer was formed with a rapid thermal processing system STEAG AST100NT, Mattson, Fremont, USA at 700 ° C in NH3 for 30 s. The wafers were coated with TiO2 and HfO2 in a flow-type ALD Refs. 13 and 14 reactor at ASM Microchemistry Ltd., Helsinki, Finland, with HfCl4 and TiCl4 as cation precursors and H2O as oxygen precursor. The deposition temperature was 300 ° C. An aluminum layer of 200 nm thickness was evaporated on the back of the wafers. Quadratic 4x4 mm^2 chips were cut, each containing one capacitor. We glued the chips on an aperture in the bottom of 35 mm polystyrene culture dishes (Falcon 3001,

Becton Dickinson, NJ) and contacted them with gilded springs. They were cleaned with hot detergent (5% Tickopur R36, Bandelin, Berlin, Germany), rinsed with Millipore water (Millipore, Billerica, MA), dried in nitrogen and sterilized with UV light for 20 min. They were coated with the Collagen TypeI solution prediluted in physiology buffer (No. C-0668, Sigma, Taufkirchen, Germany) by adsorption from a 0.5 mg/ml solution in 1% (v/v) PBS overnight.

Myogenic line cell cultures

C2C12 mouse myogenic cells were seeded at 5.000cells/cm^2 and cultured in Dulbecco's modified Eagle's medium (DMEM) supplemented with 2mM L-glutamine (Sigma, Aldrich Italy), 100U/ml penicillin, 100µg/ml streptomycin, 100µg/ml gentamycin and 20% heat-inactivated bovine serum (FBS) (Gibco BRL, Life Technologies, Germany) and maintained at 37°C in a humidified atmosphere of 5% CO_2. Cell differentiation and myoblast fusion were obtained by shifting to DMEM supplemented with 2% heat-inactivated bovine serum, 2mM L-glutamine, 100U/ml penicillin, 100µg/ml streptomycin, and 100µg/ml gentamycin (Sigma Aldrich, Italy). Experiments were performed on C2C12 myotubes from the third day of culture in fusion medium.

Primary cultures of myoblasts and myotubes

Primary myoblast cultures were derived from hind limb muscles of a 1-5 days old CD1 mouse. Muscle cells were dissociated by enzimatic digestion with trypsin (Sigma Aldrich, Italy) and of collagenase type I (Sigma Aldrich, Italy) solution at 37°C until the mixture is a melted slurry. Cells from this culture were grown on collagen type I-coated chip in Ham's nutrient mixture F-10 (Gibco BRL, Life Technologies, Germany) supplemented with 20 % horse serum (Gibco BRL, Life Technologies , Germany) and penicillin-streptomycin (100 U and 100 µg ml^{-1}, respectively; Sigma, Italy). To induce cells differentiation and myotube fusion the medium was replaced, 1 day after the plating, with DMEM (Sigma Aldrich, Italy) fusion medium supplemented with 2% heat-

inactivated bovine serum (Gibco BRL, Life Technologies , Germany), 2mM L-glutamine, 100U/ml penicillin, 100µg/ml streptomycin, and 100µg/ml gentamycin (Sigma Aldrich, Italy). Cells were maintained at 37°C in a humidified atmosphere of 5% CO_2.

Adult muscle fibre cultures

Flexor Digitorum Brevis (FDB) muscle was dissected out and placed in Tyrode solution (NaCl 140 mM; KCl 2 mM; CaCl2 0.5 mM; MgCl2 2 mM; HEPES 10 mM; glucose 5 mM) containing 0.2% type I collagenase and 10% foetal bovine serum (FBS) for 1 hour at 48C and then for 1 hour at 378C. After three washes in Tyrode solution containing 10% FBS to block the collagenase effect and stabilize the fibres, the muscle was gently dissociated by several passages through a Pasteur pipette with a large opening in a glass falcon test tube to obtain single fibres. Isolated fibres were plated on…… covered with mouse laminin, which produced fibre attachment within 1 hour. Fibres were maintained in Tyrode solution supplemented with 10% FBS and 1% penicillinstreptomicyn-amphotericin in an incubator, with 5% CO2 at 36.5 °C.

$[Ca^{2+}]$ Imaging

Cytosolic free $[Ca^{2+}]_i$ was measured in primary and C2C12 myoblasts and myotubes as well as FDB dissociated fibers loaded with the Ca^{2+} -sensitive intracellular probe fluo-4 (Molecular Probes, Invitrogen). Briefly, cells were loaded with 3µM fluo-4 in incubation buffer (125mM NaCl, 5mM KCl, 1mM $MgSO_4$, 1mM KH_2PO_4, 5.5mM glucose, 1mM $CaCl_2$, 20mM Hepes and 1% bovine serum albumine, pH 7.4 with NaOH) for 30 min at 37°C. After loading with Fluo-4, cells were washed twice for 10 minutes with incubation buffer without BSA at 37°C to retain the indicator in the cytosol. After a minimum of 30 minutes calcium signals were recorded.
Chips were then moved to the experimental set up. For calcium imaging recording we used an upright Olympus BX51W and water immersion objectives (LumPlanFI 40x/0.8 water and LumPlanFI 10x/0.3 water) for large numerical aperture. We minimized stimulation intensity via neutral density filters, according to required time sampling, to reduce fluorophore's photobleaching. Data were collected with a cooled CCD camera (Leica

DFC 350FX). Electrical pulse were generated by waveform generator (Agilent, 33250A) connected to the socket of the semiconductor chip. We used stimulation pulses with square and edge wave forms, at 1 V of amplitude and 1 msec of duration in both single pulse and different frequencies according to the experiment.

To compare calcium transients between different cells we carried on the following analysis. Time sequences were normalized on first frame acquired (F0), in order to get rid off of photobleaching, then to appreciate only intensity changes, F0 was subctracted from sequence by means of Image-Pro 6.0 (MediaCybernetics, USA). Then we selected ROI in nuclear, perinuclear and cytoplasmatic regions and performed a time measurement analysis with NIS-Elements A.R. 2.30 (Nikon Instruments, USA).

NFATC3 immuno-histochemical staining with peroxidase

Myotubes 8 days old from differentiatin media were chronically stimulated with stimuli of 1V of amplitude, 1 msec of duration in 5 seconds trains at 10 Hz with a resting time of 55 seconds for 1 to 3 days; then they were directly fixed on semiconductor chip with 4% formaldeide. They were washed with 4% PFA and with PBS, incubated with NH4Cl for 10 minutes and blocked with 0.3% H2O2 in 7% HS. After PBS washing, they were incubated 15 minutes in avidin, washed with PBS and incubated with Biotin. AntiBody: anti-NFATC3 polyclonal (rabbit) 1:500 in 0.5% BSA in PBS, 1 hour at 37°C, then added the secondary antibody biotinylatyed for 1 hour. After washing with PBS, the cells were incubated with ABC for one hour at RT, washed with PBS and incubated for 5 minutes for equilibration in TRIS 0.25 M. The cells were then incubated 20 minutes in DAB solution with 30% H_2O_2 and finally washed again with PBS.

Alpha-bugarotoxin Staining

Myotubes, 8 days after the transfer to differentiation medium, were exposed to 1 ng of neural agrin (RD System) added to DMEM supplemented with 2% heat-inactivated bovine serum for two hours. Then, without changing agrin-growing media they were prestimulated with ECS of square wave pulses of 1 V of amplitude, 1 msec of duration at 1Hz for two hours. After this pre-stimulation pahse, the ECS protocol was changed to chronic stimulation cycles of 1V of amplitude, 1 msec of duration in trains of 5 seconds at 10 Hz with a resting interval of 55 seconds overnight. Then, cells were fixed directly on semiconductor chips, with 4% formaldeide (Sigma), washed with PBS then incubated for one hour with alpha-bungarotoxins conjugated with alexa 312 green. For calcium transient-AchR localization studies on living cells, fluo-4 was loaded as described, followed by 30 minutes of incubation with alpha-bungarotoxins conjugated with alexa 416 red.
Images for evaluating AchR clustering areas were collected in a double-blind experiments, taking care in exposing samples to identical stimulus intensity conditions and acquiring data with same camera parameters.In order to exclude myotubes which were not coupled to devices only those showing calcium transients were chosen. For each myotube, the number and area of clusters were evaluated, via a threshold image analysis performed by plug-in implemented in Elements A.R. 2.30 (Nikon Instruments, USA).

TIRF Microscopy

We used commercial White-Light TIRF™ apparatus (Nikon Instruments, USA), mounted on Nikon TE2000E stage (Nikon Instruments, USA), in order to achieve the best signal-to-noise ratio in studying the features of the cell membrane in adhesion. The total internal reflection at glass coverslip-water interface was obtained by means of an objective based approach (CFI Plan Apochromat TIRF 60x/1.45 oil) with a penetration depth from about 80 nm to 130 nm. Filter cubes have emission bands of 515-555 nm for EYFP and Alexa Fluor 514, and 578-632 nm for Alexa

Fluor 568. Epifluorescence images were taken at the same focal plane changing the configuration of the TIRF illuminator. Images were analyzed by Image-Pro 6.0 (MediaCybernetics, USA). Images were acquired with the same objective mentioned above (72 nm/pixel) and 2 Mpixel CCD camera DS-2MBWc (Nikon Instruments, USA).

RESULTS

The importance of the interface

The Electric Capacitive Stimulation (ECS) is mediated by a *Transductive Extracellular Potential* (TEP) at the interface between electrogenic cells, such as neurons and myotubes, and semiconductors. A large *TEP* results from high currents through membrane and silicon dioxide, and from a low conductance of the junction (Fromherz, 2002)

When a voltage step is applied to oxidized highly doped silicon with an attached cell, we expect a polarization of oxide and cell membrane as indicated by the capacitors in the circuit of Fig. 1(a). Subsequently, the membrane can discharge through a resistor given by a film of electrolyte between oxide and membrane (Braun and Fromherz, 1997).

The dynamics of the voltage across the attached membrane $V_{JM} = V_M - V_J$ (potentials V_M and V_J in cell and junction) is determined by Eq. (1) with the capacitances C_S and C_M per unit area of oxide and membrane and the conductance g_J per unit area of the electrolyte film:

$$[C_M+(1+\beta_M) \times Cs] \times dV_{JM}/dt + (1 + \beta M)g_J V_{JM} = - Cs \times dV_{SB}/dt \qquad \text{eq. 1}$$

$\beta M = A_{JM}/A_{FM} < 1$ is the ratio of attached and free membrane area, and $V_{SB} = V_S - V_B$ is the voltage applied between solid and bath (potentials V_S and V_B in silicon and bath).

As demonstrated by Eq 1, recording and stimulation of muscle cell activity are promoted by a small distance *d*J, a high specific resistance *ρ*J, and a large radius *a*J of the cell-chip junction (fig.1a). Efficient recording requires high ion conductances in the attached membrane, efficient stimulation a high area specific capacitance *c*S of the chip. (Fromherz, 2002). The wide surface covered by developing mature myotubes or by FDB fibers over the EOS spot allows a large area of adhesion, and elect them as good candidates for the myoelectronics junction. However, in order to assure a long term coupling of myotubes and fibers and prevent myotubes early detachment , a specific coating was designed with nanolayers of collagen to assure longer adhesion during stimulation protocols. Actually, myoblast and myotubes showed unsafe behaviour when cultivated over non-coated silicon surfaces, presenting a defined borderline between coated and non coated zones.

The size and the quality of the interface in relation to the coating conditions adopted on the silicon chip compared to the coar-coat conductor model was analysed in specifically designed experiments . For this purpose TIRF microscopy was used to study the average distance, which must be below 100 nm to grant good coupling, and the average area of adhesion. We choose different conditions and cell models to study the hybrid junction at different development stages. Primary myogenic cultures and C2C12 immortalized myoblast, myotubes and dissociated adult FDB muscle fibers were examined and cultivated over silicon glass coated to reproduce the same conditions of the silicon chips on transparent material. Actually, it was not possible to use TIRF microscopy directly on the chip device since they are not transparent and inverted microscope is necessary to produce the total internal reflection fluorescence effect, required to exploit the unique properties of an induced evanescent wave or field in a limited specimen region immediately

adjacent to the interface between two media having different refractive indices.

The conditions of cells growing on chip were simulated on transparent substrates. Examples of TIRF images of the adhesion regions are shown in Figure 2. The majority of C2C12 myogenic cells at 90% of confluence showed a close adhesion between the 80 - 150 nm on the whole cell area surface in spite of the presence of some irregular adhesion regions detectable as spotted areas (see Fig 2B). Myotubes derived from C2C12 cells showed close and uniform junctions of adhesion on the surface below the 150 nm organized in regions of an average area of 500 μm^2 along the whole length of the myotubes, while other regions were left free and detached or with longer distance and weaker adhesion (Fig 2C). Moreover, in a multilayer myotube culture, typical for 6 days old myotubes, only deep myotubes developed adhesion regions over the silicon base surface, while upper myotubes did not any fluorescence adhesion staining (fig 2D). Primary cultures of murine satellite muscle cells were also examined with TIRF. Primary myotubes were contaminated by the presence of fibroblasts and showed less regions of close adhesion, compared to C2C12 myotubes. This was due to the fact that fibroblasts tend to grow below the myotubes offering them a base matrix which interferes with the hybrid cell-EOS junction formation (data not show). FDB dissociated adult muscle fibers cultured over a laminin layer coated silicon surface were also examined to determine the better coating condition to obtain adhesion regions below the 100 nm. The fibers generally form long regions of close adhesions along the whole length of the fiber membrane organized with striated patterns likely related with the costameric pattern (fig. 2D). However, not all fibers plated showed those regions of adhesion and, only some fibers were attached with the silicon surface strongly enough to assure a good coupling.

Electric Stimulation and Calcium Transients

To explore the semiconductor-muscle cells coupling and the related Excitation-Contraction Coupling of myogenic cells, myotubes and adult

muscle fibers cultured over the coated semiconductor planar device, calcium transients were monitored with FLUO-4 sensitive dye. The high specificity and spatial resolution of the semiconductor capacitor excitation system could be fully appreciated as only cells growing over the EOS spot were excited in contrast to adjacent cells which remained quiescent.

Myoblasts are generally considered to be bad responsive to electrical pulses since they lack a well developed SR. Unexpectedly, we observed that C2C12 (fig 3A-C) and primary (not shown) myoblasts coupled on the EOS spots responded to stimulation with synchronized calcium waves (Fig 3C), while cells growing out of the oxide semiconductor capacitor did not display any fluorescent signal. These observations demonstrated i) that myoblasts were fully responsive to ECS with large calcium waves and ii) that ECS was very specific as cells were not sensing capacitive stimulation even if close to the borderline up to few micrometers (fig 3a). This observations are in line with suggestions that electrical activity stimulates IP3-associated Ca2+ signlas (Valdes et al., 2007; Molgò et al., 2004).

To verify that electrical pulses applied below the myoblast membrane did not cause electroporation, ECS was applied in a buffer solution containing Evans Blue and cells were examined to see whether infiltration or penetration of coloured molecules were detectable after the stimulation. No cells positive to Evans Blue were found, indicating that ECS with the stimulation parameters used did not induce electroporation of the membrane (data not shown). To further study the origin of the calcium waves in myoblasts, the stimulation was repeated in a calcium-free buffer. Calcium slow transients within myoblast cytoplasm were observed under those circumstances as in the presence of extracellular calcium, suggesting that calcium release origin was intracellular (data not shown).

Experiments carried out on C2C12 and primary myotubes showed that both cell types respond similarly to ECS (fig 3D-E). Fast calcium transients were detected in the vast majority of myotubes which were well coupled over the EOS spot and activated by ECS. Compared to C2C12 myotubes,

a smaller fraction of primary myotubes responded to stimulation, thus showing a weaker coupling caused probably by the presence of fibroblasts located between the myotube and the capacitor (data not shown).

The kinetics of the calcium transients was very different in confluent myoblasts compared to mature myotubes (see fig. 4F). In myoblasts, calcium waves last for several seconds and can be considered as slow calcium waves (fig 3E). Differences can be detected with regard to the intracellular location: nuclear and perinuclear transients last longer than peripheral cytoplasmic waves (fig 3). Morover, myoblasts slow calcium waves appeared to respond differently to stimulation frequency. The duration of the calcium transient increases when a train of pulses at high frequency (30 – 40 Hz) were applied instead of a single pulse (Fig. 3E and 3F). On the other hand in C2C12 and primary myotubes (not shown) the calcium transient was faster (fig. 4F) and the fluorescence emission had similar time course in cytoplasm, perinuclear and nuclear regions.

Response to long term ECS

We next examined the relationship between calcium transient and myotubes contraction to explore the EC coupling within the semiconductor capacitive stimulation along myotubes maturation. Primary myotubes showed a good excitation by ECS. After 4-7 days of differentiation primary myotubes show frequent spontaneous contraction, and all myotubes coupled on the EOS responded at ECS with vigorous contractions.

C2C12 myotubes 6 days old showing 80% of excitation-calcium coupling, according with calcium transient, did not display comparable contractile responses. In fact only 10% of myotubes responded with full EC coupling to the stimulation. Spontaneous contractions in myotubes cultured on silicon semiconductors were very rare, in particular in comparison with myotubes cultured on plastic and on coated glass. However, after 2 hours of stimulation at low frequencies (0.5 or 1 Hz, 1V, 1ms) 90% of myotubes showed visible contractions in response to ECS. These observations are

in accordance with previous studies (Fujita et at, 2007), that provide evidence that electric stimulation induces sarcomere assembly in C2C12 myotubes and this leads to visible contraction. Based on these observations, we applied ECS for 6 hours at low frequency and then we changed it to chronic stimulation pattern for 24 hours using 5 seconds trains at 10 Hz every 55 seconds to induce plastic changes in myotubes. Contractions of myotubes were monitored optically before moving to chronic ECS.

To test the coupling in adult mature muscle fibers, we stimulated FDB fibers which responded at ECS with visible contractions modulated according to the stimulation parameters. In particular we observed a better modulation using voltage ramps rather than square pulse. The voltage ramps showed to integrate the signal along the duration of the stimulus, increasing the capacitive gating of ion channels along the fiber or the cell membrane, according to previous observation (Shoen and Fromherz, 2007).

NFAT-c3 translocation induced by long term ECS

To assess the potential effect of long term ECS on muscle cell plasticity we explored the effect of a prolonged low frequency stimulation on 6 days old C2C12 myotubes. As previously described (Kubis et al., 2002) stimulation at 10 Hz for 5 s followed by 55 seconds of rest, induces in myotubes phenotype changes characterized by a fast-to-slow transition. In particular, a transition in myosin expression from the myosin fast isoform to slow isoform has been observed (Meissner et al., 2000), Slow-type-specific gene expression in skeletal muscles has been shown to be controlled by a signaling pathway where calcineurin a calcium-regulated serine/threonine phosphatase is involved (Meissner et al., 2001; Serrano et al., 2001; Tothova et al., 2006). Activation of calcineurin in skeletal muscle fibres and in myotubes selectively up-regulates slow-fiber-specific gene promoters. Transcriptional activation of slow-fiber-specific transcription is mediated by a combinatorial mechanism involving proteins

of the NFAT and MEF2 families (Chin et al. 1998). Calcineurin activity and the related NFAT nuclear translocation are not sensitive to transient high-amplitude oscillation in [Ca2+]i but respond preferentially to sustained low-amplitude elevations of [Ca2+]I (Dolmetsch et al. 1997).

Based on the above evidence, we explored the endogenous NFAT nuclear translocation to assess whether fine transcriptional regulation could be elicited by ECS stimulation. In C2C12 myotubes not all NFAT isoforms are and we choose to study the NFAT-C3, since it is always expressed by mature C2C12 myotubes expressed (Delling et al., 2000). The endogenous NFAT-C3 was detected using the immunostaining with a specific antibody in myotubes coupled on the EOS in the semiconductor silicon microchip in three distinct conditions: i) non-stimulated, ii) stimulated at 0,5 Hz frequency and iii) stimulated at 10 Hz frequency. Only the myotubes coupled with the EOS and stimulated for 24 hours at 10 Hz displayed nuclear translocation, while no translocation was detected in myotubes non stimulated or stimulated at 0.5 Hz in the same chip (see Fig. 4G).

Towards an artificial NMJ

The results obtained with the NFAT translocation provided a strong demonstration that the myocell-EOS junction can be used to induce functional adaptation during in vitro differentiation or regeneration process of the muscle. The high resolution and the stimulation conditions close to the physiological ones prompted us to use the ECS in combination together with a chemical stimulation to develop an artificial neuro-muscle-junction model.

To explore the effects of calcium transients induced by ECS on NMJ development we stimulated 6 days old C2C12 myotubes coupled with EOS on silicon microchips. Before ECS, a pre-treatement of two hours with agrin was applied and was followed by agrin-ECS co-stimulation

overnight. At the end of the stimulation myotubes were stained with alpha-bungarotoxins conjugated with alexa 312 green and displayed a greater clustering (fig. 5a and b) in agrin-ECS costimulation condition compared to myotubes exposed to agrin alone. More precisely, when ECS and agrin were associated, the cluster number was reduced and their size was increased.

To confirm these findings in more controlled conditions we thought to check which myotubes were effectively coupled and responsive to ECS. To this end, we loaded myotubes with fluo-4 for 30 minutes before labeling with alpha-bungarotoxins conjugated with alexa 416 red for the next 30 minutes. We then stimulated myotubes with single pulses to identify with total certainty the responsive cells showing a clear calcium transient. At the end of the stimulation, while myotubes stimulated with agrin but not with ECS revealed many AchR clusters (fig.5e-f), agrin-ECS co-stimulated myotubes showed less clusters but with greater total area (fig5g-h). Interestingly, the clusters were organized around the EOS regions in agrin-ECS stimulated myotubes, while they were more dispersed in myotubes on the same microchip but outside EOS regions or in agrin stimulated control. On the whole, these results are strongly supporting the view that intracellular calcium transients induced by ECS are adequate to modulate the agrin-dependent mechanism of postsynaptic organization during the synaptogenesis at NMJ level.

DISCUSSION

“Myoelectronics” opens new perspectives to muscle research and applied neuroengineering. Indeed the use of electrogenic cells coupled with semiconductors leads to non invasive and single cells long lasting interfacing. Moreover the micro- and nano-electronic engineering offer today the chance to investigate the complexity of developing cell networks and to explore the cell plasticity. So far, neurons within neural networks have been explored by several studies (Zeck and Fromherz 2001; Maher

et al., 1999), but not yet muscle cells. In this scenario we realized a first skeletal myo-silicon junction to interface with semiconductor skeletal myogenic cells at different developmental stages. For this purpose, primary and immortalized myogenic cell lines C2C12 myoblasts were coupled on electrolyte-oxide-semiconductor and slow calcium waves were evoked by capacitive stimulation. The results showed a close coupling of the junction and unexpected responsive effects of non-electrogenic cells such as myoblasts to ECS, suggesting a possible role of voltage sensitive channels and calcium channels at this early stage. On the other side, in mature myotubes we observed contractions and fast calcium transients that were efficiently modulated by ECS evoked by the silicon chip. The same fast calcium transients and mechanical activity was also achieved in single dissociated muscle fibers from FDB. The stimulation device was also suitable to induce a long term ECS along hours and days. The effects of this long lasting stimulation were studied on C2C12 myotubes monitoring endogenous NFAT-C3 nuclear translocation under the effect of 10 Hz ECS trains, showing activity and calcium dependent effects of muscle plasticity. Finally, in the presence of agrin, a synaptogenic neural factor, the formation of agrin-induced clusters of Ach Receptors, was enhanced by the ECS evoked by the silicon junction.

The results of this study represent a fundamental step in neuro- and myo-electronics, putting the basis for future exploration of biological cellular systems complexes networked and self organized. The interactions of neural networks with myotubes networks connected by a closed electronic circuit designed for recording and for inducing biological and electrical signals, will reveal new aspects of how neuromuscular system develops, interacts and works under the integration of information (the neuro-system) and embodied conditions (the myo-system).

In general terms, it is important that cell-electronic interfacing is non-invasive for the cells and non-corrosive for the chips: it must rely on capacitive effects across the chip-electrolyte interface. When a muscle cell is excited, that it occurs on the myo-silicon chip, ion channels open in the cell membrane. Current flows along the seal of cell and chip, and gives

rise to a voltage on the open gate oxide of a field-effect transistor. For stimulation, a voltage transient is applied to an electrolyte-oxide-silicon capacitor. The resulting extracellular voltage opens ion channels such that the muscle is excited.
Moreover, current flowing along the seal of cell and chip, could be probed as already indicated by field-effect-transitor integrated in the chip, giving rise to a voltage on the open gate oxide. Integrated iono-electronic system are obtained by the outgrowth of myotubes networks on the surface of the silicon chip, by implementing electrical circuits in the chip and by two-way interfacing of the muscolar and the electronic components.

According to the model suggested, to achieve sensible coupling, the cleft distance between the cell membrane and the dioxide layer of the semiconductor must be around 100-300 nm (Fromherz, 2003). However this is a critical step. In particular for primary cell culture, proliferating cells tend to develop extracellular matrix and multilayers which isolate myotubes from the semiconductor surface active area. Moreover, contracting myotubes tend to detach from the surface, loosing contacts and coupling. To achieve a good coupling is so necessary to design efficient coating conditions with characteristics of biocompatibility, elasticity and thickness. We tested several coating conditions using autoassembling nanolayers of collagen, laminin or polilysyin where muscle cells grow over our silicon chip developping close and large adhesion regions and establishing the necessary conditions to be coupled and responsive to ECS. This is a fundamental step to design a system suitable for chronic stimulation. ECS offers a way to polarize the cell membrane, to modulate hyper- or de-polarization and to induce action potentials (Schoen and Fromherz 2007). On skeletal muscle cells this leads to ECC. Our stimulating conditions proved to be non invasive, with a single cell resolution and to be used for long term. Moreover, our set up could be programmed and controlled remotely directly within the incubator via a software designed on labview platform to schedule different timed protocols adapting wave forms, frequency, voltage and amplitudes according to the cell development stage and experimental stimulations needed.

In particular, when a muscle cell is stimulated, a voltage transient is applied to an electrolyte-oxide-silicon capacitor. The resulting extracellular voltage opens ion channels so that the muscle is excited. The excitation induces action potential which is propagated by Na+ channels along the sarcolemma and it is probed by sarcolemmal slow voltage gated L-type Ca2+ channel (dihydropyridine receptor, DHPR), which are coupled with Ca2+ release channel (ryanodine receptor, RyR1), localized transmembrane on Calcium internal stores, i.e. Sarcoplasmic Reticulum (SR). DHPR induces calcium release from SR lumen to cytoplasm trough RyR1, and [Ca++]i leads to contraction via troponin-actin-myosin pathway. This mechanism is defined Excitation-Contraction coupling (ECC) (Sandow, 1965; Schneider & Chandler, 1973; Rios et al. 1991).

To test our system, we chose the skeletal muscle cell line C2C12 as biological model as C2C12 myotubes show great similarities in Ca2+ signalling to adult muscle fibres (Schuhmeier & Melzer, 2004; Ursu et al. 2005). We verified Chip-ECC connection also on primary myoblasts, myotubes and dissociated FDB fibers to control the efficiency of the system and the reproducibility on primary cells conditions. In this study, C2C12 myotubes were used also for in vitro studies on muscle plasticity and synaptogenesys where the electrical stimulation acts as the modulator of muscle cell development in vitro.

In parallel with in vivo stimulation-depended activity, cross-innervation and electrical stimulation, experiments of ECS demonstrated a complete and reversible transformation of pre-existing myofibers by changing patterns of neuronal firing (Williams et al., 1986; Pette and Vrbova 1992). Many studies have identified sets of specific contractile proteins and enzymes of intermediary metabolism, the selective expression of which regulates the physiological and biochemical diversity among skeletal myocites (Saltin and Gollnick 1983; Booth and Baldwin 1996; Schiaffino and Reggiani 1996). In fact neuronal stimulation of muscle ECC induces changes in the intracellular levels of several signalling related molecules such as nitric

oxide, cyclic AMP but also of intermediate-early gene expression and their product (c-fos) or molecular chaperones (hsp70) (Michel et al. 1994; Neufer et al., 1996; Williams and Neufer 1996) In this stage [Ca2+]i plays as a major actor also as second messenger in several pathways involved in muscle plasticity, such as the calmodulin-calcineurin-NFAT (Chow et al, 1997; Crabtree, 1999; Liu et al., 2001; Olson and Williams, 2000) or the PGC-1α (Ojuka et al., 2003) pathways.

Electrical-dependent signalling has been deeply investigated in skeletal muscle cells in past years. The intermediate messenger in these pathways is free calcium transient, evoked by electrical activity through membrane depolarization. Experimental evidence showed how [Ca2+]i not only acts to be the intermediate element in the EC coupling, released by RYR1 for fast calcium transients, but [Ca2+]i plays also the role in phospholipase C/inositol 1,4,5-trisphosphate-dependent slow calcium waves (Jaimovich et al., 2000; Estrada et al., 2001). Experiments indicate that DHPRs act as voltage sensors activating Gbetagamma/phosphatidylinositol 3-kinase gamma signaling pathway involved in phospholipase C activation and the generation of the slow calcium signal induced by electrical tetanic stimulation (Eltit et al, 2006). This slow calcium signal has a predominant nuclear component, where Ip3 receptors are also located, and functional calcium store in isolated nuclei has been described (Cardenas et al., 2005).

Capacitive stimulation by EOS shows control of ECC over myogenic cells, and fast calcium transients are precisely detectable when excited with single pulses. However, when myotubes are stimulated at higher frequencies (30-40 Hz), a second slow waves can be monitored as indicated by previous studies. Interestingly, coupling confluent myoblasts with EOS, we observed in our studies that they respond to electrical pulses presenting slow calcium waves with kinetics consistent with previous observations in myotubes (Estrada et al., 2001) while they do not respond as expected with fast calcium transient. Our results suggest a possible role of voltage sensitive receptors or channels at myoblast stage which lead to calcium waves, even if they appear to lack of mature ECC

(Tarroni et al. 1997) and the relative ECC apparatus architectures (Jujita et al., 2007; Lorenzon et al., 2000). In fact, previous studies also suggested that primary myoblasts can show electrical field effects with pathways which lead to morphology alterations and gene expression regulations (Stern-Straeter et al, J.Cell.Mol.Med, 2005).

We can speculate according to our and previous observations that in C2C12 myotubes there is some key step missing during maturation to obtain correct contracting and functional myotubes. Also in 3D tissue engineering studies (Dennis et al, 2001) there is evidence that electrically stimulated contractile activity improves performance of small artificial muscles, called myoids. In this context ECS might represent a way to guide in vitro muscle development at sub-cellular level, evoking action potentials in focused regions on myotubes or myoids membranes in a junction like model.

Moreover, in myoblasts and myotubes stimulated via ECS, calcium release appears to localize in nuclear and perinuclear regions. These observations are consistent with experimental indications about nuclear IP3 receptors which regulate local Ca2+ transients (Jaimovich et al, 2000) and nuclear calcium storage (Cardenas et al., 2005). These results indicate different pathways for [Ca++]i playing different roles in calcium signaling which can be controlled by ECS during in vitro muscle differentiation.

The calcium transients triggered by ECS play the role of intracellular signals in myotubes, triggering distinct pathways, according to their frequency, amplitude and duration. Recent studies demonstrate that calcineurin activity and the resulting nuclear translocation of NFAT are insensitive to transient, high-amplitude oscillations in [Ca2+]i that activate other calcium-dependent events (e.g., NF-kB or c- Jun amino-terminal kinase). Rather, the calcineurin-NFAT pathway responds preferentially to sustained, low-amplitude elevations of [Ca2+]i (Timmerman et al. 1996; Dolmetsch et al. 1997). This ability of a calcineurin-dependent signaling pathway to discriminate between different patterns in the amplitude and

duration of changes in [Ca2+]i, in conjunction with previous data characterizing differences in intracellular calcium concentrations among specialized myofiber subtypes, provided the basis for the view that a calcineurin-dependent pathway influences fiber-type-specific gene expression. Tonic motor nerve activity at 10–15 Hz is characteristic of slow-twitch fibers (Hennig and Lomo 1985) and results in a sustained elevation of [Ca2+]i within a concentration range between 100 and 300 nM (Chin and Allen 1996), a pattern predicted to activate calcineurin. In fast myofibers, resting [Ca2+]i is maintained at levels of only 50 nM (Westerblad and Allen 1991), and the high amplitude (10 μM) calcium transients evoked by motor nerve activity are predicted to be of insufficient duration to evoke calcineurin-stimulated signaling. Chronic stimulation at 10 Hz of the motor nerve innervating fast myofibers results in sustained elevations of [Ca2+]i and promotes fast-to-slow fiber transformation (Williams et al. 1986; Sreter et al. 1987). Calcineurin and several NFAT isoforms are abundant in skeletal muscles (Hoey et al. 1995), and we wanted to induce the C2C12 isoform NFAT-c3 to translocate in the nucleus as a positive control that ECS induces calcium dependent activity.

Calcium signaling activates the phosphatase calcineurin and induces movement of NFATc proteins into the nucleus, where they cooperate with other proteins to form complexes on DNA. It is demonstrated that this pathway is implicated as regulator of developmental cell-cell interaction and of muscle plasticity (Olson 2002; Delling et al., 2000; Crabtree, 1999). C2C12 myotubes show endogenous NFAT-C3 nuclear translocation when excited by ECS with short 10 Hz trains of 5 seconds per minute. The nuclear translocation is limited to myotubes located over micro stimulating spots and excludes all other myotubes growing even few micrometer outside the EOS region.

The effectiveness of ECS on myotubes developing over silicon chips inspired us to apply it to modulate other calcium dependent pathways. a molecular receptor, relevant for both neural and muscular system, the Acetyl Colin Receptor (AchR) was chosen.It is commonly accepted that AchR channels activity controls myoblast fusion into myotubes during

myogenesis, with evidence that endogenous AchR compounds in vitro are spontaneously activated by autocrine cholinergic agonist (Krause *et al.* 1995), and after fusion myotubes develop AchR spontaneous clusters which can keep a role in late maturation (Bandi et al., 2005).

Post synaptic differentiation mechanisms have been deeply investigated for the neuromuscular junction (NMJ). The main actor is the protein Agrin released from the nerve endings (McMahan and Wallace, 1989), which triggers the AchR clustering on myotubes surface. Agrin acts via an intracellular signalling cascade triggered upon binding to the complex tyrosine MuSK receptor and possibly to others co-receptors (Glass et al., 1996). This leads to AchR clustering through cytosolic protein rapsyn (Gautam et al., 1995) and nitric oxide (Jones and Werle, 2000). In this scenario calcium plays a fundamental role both at extracellular level to activate MuSK and at intracellular level in the agrin signaling patways (Borges et al., 2002; Megeath and Fallon, 1998). Calcium fluxes are likely to act downstream of the early events in the agrin signalling cascade (Boges et al., 2002) and several data suggest that agrin-induced calcium transients may serve as a control point for postsynaptic differentiation (Megeath et al., 2003).

At NMJ level, [Ca2+]i is essential at presynaptic level to induce the neurotransmitter Ach release in the cleft when an action potential depolarizes the synapses and voltage sensitive channels Ca2+ channels opens. In addition, the mobilization of intracellular Ca2+ at post-synaptic level has been demonstrated to regulate the formation and/or the maintenance of agrin-induced AchR clustering (Megeath and Fallon,1998; Megeath et al., 2003). Neural Agrin is a protein secreted by axon terminal during development (Sanes and Lichtman, 2001) and acts in synaptogenesys differentiation together with Neuregulin (Carraway and Burden, 1995), electrical activity (Goldman and Brenner, 1988) and extracellular matrix proteins (Weston et al., 2007; Tseng et al., 2003). In particular, agrin activation of muscle specific kinase (MuSK) initiates postsynaptic development on skeletal muscle that includes the

aggregation of acetylcholine receptors (Glass et al. 1996; Gautam et al. 1996). Its action is regulated also by neurotrophins (Wells et al, 1999) and many other factors, even if the exact role of neural agrin is still not clear since AChR clusters have been found in the embryo in the absence of innervation (5–8) as well as in pure myotube cultures (9–12), which indicates that signals other than neural agrin can trigger the mechanism that leads to AchR cluster formation.

The aim of the present experiments was to find experimental evidence of artificial hybrid neuro-muscle-junction (NMJ) model to restore loss of function of denervated muscles or to improve in vitro engineering of muscle tissue with local organized NMJ like architecture coupled with non invasive external microdevice.

Since nerve-muscle connectivity is shaped by the activity-dependent elimination of synapses on multiply innervated myofibers (Lichtman and Colman, 2000), synapse-like activity could guide the development or regeneration of innervated muscle in vitro. A detailed knowledge of postsynaptic differentiation mechanisms at NMJ is available, in particular, the formation of synapses is directed by the neurotrophyn agrin, secreted by the motor nerve terminal (McMahan and Wallace, 1989). Posynaptic differentiation can be induced in culture adding agrin to the media culture to induce the formation of Acetylcholine receptor (AchR) clusters on the myotube surface (Borges and Ferns, 2001). Calcium plays at least two role in agrin-induced AchR clustering. Extracellular calcium is necessary for agrin to activate MuSK, while intracellular calcium plays an integral role in the agrin signaling pathway (Borges et al, 2002).

The present experiments showed that long term ECS on C2C12 myotubes exposed to agrin caused a reduced number of AchR clusters, but cluster average area was increased, suggesting that clusters tended to fuse when myotubes contract actively. Based on the above observations, we can postulate that the reduced numbers of clusters and the their increased area on myotubes locally stimulated with ECS is an electrical depend AchR clustering modulation, where cytosolic [Ca++] plays a major role.

There is evidence that during the synaptogenesis, postsynaptic nuclei are activated and transcription is up regulated whereas extrasynaptic nuclei are downregulated and switched off (Ravel-Chapuis et al., 2007). In preliminary data, not presented here, we observed that on myotubes ECS-agrin stimulated, bigger clusters appear to concentrate close on the surface directly in contact with EOS. In z-stack observations under video confocal studies, we noted that big clusters tend to move down to the adhesion region, along the junction direction. With the present level of technology it is possible to designe new silicon chips with matrixes of capacitors integrated at nano scales (Vogel, 2007), to modulate electric stimulation in a small nanometer area above the myotubes surface. Moreover technical problems like dielectric dead layer effects are likely close to solution (Stengel and Spaldin, 2006). Finally, combining microfluidic local delivery of agrin and other synaptic molecules (Folch, 2006) with nano-eos electrical stimulation on focused myotube membrane, a first step towards in vitro NMJ development and muscle reorganization will be achieved. Moreover, new possibility will opened to the study of synaptogenesys and calcium related pathways.

To conclude, the present experiments represent a new and important step in neuro- and myo-electronics and set the basis for a future exploration of neuro-muscle-embodiment understandings in neurophysiology and neurorobotics (Ziemke, 2008; Pfeifer et L., 2007; Beer, 2004; Rudrauf D et al., 2003; Thompson and Varela, 2001; Beer et al., 1995; Chen and Beer, 1997) at cellular and molecular level.

REFERENCES

1) Cardenas C, Liberona JL, Molgo J, Colasante C, Mignery GA, Jaimovich E (2005) Nuclear inositol 1,4,5-trisphosphate receptors regulate local Ca2+ transients and modulate cAMP response element binding protein phosphorylation. J Cell Sci. Jul 15;118(Pt 14):3131-40.
2) Carraway, K.L., III, and Burden, S. J. (1995) Curr. Opin. Neurobiol. 5, 606–612.
3) Chiel HJ and Beer RD (1997) The brain has a body: adaptive behavious emerges from interactions of nervous system, body and environoment. Trend Neurosci. 20:553-557.
4) Chow CW, Rincon M, Cavanagh J, Dickens M and Davis RJ (1997). Nuclear accumulation of NFAT4 opposed by the JNK signal transduction pathway. Science 278, 1638–1641.
5) Crabtree GR (1999). Generic signals and specific outcomes:signaling through Ca2+, calcineurin, and NF-AT. Cell 96, 611–614
6) Elena Bandi, Annalisa Bernareggi, Micaela Grandolfo, Chiara Mozzetta, Gabriella Augusti-Tocco,Fabio Ruzzier and Paola Lorenzon (2005) Autocrine activation of nicotinic acetylcholine receptors contributes to Ca2+ spikes in mouse myotubes during myogenesis Physiol 568.1 pp 171–180 171
7) Beer RD (2004) Autopoiesis and cognition in the game of life. Artif Life. vol. 10 (3) pp. 309-26.
8) Beer RD, Chiel HJ, Quinn RD and Ritzmann RE (1998) Biorobotic approaches to the study of motor systems. Curr Opin Neurobiol. 8:777-782.
9) Booth, F.W. and K.M. Baldwin. 1996. Muscle plasticity: Energy demand and supply processes. In The handbook of physiology: Integration of motor, circulatory, respiratory and meta-Calcineurin and muscle fiber type bolic control during exercise (ed. L.B. Rowell and J.T. Shepard), pp. 1075–1123. American Physiology Society, Bethesda, MD

10) Borges L S, Y Lee, M Ferns (2002) Dual role for calcium in agrin signaling and acetylcholine receptor clustering. J Neurobiol. vol. 50 (1) pp. 69-79.

11) Borges L S, M Ferns (2001) Agrin-induced phosphorylation of the acetylcholine receptor regulates cytoskeletal anchoring and clustering. J Cell Biol. vol. 153 (1) pp. 1-12.

12) Braun, D., and P. Fromherz. 2004. Imaging neuronal seal resistance on silicon chip using fluorescent voltage-sensitive dye. Biophys. J. 87:1351–1358

13) Braun D and Fromherz P (2000) Fast Voltage Transient in Capacitive Silicon-to-Cell Stimulation Detected with a luminescent Molecular Electronic Probe. Phys Rev Lett. vol. 30 (1) pp. 17-26.

14) G. Crabtree, E. Olson 2002 NFAT SignalingChoreographing the Social Lives of Cells. Cell, Volume 109, Issue 2, Pages S67-S79

15) Delling U, J Tureckova, H W Lim, L J De Windt, P Rotwein, J D Molkentin (2000) A calcineurin-NFATc3-dependent pathway regulates skeletal muscle differentiation and slow myosin heavy-chain expression. Mol Cell Biol vol. 20 (17) pp. 6600-11.

16) Dennis R G, P E Kosnik, M E Gilbert, J A Faulkner (2001) Excitability and contractility of skeletal muscle engineered from primary cultures and cell lines. Am J Physiol, Cell Physiol. vol. 280 (2) pp. C288-95

17) Eltit JM, García AA, Hidalgo J, Liberona JL, Chiong M, Lavandero S, Maldonado E, Jaimovich E. (2006) Membrane electrical activity elicits inositol 1,4,5-trisphosphate-dependent slow Ca2+ signals through a Gbetagamma/phosphatidylinositol 3-kinase gamma pathway in skeletal myotubes. J Biol Chem. 2006 Apr 28;281(17):12143-54

18) Estrada M, Cárdenas C, Liberona JL, Carrasco MA, Mignery GA, Allen PD, Jaimovich E. (2001), Calcium transients in 1B5 myotubes lacking ryanodine receptors are related to inositol trisphosphate receptors. J Biol Chem. 2001 Jun 22;276(25):22868-74. Epub Apr 11.

19) Fromherz P, Offenhäusser A, Vetter T, Weis J. (1991) A neuron-silicon junction: a Retzius cell of the leech on an insulated-gate field-effect transistor, Science May 31;252(5010):1290-3

20) Fromherz P and Klingler J (1991) Core-coat conductor of lipid bilayer and micromachined silicon Biochimica et Biophysica Acta (BBA) - Biomembranes Volume 1062, Issue 1, 11 February 1991, Pages 103-107

21) Fromherz, 2002, Neuroelectronics interfacing: semiconductor chips with ion channels, nerve cells, and brain, in Nanoelectronics and Information technology, Rainer Wasser, Willey-VCH, Berlin, 781-810

22) Fujita H, Nedachi T, Kanzaki M. (2007) Accelerated de novo sarcomere assembly by electric pulse stimulation in C2C12 myotubes. Exp Cell Res. 2007 May 15;313(9):1853-65. Epub Mar 12.

23) Gautam M, Noakes PG, Moscoso L, Rupp F, Scheller RH, Merlie JP, Sanes JR (1996) Defective neuromuscular synaptogenesis in agrindeficient mutant mice. Cell 85:525–535.

24) Glass DJ, Bowen DC, Stitt TN, Radziejewski C, Bruno J, Ryan TE, Gies DR, Shah S, Mattsson K, Burden SJ, Distefano PS, Valenzuela DM,Dechiara TM, Yancopoulos GD (1996) Agrin acts via a MuSK receptor complex. Cell 85:513–523.

25) Gleixner R and Fromherz P, (2006) The Extrtacellular Electrical Resistivity in Cell Adhesion, Biophysical Journal. V90, 2600-2611

26) Hennig R and Lomo T (1985). Firing patterns of motor units in normal rats. Nature 314, 164–166.

27) Schoen I, Fromherz P (2007) The mechanism of extracellular stimulation of nerve cells on an electrolyte-oxide-semiconductor capacitor, Biophys J vol. 92 pp. 1096-111

28) Jaimovich E, Reyes R, Liberona JL, Powell JA. (2000), IP(3) receptors, IP(3) transients, and nucleus-associated Ca(2+) signals in cultured skeletal muscle. Am J Physiol Cell Physiol.;278(5):C998-C1010

29) Tothova J, Blaauw B, Pallafacchina G, Rudolf R, Argentini C, Reggiani C, Schiaffino S (2006) NFATc1 nucleocytoplasmic shuttling is controlled by nerve activity in skeletal muscle. J Cell Sci. vol. 119 (Pt 8) pp. 1604-11.

30) Krause RM, Hamann M, Bader CR, Liu JH, Baroffio A & Bernheim L (1995). Activation of nicotinic acetylcholine receptors increases the rate of fusion of cultured human myoblasts. J Physiol 489, 779–790.

31)Kubis HP, R J Scheibe, J D Meissner, G Hornung, G Gros (2002) Fast-to-slow transformation and nuclear import/export kinetics of the transcription factor NFATc1 during electrostimulation of rabbit muscle cells in culture. J Physiol (Lond). vol. 541 (Pt 3) pp. 835-47.

32)Liu Y, Cseresnyes Z, Randall WR, Scheider (2001). Activity-dependent nuclear translocation and intranuclear distribution of NFATc in adult skeletal muscle fibers. Journal of Cell Biology 155, 27–39.

33)Lorenzon P, Grohovaz F, Ruzzier F. Voltage- and ligand-gated ryanodine receptors are functionally separated in developing C2C12 mouse myotubes (2000) J Physiol. Jun 1;525 Pt 2:499-507

34)Meissner J D, G Gros, R J Scheibe, M Scholz, H P Kubis (2001) Calcineurin regulates slow myosin, but not fast myosin or metabolic enzymes, during fast-to-slow transformation in rabbit skeletal muscle cell culture. J Physiol (Lond) vol. 533 (Pt 1) pp. 215-26.

35)Meissner J D, H P Kubis, R J Scheibe, G Gros (2000) Reversible Ca2+-induced fast-to-slow transition in primary skeletal muscle culture cells at the mRNA level. J Physiol (Lond). vol. 523 Pt 1 pp. 19-28.

36)MichaelP. Maher[a,] , Jerome Pine[b], John Wright[c] and Yu-Chong Tai[c] (1999) The neurochip: a new multielectrode device for stimulating and recording from cultured neurone, Journal of Neuroscience Methods Volume 87, Issue 1, 1 Pages 45-56

37)Megeath, L. J., and Fallon, J. R. (1998) J. Neurosci. 18, 672–678

38)Megeath, L. J., Kirber, M. T., Hopf, C., Hoch, W., and Fallon, J. R. (2003) Neuroscience 122, 659–668

39)Molgó J, Colasantei C, Adams D S, Jaimovich E (2004) IP3 receptors and Ca2+ signals in adult skeletal muscle satellite cells in situ. Biol Res. vol. 37 (4) pp. 635-9.

40)Olson EN and Williams RS (2000). Calcineurin signaling and muscle remodeling. Cell 101, 689–692.

41)Ojuka E O, Jones T E, Han D, Chen M, Holloszy J O (2003) Raising Ca2+ in L6 myotubes mimics effects of exercise on mitochondrial biogenesis in muscle. FASEB J. vol. 17 (6) pp. 675-81.

42) Pfeifer R., Lungarella, Fumiya Iida (2007) Self-organization, embodiment, and biologically inspired robotics. Science. vol. 318 (5853) pp. 1088-93

43) Ravel-Chapuis A., M Vandromme, J Thomas, L Schaeffer (2007) Postsynaptic chromatin is under neural control at the neuromuscular junction. EMBO J. vol. 26 (4) pp. 1117-28.

44) Rudrauf D, Lutz A, Cosmelli D, Lachaux JP, Le Van Quyen M (2003) From autopoiesis to neurophenomenology: Francisco Varela's exploration of the biophysics of being. Biol Res. vol. 36 (1) pp. 27-65.

45) Saltin, B. and P.D. Gollnick (1983). Skeletal muscle adaptability: Significance for metabolism and performance. In Handbook of physiology: Skeletal muscle (ed. L.D.D. Peachey), pp. 555–632. American Physiological Society, Bethesda, MD.

46) Sanes, J. R., and J. W. Lichtman. (2001). Induction, assembly,maturation and maintenance of a postsynaptic apparatus. Nat. Rev.Neurosci. 2:791–805.

47) Schiaffino, S. and C. Reggiani. (1996). Molecular diversity of myofibrillar proteins: Gene regulation and functional significance. Physiol. Rev. 76: 371–423.

48) Schoen and Fromherz (2007) The Mechanism of Extracellular Stimulation of Nerve Cells on an Electrolyte-Oxide-Semiconductor..*Biophys. J.*.; 92: 1096-1111

49) Schuhmeier RP and Melzer W (2004). Voltage-dependent Ca2+ fluxes in skeletal myotubes determined using a removal model analysis. J Gen Physiol 123, 33–51.

50) Serrano A L, M Murgia, G Pallafacchina, E Calabria, P Coniglio, T Lømo, S Schiaffino (2001) Calcineurin controls nerve activity-dependent specification of slow skeletal muscle fibers but not muscle growth. Proc Natl Acad Sci USA. vol. 98 (23) pp. 13108-13.

51) Straub B, Meyer E, Fromherz P. Recombinant maxi-K channels on transistor, a prototype of iono-electronic interfacing. (2001) Nat Biotechnol. Feb;19(2):121-4.

52) Tarroni P, Rossi D, Conti A, Sorrentino V. (1997) Expression of the ryanodine receptor type 3 calcium release channel during development

and differentiation of mammalian skeletal muscle cells. J Biol Chem. Aug 8;272(32):19808-13

53) Thompson E, Varela F (2001) Radical embodiment: neural dynamics and consciousness. Trends Cogn Sci. vol. 5 (10) pp. 418-425.

54) Tseng C, Zhang L, Cascio M, Wang Z (2003) Calcium plays a critical role in determining the acetylcholine receptor-clustering activities of alternatively spliced isoforms of Agrin. J Biol Chem. vol. 278 (19) pp. 17236-45.

55) Cassanelli S and Fromherz P (1999) Transistor probes local potassium conductances in the adhesion region of cultured rat hippocampal neurons.J Neurosci. Aug 15;19(16):6767-73.

56) Eric Vogel Technology and metrology of new electronic materials and devices Nature Nanotechnology 2, 25 - 32 (01 Jan 2007) Review

57) Ursu D, Schuhmeier RP and Melzer W (2005). Voltage-controlled Ca2+ release and entry flux in isolated adult muscle fibres of the mouse. J Physiol 562, 347–365.

58) Valdés JA, Hidalgo J, Galaz JL, Puentes N, Silva M, Jaimovich E, Carrasco M A (2007) NF-kappaB activation by depolarization of skeletal muscle cells depends on ryanodine and IP3 receptor-mediated calcium signals. Am J Physiol, Cell Physiol. vol. 292 (5) pp. C1960-70

59) R. Weis and P. Fromherz, Phys. Rev. E 55, 877 (1997).

60) Wells DG, McKechnie BA, Kelkar S, Fallon JR. (1999) Neurotrophins regulate agrin-induced postsynaptic differentiation. Proc Natl Acad Sci U S A. 2;96(3):1112-7

61) Wallrapp, F., and P. Fromherz. (2006). TiO2 and HfO2 in electrolyte-oxide-silicon configuration for applications in bioelectronics. J. Appl. Phys. 99:114103.

62) Weston C A, Teressa G, Weeks B S, Prives J (2007) Agrin and laminin induce acetylcholine receptor clustering by convergent, Rho GTPase-dependent signaling pathways. J Cell Sci. vol. 120 (Pt 5) pp. 868-75.

63) Zeck G and Fromherz Z, 2001, Noninvasive neuroelectronic interfacing with synaptically connected snail neurons immobilized on a semiconductor chip, Proc Natl Acad Sci U S A., 2001 vol. 98 pp. 10457-62

64)Ziemke T (2008) On the role of emotion in biological and robotic autonomy. BioSystems . vol. 91 (2) pp. 401-8

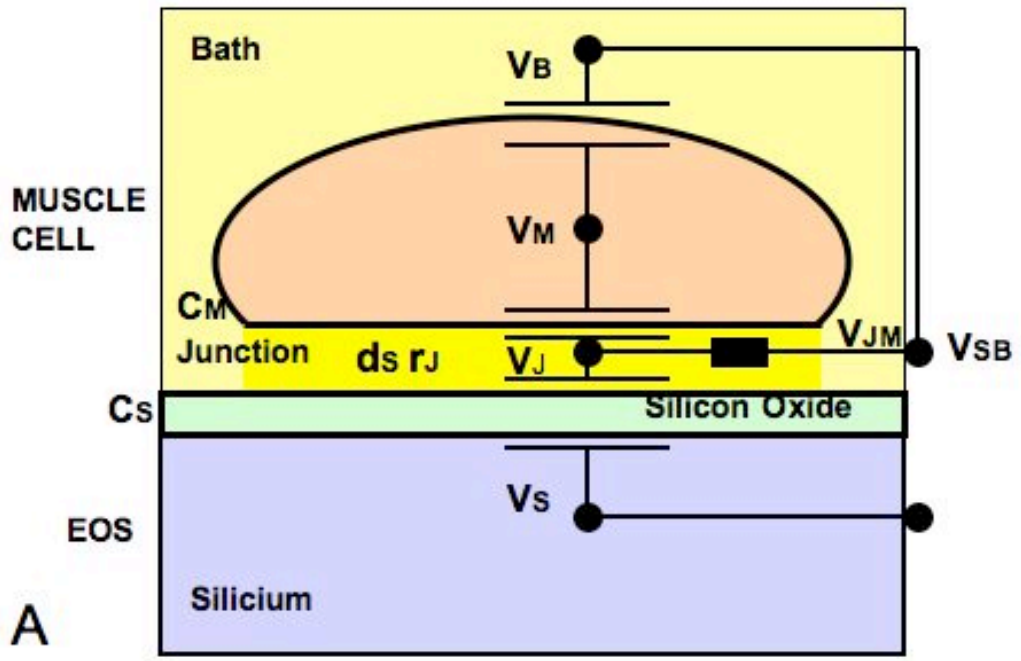

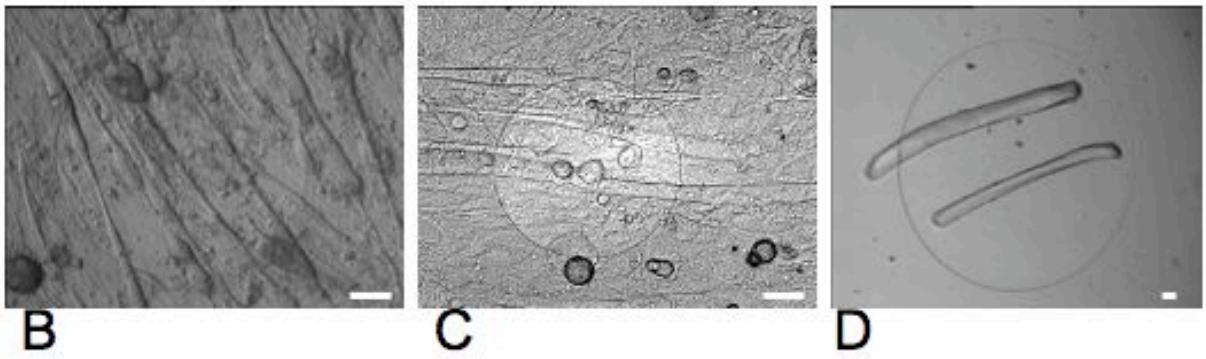

Fig. 1

Figure 1

Silicon-Muscle Junction. A) Schematic Cross Section (not in scale) of the muscle-chip junction. The Chip is insulated by silicon dioxide that is coated with extracellular matrix protein. A Muscle Cell is attached to the Electrolite-Oxide-Semiconductor capacitive stimulation spot (EOS). The cleft in the junction of thickness dJ (around 80 nm) between the cell membrane (area-specific capacitance CM) is filled with an electrolyte of resistivity rJ. When the electrical voltage VS – VB between EOS and bulk electrolyte is changed, the voltages VM – VJ and VM -VB across the attached and free membrane change giving rise in the muscle cell and to EC coupling detected with calcium sensitive dye and contraction observation. B-C-D) Micrographs (bar 10 um) of C2C12 myotubes (A), Primary Myotubes (C) and FDB dissociated muscle fibers (D) located on the EOS stimulation spot area (circles in the center).

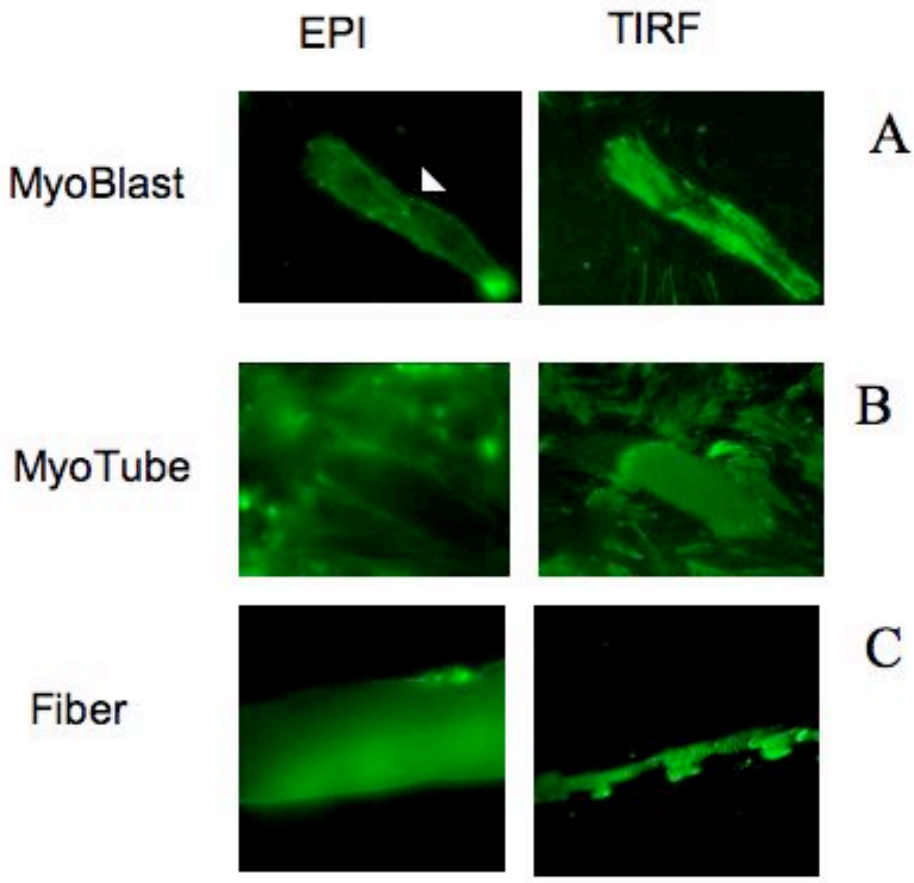

Fig. 2

Figure 2.

TIRF microscopy of adhesion regions (80-150 nm) of C2C12 myoblasts, myotubes and FDB muscle fiber stained live with FM dye. In A, myoblasts show a wide but irregular adhesion over the surface coated with collagen nanolayer. In this image two close myoblasts are fusing each other. Under epifluorescence (EPI) is visible the fusing membrane borderline (arrow), while in tirf the same region is free. In B, a myotube under epifluorescence does not show any fluorescence on the adhesion range (80-150 nm), whereas under TIRF, a large and compact adhesion region is localized under the cell membrane. In figure C a dissociated FDB muscle fiber shows a typical homogeneous pattern in epifluorescence, while small and striated adhesion regions are evident in TIRF. FDB fibers tend to develop weak and smaller adhesion regions compared the large size of the fiber but they are often sufficient for efficient fiber-silicon coupling.

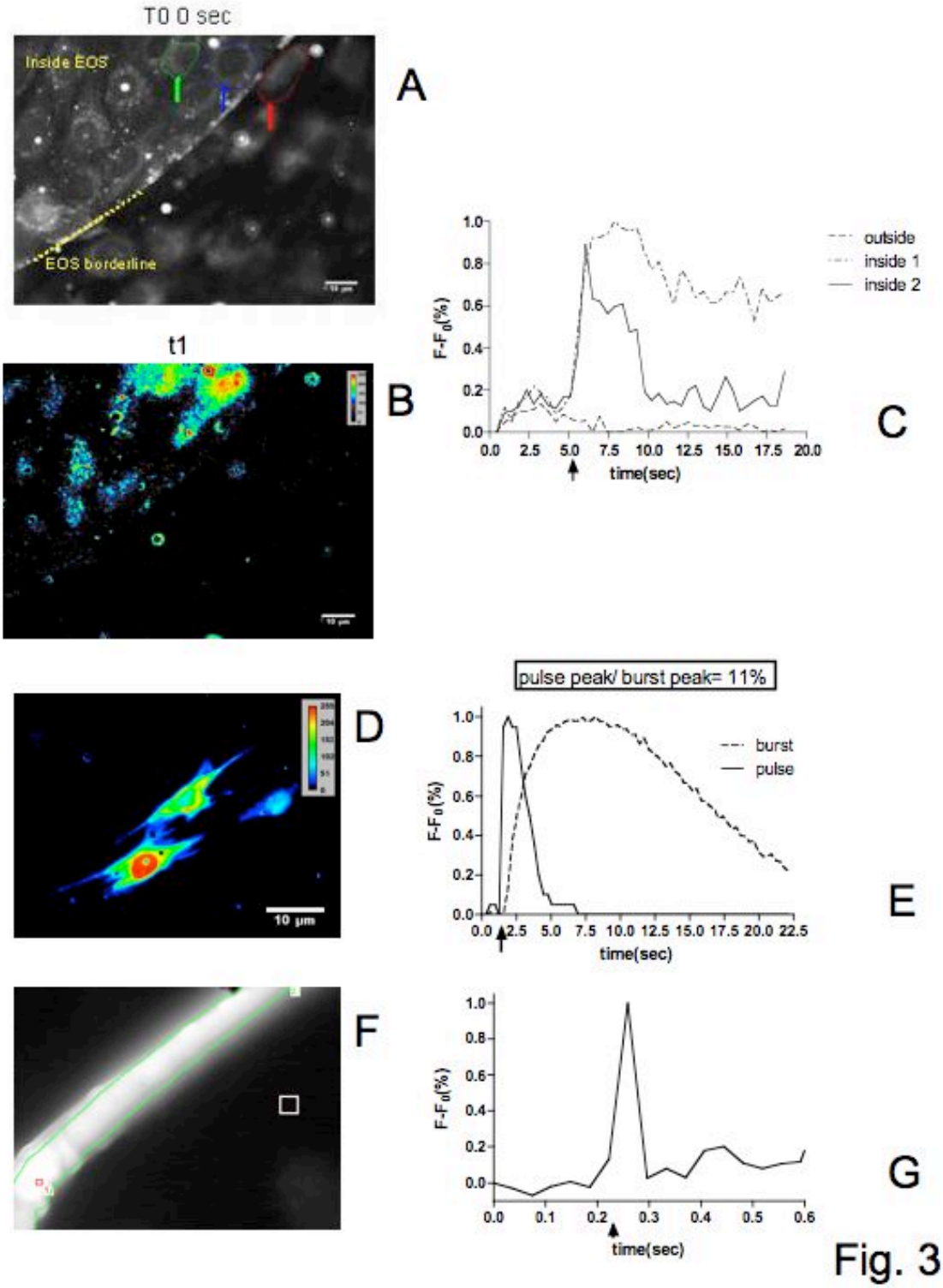
T0 0 sec
Inside EOS
EOS borderline
A
t1
B
C
outside
inside 1
inside 2
F-F0(%)
time(sec)
D
10 μm
pulse peak/ burst peak= 11%
burst
pulse
E
F
G

Fig. 3

Figure 3

Calcium transients evoked by ECS in myoblasts and FDB muscle fibers. Confluent C2C12 myoblasts are coupled with electrolyte oxide semiconductor (EOS) on silicon chip. In epifluorescence picture of basal [Ca++]i, two myoblasts within EOS region are indicated by arrows and circles and a third cell is indicated outside the bordeline of EOS (A). During ECS only in myoblasts within the EOS slow [Ca++]i waves are evoked (B), in particular long lasting waves are located within the nuclear regions (inside 1 trace in C) and slow faster waves on cytoplasmic regions (inside 2 trace in C). Outer EOS myoblast doesn't show any variation of basal [Ca++[i (outside trace in C).

In myoblasts slow [Ca++]i waves are also modulated by ECS amplitude and frequency. In D myoblasts show slow waves evoked by ECS. A single square pulse of 1 V and 1 ms of duration evokes a slow calcium wave. When a 30 Hz ECS train of 1 sec is applied to the chip, slow [Ca++]i waves are longer and higher in amplitude (E).

In F a single FDB muscle fiber is coupled to the EOS and single square pulses are applied, evoking fast [Ca++]I transients (G).

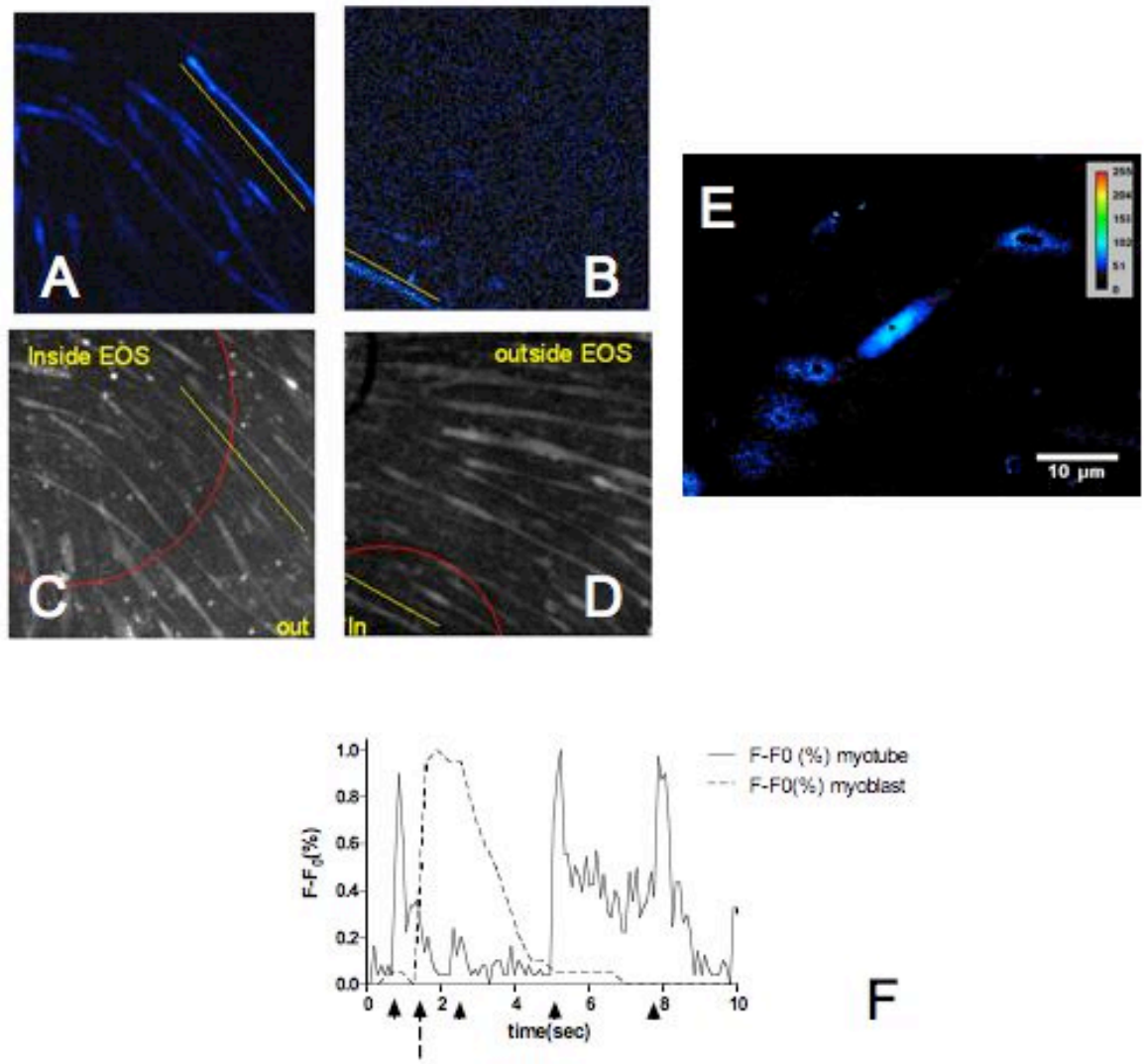
A
B
E
Inside EOS
outside EOS
C
out
In
D
10 µm
F-F0 (%) myotube
F-F0(%) myoblast
F-F0(%)
1.0
0.8
0.6
0.4
0.2
0.0
0
2
4
6
8
10
time(sec)
F
G
In
Out
Out
In
H

Fig. 4

Figure 4

C2C12 Myotubes coupled with EOS under long term ECS. Myotubes growing over silicon chip with integrated EOS cover the whole surface. In C and D, in red is highlighted the EOS borderline and are well visible in epifluorescence profiles of myotubes loaded with calcium sensitive dye. In A and B the same myotubes under ECS show [Ca++]i transients only if coupled with one or more adhesion regions inside EOS area (A), while outside the ESO no myuotubes present [Ca++]i transients (B). In fig. F fast [Ca++]i kinetic of calcum transients evoked by ECS on single myotube (in E the explored myotube with Region of Interest located in a nucleus). Three ECS pulses of square wave, at 1V, 1 ms duration evoke three distinct calcium transients (F). They are compared with the slow calcium wave evoked by similar single pulse in a myoblast of fig 3E (expanded here on the same time scale).

In G and E, NFATC3 endogenous immuno-histochemical staining with DAB-peroxidase in myotubes nuclei after 12 hours of long term ECS 5 sec trains at 10 HZ with a resting time of 55 seconds. Picture at 10x (G) shows the translocated nuclei concentrated over the EOS region (left side), while outside myotubes present no nuclear translocation (right side). The EOS border is indicated by an arrow. In particular, at 60x (E) arrows indicate positive translocated nuclei on a myotube over EOS region (bottom side), and negative non translocated nuclei on a myotube outside the EOS (top side).

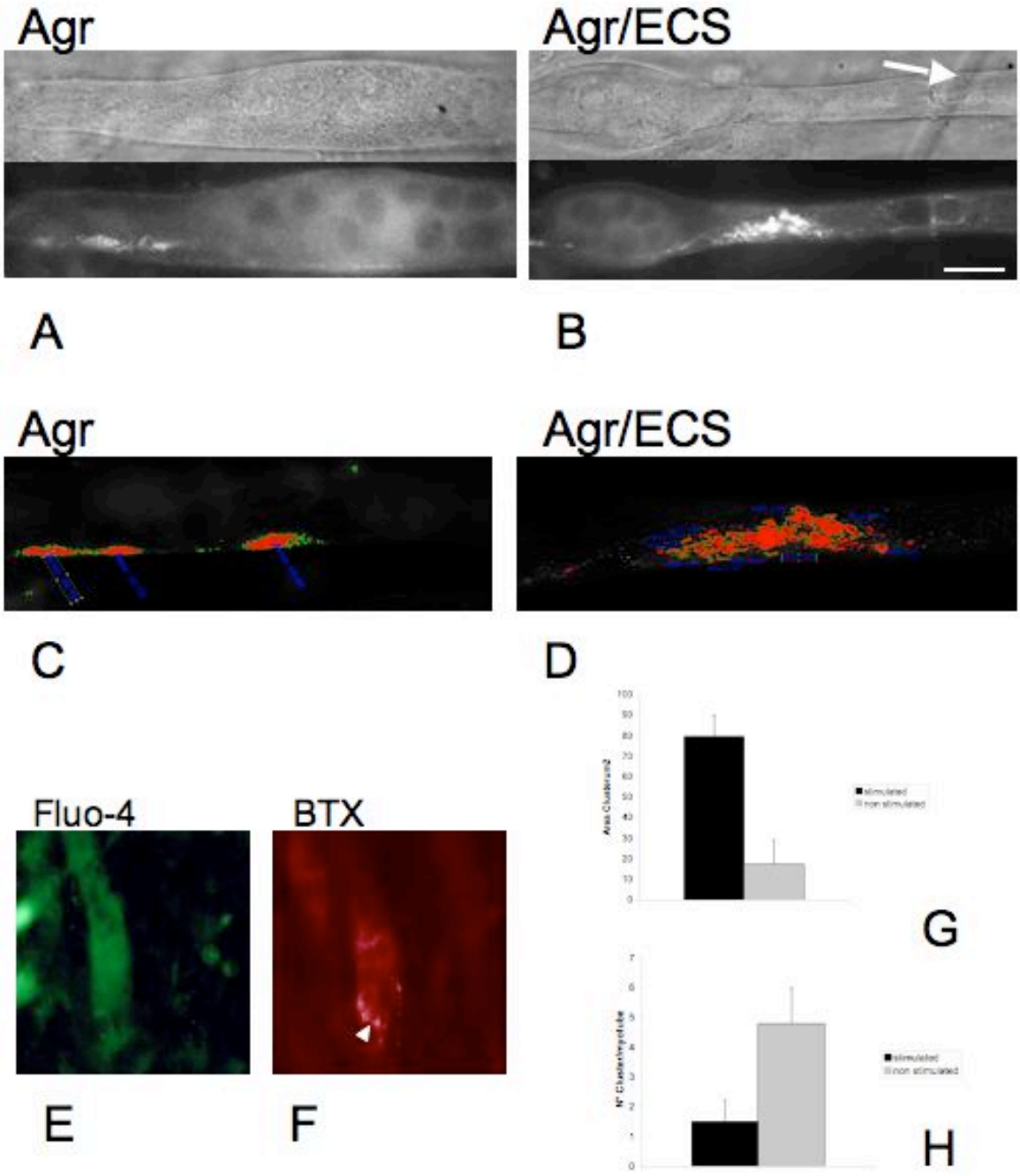

Fig. 5

Figure 5

C2C12 myotubes growing over silicon EOS chip, show AchR clustering agrin-induced and ECS-modulated. Single myotubes exposed for 12 Hr to neural agrin alone (A) or together with long term ECS at 10 hz (B). Scale bar 10 μM. Top sides are contrast microscope pictures, on the right side of 5B an arrow indicates the bordeline of EOS coupled with a myotube. Bottom side of the pictures is epifluorescence microscopy images for AchR clusters of live staining with green coniugated alphaugarotoxin. While myotubes exposed only to agrin present several small clusters (A), myotubes under chronic ECS present reduced number of clusters but larger in the area (B). Clusters images have been manipulated to filter and quantify data by bioinformatics analysis (C and D). To exclude uncoupled myotubes, after long term ECS, cells on chip were loaded with calcium sensitive day (E) to screen for ECS calcium transient responsive myotubes and stained live for alphabungarotoxin red coniugated. Once selected the coupled myotubes, they have been studied for AchR clusters (F). On the same silicon chip semiconductor coupled myotubes long termed stimulated with ECS present less cluster (H) but with with larger areas (G) than resting unstimulated myotubes.

CONCLUSION

EC coupling of the skeletal muscle is a complex system and the network of molecular players and pathways is far to be understood. The elegant architecture which links and involves SR, sarcolemma and myofibrils, designs regular patterns functionally related to Calcium pathways within skeletal muscle cells. In this context several SR proteins play multifunctional roles. Our results show how a functional SR calcium-binding protein, like Csq1, when mutated or missing causes a re-organized C2+ stores, disrupting the muscle structure and leading to impaired calcium handling (chapter 1). These alterations cause myopathies and develop pathogenic conditions, like the MH episodes we have described for the Cs1-null mice (chapter 2). On the other side, the structural SR protein Ank1.5 could play a specific role not restricted to a correct positioning of the SR at specific sarcomere regions and may contribute to the generation of myopathies, and EC coupling dysfunctions (chapter 3). This scenario suggests a complex concertated network of SR, Sarcoplasm and myofibrillar proteins in skeletal muscle.

Our new technique of hybrid semiconductor microchips coupled with single fibers and primary satellite cells culture offers high spatial resolution and long term single cell EC induced modultation (chapter 4). This innovative device combined together with our KO mice models, offers a deeper level of investigation which can reveal more hidden aspects of the relations between different players involved in the calcium singnaling EC coupling-related and its role in the development, regeneration, aging and plasticity of the skeletal muscle.

AKNOWLEDGMENT

AKNOWLEDGMENT

I must thank first of all my mentor, Prof. Carlo Reggiani: a wise boss and a friend. He guided me with patient and knowledge trough the fantastic world of muscle science, which I have learned to love. He teached me how to make and, more important, how to understand what real science is. He offered me a lot of chance and opportunities to grow as a young scientist.
I want to thank Dr Stefano Vassanelli, who gave me the chance to take up the project of chips and turn it into reality.; Prof. Feliciano Protasi, a nice guy and brilliant proactive scientis, and his team, Dr. Cecilia Paolini and Dr Marco Dainese for their collaboration on Calsequestrin project; and Prof. Vincenzo Sorrentino, an acute and skilled scientist, and his team, Dr. Emiliana Giacomello and Dr. Vincenza Cusimano, for their collaboration in the Ankkyrins project.
I thank my lab colleagues, Dr Luciana Toniolo, Dr Marta Canato, Dr Nicola Cacciani and Dr Bert Blaauw for sharing with me these three past years of science and challenges. I want to thank also Prof. Aram Megighian for his kind suggestions and tips in neuroscience.
I thank also all the other department people, in particular special thanks go to Dr Michele Scorzeto and Dr Stefano Girardi, I am glad to have found good friends and supportive colleagues at the same time.
Finally I thank my parents and Maddalena, for their ever present support and trust.

Εν Το Παν